SRESA's International Journal of

LIFE CYCLE RELIABILITY AND SAFETY ENGINEERING

Vol.4 **Issue No.1** **Jan–March 2015** **ISSN – 2250 0820**

Special issue

on

"Prognostics & Structural Health Management"

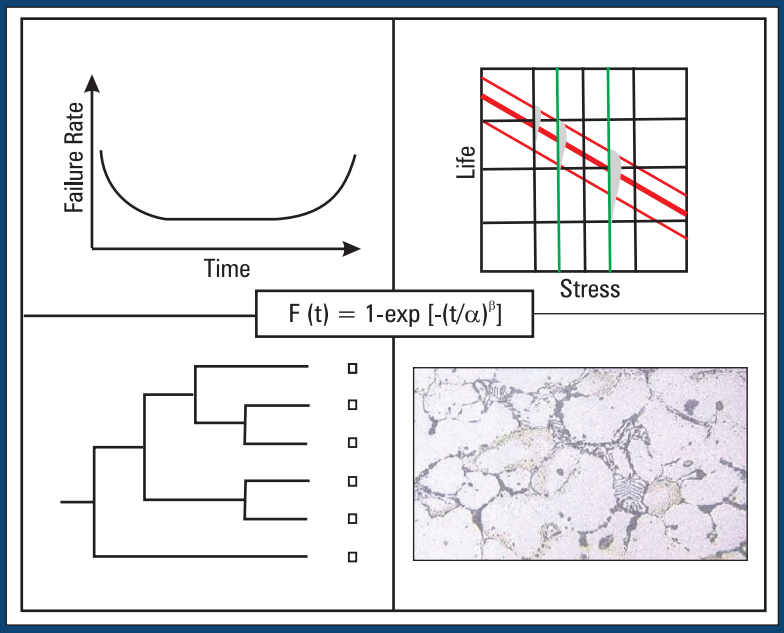

Guest Editor:
Dr. Achintya Haldar

Society for Reliability and Safety

website: http://www.sresa.org.in

SRESA Journal of Life Cycle Reliability and Safety Engineering

Extensive work is being performed world over on assessment of Reliability and Safety for engineering systems in support of decisions. The increasing number of risk-based / risk-informed applications being developed world over is a testimony to the growth of this field. Here, along with probabilistic methods, deterministic methods including Physics-of-Failure based approach is playing an important role. The International Journal of Life Cycle Reliability and Safety Engineering provides a unique medium for researchers and academicians to contribute articles based on their R&D work, applied work and review work, in the area of Reliability, Safety and related fields. Articles based on technology development will also be published as Technical Notes. Review articles on Books published in the subject area of the journal will also form part of the publication.

Society for Reliability and Safety has been actively working for developing means and methods for improving system reliability. Publications of quarterly News Letters and this journal are some of the areas the society is vigorously pursuing for societal benefits. Manuscript in the subject areas can be communicated to the Chief Editors. Manuscript will be reviewed by the experts in the respective area of the work and comments will be communicated to the corresponding author. The reviewed final manuscript will be published and the author will be communicated the publication details. Instruction for preparing the manuscript has been given on inside page of the end cover page of each issue. The rights of publication rest with the Chief-Editors.

SCOPE OF JOURNAL

System Reliability analysis	**Structural Reliability**	**Risk-based applications**
Statistical tools and methods	Remaining life prediction	Technical specification optimization
Probabilistic Safety Assessment	Reliability based design	Risk-informed approach
Quantitative methods	Physics-of-Failure methods	Risk-based ISI
Human factor modeling	Probabilistic Fracture Mechanics	Risk-based maintenance
Common Cause Failure analysis	Passive system reliability	Risk-monitor
Life testing methods	Precursor event analysis	Prognostics & health management
Software reliability	Bayesian modeling	Severe accident management
Uncertainty modeling	Artificial intelligence in risk and reliability modeling	Risk-based Operator support systems
Dynamic reliability models	Design of Experiments	Role of risk-based approach in Regulatory reviews
Sensitivity analysis	Fuzzy approach in risk analysis	Advanced electronic systems reliability modeling
Decision support systems	Cognitive framework	Risk-informed asset management

SRESA AND ITS OBJECTIVES

a) To promote and develop the science of reliability and safety.

b) To encourage research in the area of reliability and safety engineering technology & allied fields.

c) To hold meetings for presentation and discussion of scientific and technical issues related to safety and reliability.

d) To evolve a unified standard code of practice in safety and reliability engineering for assurance of quality based professional engineering services.

e) To publish journals, books, reports and other information, alone or in collaboration with other organizations, and to disseminate information, knowledge and practice of ensuring quality services in the field of Reliability and Safety.

f) To organize reliability and safety engineering courses and / or services for any kind of energy systems like nuclear and thermal power plants, research reactors, other nuclear and radiation facilities, conventional process and chemical industries.

g) To co-operate with government agencies, educational institutions and research oganisations

SRESA's International Journal of

LIFE CYCLE RELIABILITY AND SAFETY ENGINEERING

Vol.4 Issue No.1 Jan–March 2015 ISSN – 2250 0820

Special issue

on

"Prognostics & Structural Health Management"

Guest Editor:

Prof. Achintya Haldar

Chief-Editors

P.V. Varde
A.K. Verma
Michael G. Pecht

SOCIETY FOR RELIABILITY AND SAFETY

Typeset & Printed

EBENEZER PRINTING HOUSE
Unit No. 5 & 11, 2nd Floor, Hind Services Industries,
Veer Savarkar Marg,
Dadar (west), Mumbai -28
Tel.: 2446 2632/ 3872
E-mail: outwork@gmail.com

Guest Editorial

Prognostics and structuring health management has become an active interdisciplinary research area all over the world. Infrastructures are deteriorating, some of them are over their design life, or they are being exposed to natural extreme events like strong earthquakes or high winds, or man-made like blasts or explosions. Due to severe shortage of resources to replace them, it is now necessary to extend their design life without exposing public to unnecessary risk. One approach has attracted a considerable amount of attention is inspecting the infrastructures as thoroughly as practicable in a timely manner to identify the defect spots,quantify their severity and then take appropriate remedial actions so that they can be used for which they were initially designed. Researchers from many different disciplines are now concentrating on developing new mathematical techniques, inspection methods, necessary instruments or sensors, sources of energy require to operate the sensors in field conditions, etc. The first two issues of 2015 of this journal Life Cycle Reliability and Safety Engineering are dedicated to these special topics.

The first paper presents a novel method to identify nonlinear large dynamic systems using a system identification-based technique in the presence of uncertainty using the Kalman filter concept. The potential benefits of particle filtering in revealing accurate statistical information on the imprecisely known model parameters or modeling errors of dynamical systems, based on limited time series data, have not been quite realized. A major numerical bottleneck precipitating this under-performance, especially for higher dimensional systems, is the progressive particle impoverishment owing to weight collapse.In this paper this problem is addressed by replacing weight-based updates through additive ones. Thus, in the context of nonlinear filtering problems, a novel additive, gain-like particle update scheme, in its non-iterative and iterative forms, is proposed based on manipulations of the innovation integral in the governing Kushner-Stratonovich equation. It is superior to the non-iterative version of the Ensemble Kalman Filter (EnKS) vis-à-vis most existing filters. Prominent in the reported numerical comparisons are variants of EnKF that also use additive updates, albeit with many inherent limitations of a Kalman filter.

The second paper proposes a variance reduction strategy for updating reliability models of dynamical systems driven by random excitations. The basic framework consists of a system identification step followed by a reliability model updating step. Both these problems are tackled within the framework of Bayesian model updating. Maximum likelihood estimation method is used as a tool for system identification, whereas, the Girsanov transformation based method is used in obtaining as estimate for the posterior probability of failure with reduced variance. Illustrative example includes shake table studies on an asymmetric, bending-torsion coupled frame.

A novel structural health assessment procedure for nonlinear structural systems is presented in the third paper. It is developed by integrating the unscented Kalman filter concept with the weighted global iteration procedure with an objective function. It is denoted as unscented Kalman filter with weighted global iteration (UKF-WGI). It is a finite elements-based time-domain system-identification technique. It can be used to assess structural health at the element level using only a limited number of noise-contaminated responses. Defect(s) with different level of severity is simulated in single and multiple member(s) and then the capabilities of the procedure are examined. The proposed method is compared with the extended Kalman filter with weighted global iteration (EKF-WGI) procedure. The proposed UKF-WGI is superior to EKF-WGI in all aspects, particularly when the level of nonlinearity is severe. Since the level of nonlinearity is expected to be unknown at the initiation of the inspection, to be on the safe side, the proposed UKF-based procedure should be used to assess structural health in the future.

In the fourth paper Wavelet Transforms have been used to enhance damage sensitive features for structural health monitoring. Although, the Continuous Wavelet Transforms have been employed, the Discrete Wavelet Transform (DWT) becomes a natural choice in view of its capability to optimally localize the space/time and frequency/scale resolution. Although, a number of alternative DWT families exist; the choice of a particular basis for enhancement of damage features is somehow arbitrary. The feature enhancement capability of several most commonly employed wavelet families are compared in order to assess their relative efficacy in this paper. The superior performance of Cohen-Daubechies-Feauveau family is observed and appears to be

the sole choice where the damage onset is at immediate vicinity of the boundary. The relative efficiencies of enhancements are demonstrated considering the possible variations of the damage locations, extents, as well as alternate features.

A major cost and management issue related to wind turbine structures is condition assessment, which, when conducted according to state-of-the-art protocols, produces very subjective and highly variable results. The related topics are discussed in this paper. This paper reports on the development of a new onsite structural condition assessment for a wind turbine tower structural system based on a wireless sensor system that is remote, compact, and quick to install. This condition assessment tool offers a cost-effective monitoring system that can be effective in increasing the safety of wind turbine tower structures and hence, enhancing their reliability of performance.

AchintyaHaldar
Guest Editor
University of Arizona, Tucson, Arizona

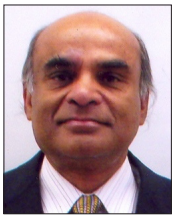

Dr. Haldar is a Distinguished Member of ASCE and a Fellow of Structural Engineering institute. He started his research career at the University of Illinois (M.S., 1973 and Ph.D., 1976). After graduation, he worked two years for Bechtel Power Corporation in Los Angeles. Then he returned to an academic career, first at Illinois Institute of Technology, then at Georgia Institute of Technology, and now at the University of Arizona (UA). He also taught courses at Hong Kong University of Science & Technology and at the Technical University of Ostrava in the Czech Republic. He conducted research at the University of Tokyo and Indian Inst. of Science, Bangalore, India. In addition, Dr. Haldar has more than 5 1/2 years of practical experience. Dr. Haldar was the founding Editor-in-Chief for "Engineering under Uncertainty; Hazards, Assessment and Mitigation." He was an associate editor of the ASCE's Journal of Structural Engineering. Dr. Haldar was a co-chair of the Probabilistic Mechanics Conference sponsored by the ASCE. He also organized Euro-SiBRAM'02 in Prague, Czech Republic. Dr. Haldar received numerous recognitions for his service and exceptional teaching at the highest level. They are listed at haldar.faculty.arizona.edu.

Dr. Haldar's research emphasizes the presence of uncertainty in engineering problems. Recently, under a research grant from the NSF, he has been working on multiple deterministic analyses to capture the presence of uncertainty. If successful, it will revolutionized engineering computations. So far, Dr. Haldar has published over 450 technical publications, including 10 books, 25 book chapters, and made numerous keynote and invited presentations worldwide. For the areas covered in this special issue, he published 1 edited book, 6 book chapters, gave 3 special lectures, over 46 referred papers, over 21 conference papers, and gave 22 special invited international presentations. He has advised a large number of graduate students. Some of them are now professor in the U.S., Canada, Jordon, Korea, Mexico, Taiwan, West Bank, etc.

Dr. Haldar received many awards for his research, including the first Presidential Young Investigator Award and the ASCE's Huber Civil Engineering Research prize. He received an Honorable Diploma from the Czech Society for Mechanics. He received the Distinguished Alumnus Award from the CEE Alumni Association, University of Illinois. He received inaugural da Vinci fellowship from the College of Engineering. ASME gave him the Honorable Recognition Award. He received John C. Park Outstanding Civil Engineer Award in from the Arizona Society of ASCE. He was selected one of 23 Scientists and Technologists of Indian Origin abroad (STIOs) by the Government of India for collaborative projects with Indian scientists and technologists. Recently he received Honorary Distinguished Visiting Professorship, Bengal Engineering and Science University, Shibpur, India, 2013-2018 and Invited Wenyuan Lecture Professorship, Tongji University, Shanghai, China, 2013.

Life Cycle Reliability and Safety Engineering
Vol.4 Issue 1 (2015) 01-13

An Ensemble Kushner-Stratonovich (EnKS) Nonlinear Filter: Additive Particle Updates in Non-Iterative and Iterative Forms

Saikat Sarkar and Debasish Roy*
Computational Mechanics Lab, Department of Civil Engineering, Indian Institute of Science, Bangalore, India
**Email: royd@civil.iisc.ernet.in*

Abstract:

Despite the cheap availability of computing resources enabling faster Monte Carlo simulations, the potential benefits of particle filtering in revealing accurate statistical information on the imprecisely known model parameters or modeling errors of dynamical systems, based on limited time series data, have not been quite realized. A major numerical bottleneck precipitating this under-performance, especially for higher dimensional systems, is the progressive particle impoverishment owing to weight collapse and the aim of the current work is to address this problem by replacing weight-based updates through additive ones. Thus, in the context of nonlinear filtering problems, a novel additive, gain-like particle update scheme, in its non-iterative and iterative forms, is proposed based on manipulations of the innovation integral in the governing Kushner-Stratonovich equation. Numerical evidence for the identification of nonlinear and large dimensional dynamical systems indicates a substantively superior performance of the non-iterative version of the EnKS vis-à-vis most existing filters. The costlier iterative version, though conceptually elegant, mostly appears to effect a marginal improvement in the reconstruction accuracy over its non-iterative counterpart. Prominent in the reported numerical comparisons are variants of the Ensemble Kalman Filter (EnKF) that also use additive updates, albeit with many inherent limitations of a Kalman filter.

Keywords: *Kushner-Stratonovich equation; Euler approximation; inner iterations; Monte Carlo filters; error estimates; nonlinear system identification*

1. Introduction

In recent years, stochastic filters based on Monte Carlo (MC) simulations have gained prominence owing to their potential in solving a large class of nonlinear estimation problems, ranging from dynamical state/parameter estimation to complex target tracking, atmospheric data assimilation etc., by combining partially observed noisy time series data acquired through experiments with the simulation tools for the dynamical system model. The original filter by Kalman and Bucy [1] may be traced back as a progenitor of most modern stochastic filters, even though the former was developed as a closed-form analytical (and not as an MC) scheme for solving strictly linear estimation problems with Gaussian noises. In stochastic filtering, the estimation problem is posed as determining the distributions of (measurable functions of) the system states, also called processes, conditioned on the filtration generated by the measurements up to the current time t. When the drift terms in the stochastic differential equations (SDE-s) representing the process and measurement dynamics are linear and the noises or diffusion terms Gaussian, the evolving conditional distribution for the estimation problem, also called the filtering distribution, is Gaussian which is determined by the evolution equations for mean and covariance, the first two moments, as prescribed by the Kalman filter [2]. Even though the idea behind this filter is simple and elegant, its sub-optimal extensions based on drift linearization, the extended Kalman filters (EKF-s) to wit [3], are often found inadequate in treating estimation problems with strong drift nonlinearity and/or noise non-Gaussianity in the process/measurement dynamics. The last class of problems typically involve non-Gaussian, possibly multi-modal conditional distributions as solutions to the estimation problems. Here a MC simulation approach, adopted by many recent filters such as the particle filters (PF-s), is preferred as evolutions of such distributions cannot generally be described by a finite hierarchical set of moments [4] except for a few special cases. For nonlinear, non-Gaussian estimation problems, the governing filtering equations describing

the evolution of the conditional distribution in the space of probability measures may be derived starting with an appropriate change of measures, which immediately yields the Kallianpur-Striebel formula [5]. Manipulations of this formula based on the principles of stochastic calculus leads to the Zakai equation [6] for the un-normalized conditional density and onwards to the Kushner-Stratonovich (KS) equation [7] for the normalized density. Unfortunately, analytical or even acceptably accurate numerical solutions to these equations are not available [8]. During the early stages of development of MC filters approximating the nonlinear filtering equations during the last quarter of the last century, success was limited partly owing to a rather restricted availability of the computational power. This probably led to a somewhat popular adoption of the analytical EKF for nonlinear filtering applications [9], even though the method was known to be potentially inaccurate and often unstable thereby requiring an elaborate tuning of the process noise covariance.

The vastly improved computational power over the last couple of decades has imparted a great fillip to the devising of innovative numerical schemes that solve the non-linear and non-Gaussian filtering problem. Amongst these, prominence may be accorded to sequential Monte Carlo (SMC) techniques, i.e. the PF-s [10-14], which are basically recursive Bayesian approaches empirically representing the posterior (or filtering) distribution through an ensemble of MC realizations of the system states, also called particles. Extensive convergence studies have been carried out for many of these numerical schemes which show that these schemes, through multiplicative weight-based updates, empirically represent the desired filtering distribution at a given time with the error decreasing (in law) proportional to only $\frac{1}{\sqrt{N}}$, where N denotes the number of particles or the ensemble size [15, 16]. Unfortunately, most SMC techniques are scourged with the problem of 'particle impoverishment', especially when applied to higher dimensional filtering problems wherein the weights tend to collapse sequentially to a point mass. Once this happens, the process upon conditioning on the measurement till the current time receives no non-trivial updates. Numerical evidence suggests that the typical ensemble size preventing 'weight collapse' increases exponentially with increasing system dimension [16]. Among the numerous research articles aiming at improving these SMC techniques, implicit sampling [17], improved re-sampling [18] and Markov chain Monte Carlo (MCMC) sampling based particle filters [19] have, amongst others, drawn attention. Since methods like implicit sampling, improved re-sampling etc. still rely on the multiplicative weight based update strategy, they are not essentially free from the problem of 'particle impoverishment'. On the other hand, MCMC schemes typically take a very large number of iterations for most problems of practical interest and may thus be computationally unwieldy. Within the MC setup, the numerical infeasibility of requiring impractically large N is, to an extent, bypassed by an MC based filter called the ensemble Kalman filter (EnKF) [20] and its variants, several of which have been successfully applied to large dimensional atmospheric data assimilation problems. Here a resolution to the problem of particle impoverishment is realized through an additive update, which is basically an MC implementation of the gain-based update term of the Kalman filter. But a major criticism of this class of approximate schemes is that they are derived heuristically and even though drift non-linearity is accounted for in some way, they are hardly equipped to treat noise non-Gaussianity [20]. There are attempts in the literature to directly solve the Zakai equation by approximating the un-normalized filtering distribution via time and space discretizations or through functional series [21-23]. For example, the conditional density is approximated using multiple Wiener and Stratonovich integrals in [21,24]. In [22,23], numerical approximations to the Zakai equation have been validated through low-dimensional problems. Even though the Zakai equation is linear and widely studied, in numerical computations it suffers from serious deficiencies [8], e.g. fast dissipation of the solution with increased time step and intermittency leading to rare but large peaks. A way of circumventing these numerical limitations would be to take recourse to the KS equation [8].

The KS equation, the parent filtering equation derivable through Ito's expansion of the Kallianpur-Striebel formula, gives the evolution of the normalized conditional distribution (or a measure-valued conditional process) via a stochastic integral expression. But, except for a few very special cases of linearity and Gaussianity, the KS equation cannot, in general, be reduced to a closed set of stochastic partial differential equations (SPDEs), which can be numerically integrated to arrive at the desired filtering distribution at a given time. Indeed a direct approximation of the KS equation, say using an Euler-type discretization, does not generally yield an

accurate and robust scheme. Many SMC methods, which attempt MC simulations based on averaging over the characteristics (i.e. the sample paths provided by the process and measurement dynamics) following a conditional Feynman-Kac formula [25] and typically leading to a weighted particle system [26], have been tried to approximate the KS equation. However, as noted before, most of these methods are not free from the curse of weight collapse, even for moderately large filter dimensions. The primary aim of this article is a resolution of this long standing problem through an efficient, yet accurate, additive particle update scheme derived through the KS equation.

Building upon our recent idea of an MC-based iterative approximation to the additive update term in the KS equation [27], we propose an entirely new version of the filter that, whilst closely following the evolutions of the estimates based on the KS equation, efficiently implements the nonlinear and strictly additive particle updates without an imperative necessity for inner iterations. This development is based on a sequence of manipulations of the update term so as to introduce an additional layer of numerical dispersion in the gain-like coefficient of the innovation. While inner iterations, as in the previous version of the filter, may still be utilized with some improvement in the estimate, the non-iterative form of the filter does yield solutions that are quite accurate even for large dimensional nonlinear filtering problems. Proofs of convergence of the modified filter, in both its non-iterative and iterative forms, are also provided.

The rest of the paper is organized as follows. Section 2 introduces the filtering problem in a generic form. In Section 3, discretization of the KS equation is discussed. The two versions of the proposed filter, non-iterative and iterative, are detailed (along with pseudo-codes) in Sections 4 and 5 respectively. Numerical illustrations are provided in Section 6 and, finally, the concluding remarks given in Section 7.

2. Statement of the Problem

Within a complete probability space $(\Omega, \mathcal{F}, P)$, supplied with an increasing filtration $\{\mathcal{F}_t, 0 \le t \le T_{\max}\}$ consisting of σ-subalgebras of $\mathcal{F}$, the system process model, typically represented as Ito stochastic differential equations (SDE-s), has the generic form

$$dX_t = b(X_t, t)dt + f(X_t, t)dB_t \tag{1}$$

for $t \in (t_{i-1}, t_i]$, i=1,2,3,… with $X_t := X(t) \in \mathbf{R}^n$ the (hidden) process vector, $b : \mathbf{R}^n \times \mathbf{R}_+ \mapsto \mathbf{R}^n$ the non-linear drift function, $f : \mathbf{R}^n \times \mathbf{R}_+ \mapsto \mathbf{R}^{n\times m}$ the diffusion matrix and $B_t \in \mathbf{R}^m$ an m-dimensional standard P-Brownian motion. Here $0 = t_0 < t_1 ... < t_i < ... < t_N = T_{\max}$ denotes an ordering of the time interval $(0, T_{\max}]$ of interest to facilitate a recursive numerical implementation of the stochastic filtering scheme. In contrast to the system process model, the measurement model is available typically in the algebraic form

$$Y_t = h(X_t, t) + \Delta\eta_t \tag{2a}$$

where $Y_t := Y(t) \in \mathbf{R}^q$ ($y_0 := 0$) is the noisy measurement process generating the sub-filtration $\mathcal{F}_t^Y$, $h : \mathbf{R}^n \times \mathbf{R}_+ \mapsto \mathbf{R}^q$ is the non-linear measurement function and $\Delta\eta_t = \eta_t - \eta_{i-1} \in \mathbf{R}^q$ a q-dimensional P-Brownian increment representing the measurement noise (assuming that the last measurement Y_{i-1} was sampled at t_{i-1}). An incremental form of the noise term $\Delta\eta_t$ is used in Eqn. (2a) so as to indicate its relative 'smallness' vis-à-vis $h(X_t, t)$, the measurement drift function. Since the nonlinear filtering (KS) equation demands SDE structures for both the system process and measurement models, we define a fictitious process $Y_t := Y(t)$ (with $Y_0 := 0$) so that the measurement equation over $(t_{i-1}, t_i]$ in terms of incremental Y_t is given by

$$\Delta Y_t := Y_t \Delta t = h(X_t, t)\Delta t + \Delta\eta_t \Delta t; \quad \Delta t = t - t_{i-1} \tag{2b}$$

Assuming the time step $\Delta t_i := t_i - t_{i-1}$ to be small, the above equation may be approximated as

$$\Delta Y_t \approx h(X_t, t)\Delta t + \Delta\eta_t \Delta t_i,$$

which corresponds to the SDE

$$dY_t \approx h(X_t, t)dt + \Delta t_i d\eta_t \tag{2c}$$

Note that the term $\Delta t \Delta\eta_t$ is of $O(\Delta t^{3/2})$ is of vis-à-vis the drift term $h(X_t, t)\Delta t \sim O(\Delta t)$. The above representation of the noise term is in keeping with the general scenario of the measurement noise being smaller than the measurement drift term by an order of magnitude in the mean square sense. The relative 'smallness' of the noise term is justifiable through the fact that most modern sensing devices used for data acquisition are very accurate with high signal-to-noise ratio. We now write $d\eta_t$ in terms of a standard P-Brownian increment $dW_t \in \mathbf{R}^q$ as $d\eta_t = \upsilon_t dW_t$ where $\upsilon_t := \upsilon(t)$ is a $q \times q$ dimensional matrix representing the measurement noise intensity. Defining $\boldsymbol{\sigma}_t = \upsilon_t \Delta t_i$ (the scaled measurement noise intensity), the measurement SDE is of the final form:

$$dY_t = h(X_t, t)dt + \boldsymbol{\sigma}_t dW_t \tag{3}$$

It is emphasized that, in implementing the new EnKS filter, $|\boldsymbol{\sigma}_t|$ need not actually be 'small' and that the noise term need not be Gaussian. Thus the measurement diffusion matrix could be of the form $\boldsymbol{\sigma}_t = \boldsymbol{\sigma}(X_t, t)$, a function of X_t. While the presentation to follow could also be adapted to non-Brownian (e.g. Poisson's) right continuous noise processes, we presently stick to the measurement SDE (3) so that we have a strictly continuous form of measurement filtration $\mathcal{F}_{t+}^Y = \mathcal{F}_t^Y$. Standard existence criteria [28] for weak solutions to the above SDEs are assumed. The purpose of stochastic filtering is then to arrive at the conditional (filtered) distribution of, say, a scalar-valued function $\phi(X_t)$, $\phi \in C_b^2$ (bounded and twice continuously differentiable), given the measurement history $\mathcal{F}_t^Y := \sigma\{Y_s \mid s \in (0,t]\}$. Thus the conditional estimate $\pi_t(\phi)$ is defined as the measure-valued process $E_P\left(\phi(X_t) \mid \mathcal{F}_t^Y\right)$ measurable with respect to $\mathcal{F}_t^Y$.

3. Discretization of the KS Equation

The filtered estimate $\pi_t(\phi)$ of $\phi(X_t)$, for $t \in (t_{i-1}, t_i]$, satisfies the KS equation (or the filtered martingale problem [29]):

$$\pi_t(\phi) = \pi_{i-1}(\phi) + \int_{t_{i-1}}^t \pi_s\left(\mathrm{L}_s(\phi)\right) ds + \sum_{\varsigma=1}^q \int_{t_{i-1}}^t \left\{\pi_s\left(\mathrm{M}_s^\varsigma(\phi)\right) - \pi_s\left(h^\varsigma(\cdot,s)\right)\pi_s(\phi)\right\} dI_s^\varsigma \tag{4}$$

$dI_t := \left\{dI_t^\varsigma\right\} = \left(\boldsymbol{\sigma}_t^T \boldsymbol{\sigma}_t\right)^{-1}\left\{dY_t - \pi_t(h)\,dt\right\}$ denotes the incremental innovation vector process and I_t^ς the ς th element of I. Here $\pi_{i-1}(\cdot) := \pi_{t_{i-1}}(\cdot)$ and L is the infinitesimal generator corresponding to the system process SDE (1) given by

$$\mathrm{L}_t(\phi(x)) := \mathrm{L}(\phi(x_t)) = \frac{1}{2}\sum_{\xi=1}^n \sum_{\eta=1}^n a^{\xi\eta}(x_t,t)\frac{\partial^2 \phi(x_t)}{\partial x_t^{\xi}\partial x_t^{\eta}} + \sum_{\xi=1}^n b^{\xi}(x_t,t)\frac{\partial \phi(x_t)}{\partial x_t^{\xi}}, \quad x_t = \left\{x_t^1,\ldots,x_t^n\right\}^T \in \mathbf{R}^n$$

$a := ff^T$ with $a^{\xi\eta}$ denoting the $(\xi,\eta)^{\text{th}}$ element of the matrix a. Similarly, b^ξ is the ξ^{th} element of the vector b. Moreover, we have $\mathrm{M}_t^\varsigma(\phi(x)) := \mathrm{M}^\varsigma(\phi(x_t)) = h^\varsigma(x_t,t)\phi(x_t)$, where h^ς, Y_t^ς are the ς^{th} elements of the vectors h and Y_t respectively. Indeed, Eqn. (4) may be interpreted as a weak form to determine the conditional measure $\pi_t(\cdot)$ with ϕ being a test function. The aim of a typical filtering method is to design a numerical scheme so that the innovation process is driven to a zero-mean martingale (corresponding to the diffusion term of the measurement SDE 3) through recursion over time t. This goal is often accomplished in two major stages, viz. prediction and update. In most MC filters, the prediction stage involves integrating the system process SDE (1) over $(t_{i-1}, t_i]$ starting with the realizations (particles) of the filtered solution at t_{i-1} as the initial conditions and hence this stage is often executed independent of (i.e. as a precursor to) the update stage. A similar strategy is adopted in developing the current filtering scheme as well. A first step in this direction would be to approximate the second term on the right hand side (RHS) of the KS Eqn. (4) as

$$\int_{t_{i-1}}^t \pi_s\left(\mathrm{L}_s(\phi)\right) ds \cong \pi_{i-1}\int_{t_{i-1}}^t \mathrm{L}_s(\phi)\, ds \tag{5}$$

Recall that Eqn. (4) is arrived at after averaging over the diffusion paths corresponding to the process noise B_t. Moreover, if the second term on the RHS of the KS Eqn. (4) is replaced by the approximation in Eqn. (5), then the first two terms (referred to as 'the prediction component') on the RHS of the KS equation, so approximated, recover Dynkin's formula for the predicted mean $E_P(\phi(X_t) \mid X(t_{i-1}) := X_{i-1})$ according to the process dynamics of Eqn. (1.1). By way of motivating the EnKS filter, a particle based representation (the unmasked form) of Eqn. (4) may be conceived of by putting back, in the prediction component, the diffusion term for the process dynamics. As a first step in deriving the unmasked additive update, as the current measurement Y_t (typically at $t = t_i$) is available, an MC setting for solving Eqn. (4) may be set up as

$$\pi'_t(\phi) = \pi'_{i-1}(\phi) + \int_{t_{i-1}}^t \pi'_s\left(\mathrm{L}(\phi)\right) dt + \sum_{\varsigma=1}^q \int_{t_{i-1}}^t \left\{\pi'_s\left(h^\varsigma\phi\right) - \pi'_s\left(h^\varsigma\right)\pi'_s(\phi)\right\} dI'^\varsigma_s \tag{6}$$

where $dI'_t := \left\{dI'^\varsigma_t\right\} = \left(\boldsymbol{\sigma}_t^T\boldsymbol{\sigma}_t\right)^{-1}\left\{dY_t - \pi'_t(h)\,dt\right\}$, $\pi'(\phi) = (1/N)\sum_{j=1}^N \phi^{(j)}$, is the ensemble-averaged approximation of the actual conditional estimate. Note that the bracketed superscript (j) over a random variable represents its j^{th} realization and that $\phi^{(j)} := \phi(X^{(j)})$. Let $\boldsymbol{\varphi} := (\phi^1,\ldots,\phi^{\hat{n}})^T$ be an $\hat{n}$ -

dimensional vector-valued function to be estimated via the filtering technique with $\phi^k(x_t) \in C_b^2$ for $k \in [1, \hat{n}]$; typically we have $\boldsymbol{\varphi}(x) := (x^1, ..., x^n)^T$ so that $\hat{n} = n$ and $\phi^k(x) = x^k$. Then an unmasked (particle based) representation of Eqn. (6) may be written as

$$\boldsymbol{\Phi}_t = \boldsymbol{\Phi}_{i-1} + \int_{t_{i-1}}^{t} \boldsymbol{\Psi}_s ds + \int_{t_{i-1}}^{t} d\boldsymbol{\Xi}_s + \frac{1}{N}\int_{t_{i-1}}^{t} \begin{Bmatrix} \boldsymbol{\Phi}_s \mathbf{H}_s{}^T \\ -\hat{\boldsymbol{\Phi}}_s \hat{\mathbf{H}}_s{}^T \end{Bmatrix} \left(\boldsymbol{\sigma}_s^T \boldsymbol{\sigma}_s\right)^{-1} \left\{ d\mathbf{Y}_s - \mathbf{H}_s ds \right\} \quad (7)$$

where $\boldsymbol{\Phi}_t := [\boldsymbol{\varphi}_t^{(1)}, ... \boldsymbol{\varphi}_t^{(N)}]$, $\boldsymbol{\Phi}_{i-1} := \boldsymbol{\Phi}_{t_{i-1}}$,

$\boldsymbol{\Psi}_t := [\mathrm{L}(\boldsymbol{\varphi}_t^{(1)}), ..., \mathrm{L}(\boldsymbol{\varphi}_t^{(N)})]$,

$d\boldsymbol{\Xi}_t := [\boldsymbol{\varphi}_t'^{(1)} f_t^{(1)} dB_t^{(1)}, ..., \boldsymbol{\varphi}_t'^{(N)} f_t^{(N)} dB_t^{(N)}]$,

$\mathbf{H}_t := [h_t^{(1)}, ..., h_t^{(N)}]$, $\hat{\boldsymbol{\Phi}}_t = [\pi_t'(\boldsymbol{\varphi}), ..., \pi_t'(\boldsymbol{\varphi})] \in \mathbf{R}^{n \times N}$,

$\hat{\mathbf{H}}_t = [\pi_t'(h), ..., \pi_t'(h)] \in \mathbf{R}^{q \times N}$

and $d\mathbf{Y}_t := [dY_t, ..., dY_t] \in \mathbf{R}^{q \times N}$. Note that the identical (column) vector elements of $\hat{\boldsymbol{\Phi}}_t$ and $\hat{\mathbf{H}}_t$ are respectively the ensemble-averaged $\boldsymbol{\varphi}$ and h respectively at the current time t. As a precursor to the rest of the derivation, it is convenient to recast Eqn. (7) as:

$$\boldsymbol{\Phi}_t = \boldsymbol{\Phi}_{i-1} + \int_{t_{i-1}}^{t} (\boldsymbol{\Psi}_s ds + d\boldsymbol{\Xi}_s) + \frac{1}{N}\int_{t_{i-1}}^{t} \begin{Bmatrix} \boldsymbol{\Phi}_s \mathbf{H}_s{}^T - \hat{\boldsymbol{\Phi}}_s \mathbf{H}_s{}^T \\ +\hat{\boldsymbol{\Phi}}_s \mathbf{H}_s{}^T - \hat{\boldsymbol{\Phi}}_s \hat{\mathbf{H}}_s{}^T \end{Bmatrix} \left(\boldsymbol{\sigma}_s^T \boldsymbol{\sigma}_s\right)^{-1} \left\{ d\mathbf{Y}_s - \mathbf{H}_s ds \right\} \quad (8)$$

A major hindrance in using Eqn. (8), an MC based unmasked representation of Eqn. (4), continues to be the problem of circularity in that the expectation of $\boldsymbol{\Phi}_t$ needs information on that of $\boldsymbol{\Phi}_t \mathbf{H}_t{}^T$, i.e. higher order expectations. This impedes a direct solution of the set of non-linear equations. Starting with Eqn. (8), an algorithm is devised in the next section to circumvent this problem.

4. The EnKS Methodology: A Non-iterative Form

Within the MC-setting used to address the problem of moment closure in Eqn. (8), a two-stage strategy is adopted in the proposed EnKS filter. First, for a given $t \in (t_{i-1}, t_i]$ in the current time interval, the process SDE (corresponding to the first three terms on the RHS of Eqn. (8)) is weakly solved using a numerical integration technique (e.g. Euler Maruyama (EM) [30], Milstein's scheme, local linearization [31, 32, 33] or stochastic Newmark [34] schemes etc.). In the second stage, an MC-based additive update term is derived using the fourth term on the RHS of Eqn. (8). Although an explicit EM scheme is considered here for numerical integration of the process SDEs, a more accurate/stable stochastic integration scheme could be adopted to enhance the reconstruction fidelity. Presently, using the explicit EM-based integration, the recursive prediction-update filtering strategy that aims at arriving at an empirical filtered distribution at time $t \in (t_{i-1}, t_i]$ is depicted below. In all the numerical work, however, we set $t = t_i$.

Prediction

$$\tilde{\boldsymbol{\Phi}}_t = \boldsymbol{\Phi}_{i-1} + \boldsymbol{\Psi}_{i-1}\Delta t + \Delta\boldsymbol{\Xi}_{i-1} \quad (9)$$

where, $\boldsymbol{\Psi}_{i-1} := \boldsymbol{\Psi}_{t_{i-1}}$, $\Delta t = t - t_{i-1}$

$$\Delta\boldsymbol{\Xi}_{i-1} := \Delta\boldsymbol{\Xi}_{t_{i-1}} = \begin{bmatrix} \boldsymbol{\varphi}_t'^{(1)} f_{i-1}^{(1)} \left(B_i^{(1)} - B_{i-1}^{(1)}\right), \\ ..., \boldsymbol{\varphi}_t'^{(N)} f_{i-1}^{(N)} \left(B_i^{(N)} - B_{i-1}^{(N)}\right) \end{bmatrix}$$

$f_{i-1} := f_{t_{i-1}}$, and $B_{i-1} := B_{t_{i-1}}$.

Additive Update

A time-discretized MC-form of the update equation, motivated by an EM-based approximation to the third term on the RHS of Eqn. (8), may be written as:

$$\boldsymbol{\Phi}_t = \tilde{\boldsymbol{\Phi}}_t + \frac{1}{N} \begin{Bmatrix} \left(\tilde{\boldsymbol{\Phi}}_t - \bar{\tilde{\boldsymbol{\Phi}}}_t\right) \tilde{\mathbf{H}}_t{}^T \\ +\bar{\tilde{\boldsymbol{\Phi}}}_t \left(\tilde{\mathbf{H}}_t{}^T - \bar{\tilde{\mathbf{H}}}_t{}^T\right) \end{Bmatrix} \left(\boldsymbol{\sigma}_t^T \boldsymbol{\sigma}_t\right)^{-1} \left\{ \Delta\mathbf{Y}_t - \tilde{\mathbf{H}}_t \Delta t \right\} \quad (10)$$

Here $\tilde{\mathbf{H}}_t := [\tilde{h}_t^{(1)}, ..., \tilde{h}_t^{(N)}] = [h^{(1)}(\tilde{X}_t), ..., h^{(N)}(\tilde{X}_t)]$ is the predicted ensemble of the measurement drift vectors. Recalling from Eqn. (2b) that $\Delta Y_t := Y_t \Delta t$, Eqn. (10) may be recast as:

$$\boldsymbol{\Phi}_t = \tilde{\boldsymbol{\Phi}}_t + \frac{1}{N} \begin{Bmatrix} \left(\tilde{\boldsymbol{\Phi}}_t - \bar{\tilde{\boldsymbol{\Phi}}}_t\right) \left(\tilde{\mathbf{H}}_t{}^T \Delta t\right) \\ +\left(\bar{\tilde{\boldsymbol{\Phi}}}_t \Delta t\right) \left(\tilde{\mathbf{H}}_t{}^T - \bar{\tilde{\mathbf{H}}}_t{}^T\right) \end{Bmatrix} \left(\boldsymbol{\sigma}_t^T \boldsymbol{\sigma}_t\right)^{-1} \left\{ \hat{\mathbf{Y}}_t - \tilde{\mathbf{H}}_t \right\} \quad (11)$$

where $\hat{\mathbf{Y}}_t = [Y_t, ..., Y_t] \in \mathbf{R}^{q \times N}$. Recall that while $\tilde{\boldsymbol{\Phi}}_t = [\tilde{\boldsymbol{\varphi}}_t^{(1)}, ..., \tilde{\boldsymbol{\varphi}}_t^{(N)}]$ contains the predicted particles within the ensemble, $\bar{\tilde{\boldsymbol{\Phi}}}_t$ is constructed using N identical column vectors of the ensemble-averaged prediction $\pi_t'(\tilde{\boldsymbol{\varphi}})$. In the initial stages of time evolution, when the innovation process could have a significant drift component owing to the measurement-prediction mismatch (i.e. a significant departure from a zero-mean martingale), the gain-type coefficient matrix

should be such (e.g. having a large norm) that the sample space is better explored. Keeping in mind that the temporal gradients of the evolving estimates have sharper gradients in this regime, one way to construct the gain-type coefficient matrix would be to incorporate information on these gradients through the previous estimates. Thus $\tilde{\mathbf{H}}_t \Delta t$ and $\tilde{\bar{\mathbf{\Phi}}} \Delta t$ may be approximated as:

$$\tilde{\mathbf{H}}_t \Delta t \approx \left(\tilde{\mathbf{H}}_t t - \tilde{\bar{\mathbf{H}}}_{i-1} t_{i-1} - \Delta \tilde{\bar{\mathbf{H}}}_t t \right) \tag{12}$$

$$\tilde{\bar{\mathbf{\Phi}}}_t \Delta t = \left(\tilde{\bar{\mathbf{\Phi}}}_t t - \tilde{\bar{\mathbf{\Phi}}}_{i-1} t_{i-1} \right) \tag{13}$$

where Ito's formula has been used in writing the approximation (12). Since this modification incorporates the filtered estimates at the previous time instant (t_{i-1}), it should be helpful in expediting filter convergence especially in regions of sample space far away from the converged solution. Thus we get;

$$\begin{aligned} \mathbf{\Phi}_t &= \tilde{\mathbf{\Phi}}_t \\ &+ \frac{1}{N} \left\{ \begin{array}{l} \left(\tilde{\mathbf{\Phi}}_t - \tilde{\bar{\mathbf{\Phi}}}_t \right) \left(\tilde{\mathbf{H}}_t^T t - \tilde{\bar{\mathbf{H}}}_{i-1}^T t_{i-1} - \Delta \tilde{\bar{\mathbf{H}}}_t^T t \right) \\ + \left(\tilde{\bar{\mathbf{\Phi}}}_t t - \tilde{\bar{\mathbf{\Phi}}}_{i-1} t_{i-1} - \Delta \tilde{\bar{\mathbf{\Phi}}}_t t \right) \left(\tilde{\mathbf{H}}_t^T - \tilde{\bar{\mathbf{H}}}_t^T \right) \end{array} \right\} \left(\boldsymbol{\sigma}_t^T \boldsymbol{\sigma}_t \right)^{-1} \left\{ \hat{\mathbf{Y}}_t - \tilde{\mathbf{H}}_t \right\} \end{aligned} \tag{14}$$

It may now be observed that, once the converged filtered estimate is available, the squared noise intensity term $\boldsymbol{\sigma}_t^T \boldsymbol{\sigma}_t$ may be replaced by the innovation covariance matrix $E_P \left(\left((Y_t - h_t) - \pi_t'(Y_t - h_t) \right) \left((Y_t - h_t) - \pi_t'(Y_t - h_t) \right)^T \right)$. However, away from the converged solution and especially during the initial stages of the filter evolution, the last covariance matrix (e.g. its norm) would typically be rather 'large'. Incorporation of this term, in lieu of $\boldsymbol{\sigma}_t^T \boldsymbol{\sigma}_t$ in Eqn. (14) would have the effect of artificially increasing the measurement noise in the initial stages, thereby enabling the diffusion term in the system process model to efficaciously explore the search space. In the MC setup that we have adopted, the innovation covariance matrix may be computed as:

$$\begin{aligned} & E_P \left(\left((Y_t - h_t) - \pi_t'(Y_t - h_t) \right) \left((Y_t - h_t) - \pi_t'(Y_t - h_t) \right)^T \right) \\ &= \frac{1}{N-1} \left(\tilde{\mathbf{H}}_t^T - \tilde{\bar{\mathbf{H}}}_t^T \right) \left(\tilde{\mathbf{H}}_t - \tilde{\bar{\mathbf{H}}}_t \right) \end{aligned}$$

Finally, introducing a scalar parameter $0 < \alpha < 1$, $\left(\boldsymbol{\sigma}_t^T \boldsymbol{\sigma}_t \right)^{-1}$ in Eqn. (14) is replaced by

$$\left(\alpha \frac{1}{N-1} \left(\tilde{\mathbf{H}}_t^T - \tilde{\bar{\mathbf{H}}}_t^T \right) \left(\tilde{\mathbf{H}}_t - \tilde{\bar{\mathbf{H}}}_t \right) + (1-\alpha) \left(\boldsymbol{\sigma}_t^T \boldsymbol{\sigma}_t \right) \right)^{-1}$$

Eqn. (14) thus takes the form:

$$\begin{aligned} \mathbf{\Phi}_t &= \tilde{\mathbf{\Phi}}_t \\ &+ \frac{1}{N} \left\{ \begin{array}{l} \left(\tilde{\mathbf{\Phi}}_t - \tilde{\bar{\mathbf{\Phi}}}_t \right) \left(\tilde{\mathbf{H}}_t^T t - \tilde{\bar{\mathbf{H}}}_{i-1}^T t_{i-1} - \Delta \tilde{\bar{\mathbf{H}}}_t^T t \right) \\ + \left(\tilde{\bar{\mathbf{\Phi}}}_t t - \tilde{\bar{\mathbf{\Phi}}}_{i-1} t_{i-1} \right) \left(\tilde{\mathbf{H}}_t^T - \tilde{\bar{\mathbf{H}}}_t^T \right) \end{array} \right\} \\ & \left\{ \alpha \frac{1}{N-1} \left(\tilde{\mathbf{H}}_t - \tilde{\bar{\mathbf{H}}}_t \right) \left(\tilde{\mathbf{H}}_t^T - \tilde{\bar{\mathbf{H}}}_t^T \right) \right\}^{-1} \\ & \left\{ + (1-\alpha) \boldsymbol{\sigma}_t^T \boldsymbol{\sigma}_t \right\} \left\{ \hat{\mathbf{Y}}_t - \tilde{\mathbf{H}}_t \right\} \end{aligned} \tag{15}$$

A more concise form of the update equation may be written as:

$$\mathbf{\Phi}_t = \tilde{\mathbf{\Phi}}_t + \tilde{\mathbf{G}}_t \left\{ \hat{\mathbf{Y}}_t - \tilde{\mathbf{H}}_t \right\} \tag{16}$$

where

$$\begin{aligned} \tilde{\mathbf{G}}_t \coloneqq & \frac{1}{N} \left\{ \begin{array}{l} \left(\tilde{\mathbf{\Phi}}_t - \tilde{\bar{\mathbf{\Phi}}}_t \right) \left(\tilde{\mathbf{H}}_t^T t - \tilde{\bar{\mathbf{H}}}_{i-1}^T t_{i-1} - \Delta \tilde{\bar{\mathbf{H}}}_t^T t \right) \\ + \left(\tilde{\bar{\mathbf{\Phi}}}_t t - \tilde{\bar{\mathbf{\Phi}}}_{i-1} t_{i-1} \right) \left(\tilde{\mathbf{H}}_t^T - \tilde{\bar{\mathbf{H}}}_t^T \right) \end{array} \right\} \\ & \left\{ \alpha \frac{1}{N-1} \left(\tilde{\mathbf{H}}_t - \tilde{\bar{\mathbf{H}}}_t \right) \left(\tilde{\mathbf{H}}_t^T - \tilde{\bar{\mathbf{H}}}_t^T \right) \right\}^{-1} \\ & \left\{ + (1-\alpha) \boldsymbol{\sigma}_t^T \boldsymbol{\sigma}_t \right\} \end{aligned}$$

In line with the traditional stochastic filtering terminology (e.g. the Kalman filter), the update term may be thought of as an innovation term $\mathbf{I}_t \coloneqq \left\{ \hat{\mathbf{Y}}_t - \tilde{\mathbf{H}}_t \right\}$, weighted by the gain-type coefficient matrix $\tilde{\mathbf{G}}_t$. A pseudo-code for the non-iterative EnKS is provided below.

Pseudo-code 1: for the non-iterative EnKS

1. Discretize the time interval of interest, say $[0, T]$, using a partition $\{t_0, t_1, ..., t_M\}$ such that $0 = t_0 < t_1 < ... < t_M = T$ and $t_i - t_{i-1} = \Delta t_i$ ($= \frac{1}{M}$ if the step size is chosen uniformly for $i = 0, ..., M-1$). Choose an ensemble size *N*.
2. Generate the ensemble of initial conditions $\left\{ \boldsymbol{\varphi}_0^{(j)} \right\}_{j=1}^N$, , or equivalently $\left\{ X_0^{(j)} \right\}_{j=1}^N$, for the system state vector. For each discrete time instant $t_i, i = 1, ..., M-1$, execute the following steps.
3. *Prediction*
   Using $\left\{ \boldsymbol{\varphi}_{i-1}^{(j)} \right\}_{j=1}^N$, the update available at the last time instant t_{i-1}, propagate each particle to the current time instant t_i using any appropriate integration scheme for SDEs, e.g. an explicit Euler-Maruyama (EM) approximation to Eqn. (1) given by:

$$\tilde{\boldsymbol{\varphi}}_i^{(j)} = \boldsymbol{\varphi}_{i-1}^{(j)} + \mathrm{L}(\boldsymbol{\varphi}_{i-1}^{(j)}) \Delta t_i + \boldsymbol{\varphi}_{i-1}'^{(j)} f_{i-1}^{(j)} \left(B_i^{(N)} - B_{i-1}^{(j)} \right)$$
$$, \quad j = 1, ..., N$$

Using $\left\{\tilde{\boldsymbol{\varphi}}_i^{(j)}\right\}_{j=1}^N$ compute $\left\{\tilde{X}_i^{(j)}\right\}_{j=1}^N$. This step is trivial if $\boldsymbol{\varphi}$ is the identity function $\boldsymbol{\varphi}(X)=X$.

Using $\left\{\tilde{X}_i^{(j)}\right\}_{j=1}^N$, compute $\left\{\tilde{h}_i^{(j)}\right\}_{j=1}^N = \left\{h\left(\tilde{X}_i^{(j)}\right)\right\}_{j=1}^N$.

Construct $\tilde{\boldsymbol{\Phi}}_i \coloneqq [\tilde{\boldsymbol{\varphi}}_i^{(1)},...\tilde{\boldsymbol{\varphi}}_i^{(N)}]$

$\hat{\tilde{\boldsymbol{\Phi}}}_i = [\pi_i'(\tilde{\boldsymbol{\varphi}}),...,\pi_i'(\tilde{\boldsymbol{\varphi}})]$,

$\tilde{\mathbf{H}}_i \coloneqq [\tilde{h}_i^{(1)},...,\tilde{h}_i^{(N)}]$, $\hat{\tilde{\mathbf{H}}}_i = [\pi_i'(\tilde{h}),...,\pi_i'(\tilde{h})]$

4. *Additive update*

Choose $\alpha \in (0,1)$; a typical prescribed value would be $\alpha \approx 0.8$, even though the method also performs well for other values in the interval indicated.

Update each particle as

$$\boldsymbol{\varphi}_i^{(j)} = \tilde{\boldsymbol{\varphi}}_i^{(j)} + \tilde{\mathbf{G}}_i\left\{\boldsymbol{Y}_i - \tilde{h}_i^{(j)}\right\},\ j=1,...,N$$

where

$$\tilde{\mathbf{G}}_i \coloneqq \frac{1}{N}\left\{\begin{matrix}\left(\tilde{\boldsymbol{\Phi}}_i - \hat{\tilde{\boldsymbol{\Phi}}}_i\right)\left(\tilde{\mathbf{H}}_i{}^T t_i - \hat{\tilde{\mathbf{H}}}_{i-1}{}^T t_{i-1} - \Delta\hat{\tilde{\mathbf{H}}}_i{}^T t_i\right)\\ +\left(\hat{\tilde{\boldsymbol{\Phi}}}_i t_i - \hat{\tilde{\boldsymbol{\Phi}}}_{i-1} t_{i-1}\right)\left(\tilde{\mathbf{H}}_i{}^T - \hat{\tilde{\mathbf{H}}}_i{}^T\right)\end{matrix}\right\}$$
$$\left\{\begin{matrix}\alpha\frac{1}{N-1}\left(\tilde{\mathbf{H}}_i - \hat{\tilde{\mathbf{H}}}_i\right)\left(\tilde{\mathbf{H}}_i{}^T - \hat{\tilde{\mathbf{H}}}_i{}^T\right)\\ +(1-\alpha)\boldsymbol{\sigma}_i{}^T\boldsymbol{\sigma}_i\end{matrix}\right\}^{-1}$$

5. If $i < M$, go to step 3 with $i = i+1$, else terminate the algorithm.

Using a filtered martingale problem setup, the existence and uniqueness of a posterior distribution satisfying the KS equation has been proved in [29] under very general conditions on the drift and diffusion fields of the system process and measurement SDEs. However, since we presently adopt Ito's theory in interpreting the weak solutions of the SDEs, somewhat more restrictive conditions, e.g. Lipschitz continuity and linear growth bound, are applied to the drift and diffusion terms.

5. An Iterative Version of the EnKS

A motivation in developing an iterative version of the EnKS is derived from the fact that iterations provide an attractive, and sometimes indispensable, tool for an update procedure involving nonlinearities, e.g. those present in the system process and/or measurement models. While the additive nature of particle updates in the EnKS eliminates the curse of 'particle collapse', an iterative form could additionally help precipitate a faster convergence of the measurement-prediction mismatch to a zero-mean martingale. In other words, using an inner layer of iterations, one could attempt a 'maximal' utilization of the current measurement within the particle update before moving over to the next time step. In order to provide an additional boost to the mixing property of the update kernel, an annealing-type non-decreasing sequence of scalar multipliers $\{\beta_0, \beta_1, ..., \beta_{\kappa-1}\}$ is artificially applied to the iterated sequence of gain-weighted innovation terms. Here κ denotes the number of inner iterations at the current time t. The sequence $\{\beta_0, \beta_1, ..., \beta_{\kappa-1}\}$ is so chosen that $\beta_\kappa \to 1$ as $\kappa \to \infty$ (to approach the original update term) and $\beta_k \le \beta_{k+1}$ for $k \in [0, \kappa-1)$. Effect of the annealing type term is similar to the temperature (herein proportional to $1/\beta_k$) in a standard simulated annealing (SA) scheme [35]. The added advantage we have over SA based schemes, is that, unlike SA where a single Markov chain is evolved and $1/\beta_k$ is slowly reduced to unity, in the present setting, an ensemble of pseudo-chains is propagated simultaneously, for a given t, allowing us to have a much faster and flexible reduction. Presently an exponential increment, $\beta_k = \exp(k+1-\kappa), k = 0,...,\kappa-1$ which is a more non-conservative schedule, is adopted. At a given time t, to initiate the inner iteration, an initial annealing term is required, for which, typically a 'large' value of $1/\beta_k$ is taken. Although the filtered estimate asymptotically improves with increasing number of κ, at a given t, keeping in mind the computational feasibility, only a few iterations (say, $\kappa = 10$) may be prescribed for a sufficiently large class of problems. With the convention $\left\{\boldsymbol{\varphi}_{t,0}^{(j)}\right\}_{j=1}^N \coloneqq \left\{\tilde{\boldsymbol{\varphi}}_t^{(j)}\right\}_{j=1}^N$ and $\left\{h_{t,0}^{(j)}\right\}_{j=1}^N \coloneqq \left\{\tilde{h}_t^{(j)}\right\}$ a generic form of the iterative update may be given as:

$$\boldsymbol{\Phi}_{t,k} = \boldsymbol{\Phi}_{t,k-1} + \beta_{k-1}\mathbf{G}_{t,k-1}\left\{\hat{\mathbf{Y}}_t - \mathbf{H}_{t,k-1}\right\},\ k = 1,...,\kappa \quad (17)$$

where

$$\mathbf{G}_{t,k} \coloneqq \frac{1}{N}\left\{\begin{matrix}\left(\boldsymbol{\Phi}_{t,k} - \hat{\boldsymbol{\Phi}}_{t,k}\right)\left(\mathbf{H}_{t,k}{}^T t - \hat{\mathbf{H}}_{i-1}{}^T t_{i-1} - \Delta\hat{\mathbf{H}}_{t,k}{}^T t\right)\\ +\left(\hat{\boldsymbol{\Phi}}_{t,k} t - \hat{\boldsymbol{\Phi}}_{i-1} t_{i-1}\right)\left(\mathbf{H}_{t,k}{}^T - \hat{\mathbf{H}}_{t,k}{}^T\right)\end{matrix}\right\}$$
$$\left\{\begin{matrix}\alpha\frac{1}{N-1}\left(\mathbf{H}_{t,k} - \hat{\mathbf{H}}_{t,k}\right)\left(\mathbf{H}_{t,k}{}^T - \hat{\mathbf{H}}_{t,k}^T\right)\\ +(1-\alpha)\boldsymbol{\sigma}_t{}^T\boldsymbol{\sigma}_t\end{matrix}\right\}^{-1}$$

$$\hat{\boldsymbol{\Phi}}_{t,k} = [\pi'_{t,k}(\boldsymbol{\varphi}),...,\pi'_{t,k}(\boldsymbol{\varphi})],\quad \pi'_{t,k}(\boldsymbol{\varphi}) \coloneqq \frac{1}{N}\sum_{j=1}^N \boldsymbol{\varphi}_{t,k}^{(j)},$$

$$\mathbf{H}_{t,k} \coloneqq [h_{t,k}^{(1)},...,h_{t,k}^{(N)}] \text{ and } \hat{\mathbf{H}}_{t,k} = [\pi'_{t,k}(h),...,\pi'_{t,k}(h)]$$

Given below is a pseudo-code for the iterative updates.

Pseudo-code 2: for the iterative EnKS

1. Follow steps 1:3 in pseudo-code 1.
   Set $k=1$ and choose κ. Compute $\beta_0 = \exp(1-\kappa)$.
2. (Iterative update)
   Using $\left\{\boldsymbol{\varphi}_{i,k-1}^{(j)}\right\}_{j=1}^{N}$ compute $\left\{X_{i,k-1}^{(j)}\right\}$.
   Using $\left\{X_{i,k-1}^{(j)}\right\}$ compute .
   $\left\{h_{i,k-1}^{(j)}\right\}_{j=1}^{N} = \left\{h\left(X_{i,k-1}^{(j)}\right)\right\}_{j=1}^{N}$.
   Compute $\boldsymbol{\Phi}_{i,k-1} := [\boldsymbol{\varphi}_{i,k-1}^{(1)},...\boldsymbol{\varphi}_{i,k-1}^{(N)}]$,

$$\pi'_{i,k-1}(\boldsymbol{\varphi}) := \frac{1}{N}\sum_{j=1}^{N}\boldsymbol{\varphi}_{i,k-1}^{(j)}$$

$$\widehat{\boldsymbol{\Phi}}_{i,k-1} = [\pi'_{i,k-1}(\boldsymbol{\varphi}),...,\pi'_{i,k-1}(\boldsymbol{\varphi})],$$

$$\mathbf{H}_{i,k-1} := [h_{i,k-1}^{(1)},...,h_{i,k-1}^{(N)}],$$

$$\pi'_{i,k-1}(h) := \frac{1}{N}\sum_{j=1}^{N}h_{i,k-1}^{(j)},$$

$$\widehat{\mathbf{H}}_{i,k-1} = [\pi'_{i,k-1}(h),...,\pi'_{i,k-1}(h)].$$

   Update each particle as

$$\boldsymbol{\varphi}_{i,k}^{(j)} = \boldsymbol{\varphi}_{i,k-1}^{(j)} + \beta_{k-1}\mathbf{G}_{i,k-1}\left\{Y_i - h_{i,k-1}^{(j)}\right\},\ j=1,...,N$$

$$\mathbf{G}_{i,k-1} := \frac{1}{N}\left\{\begin{matrix}\left(\boldsymbol{\Phi}_{i,k-1}-\widehat{\boldsymbol{\Phi}}_{i,k-1}\right)\begin{pmatrix}\mathbf{H}_{i,k-1}{}^{T}t_i - \widehat{\mathbf{H}}_{i-1}{}^{T}t_{i-1}\\ -\Delta\widehat{\mathbf{H}}_{i,k-1}{}^{T}t_i\end{pmatrix}\\ +\left(\widehat{\boldsymbol{\Phi}}_{i,k-1}t_i - \widehat{\boldsymbol{\Phi}}_{i-1}t_{i-1}\right)\left(\mathbf{H}_{i,k-1}{}^{T} - \widehat{\mathbf{H}}_{i,k-1}{}^{T}\right)\end{matrix}\right\}$$
$$\left\{\begin{matrix}\alpha\frac{1}{N-1}\left(\mathbf{H}_{i,k-1}-\widehat{\mathbf{H}}_{i,k-1}\right)\left(\mathbf{H}_{i,k-1}{}^{T}-\widehat{\mathbf{H}}_{i,k-1}{}^{T}\right)\\ +(1-\alpha)\boldsymbol{\sigma}_i{}^{T}\boldsymbol{\sigma}_i\end{matrix}\right\}^{-1}$$

3. Set $k=k+1$. If $k<\kappa$, set $\beta_k = \exp(k+1-\kappa)$ and go to step 2;
   else if $i<M$, go to step 3 in *pseudo-code 1* with $i=i+1$;
   else terminate the algorithm.
   Based on the notion of stochastic Picard's iterations often used to prove the existence and uniqueness of solutions to SDEs, the existence and uniqueness of solution (i.e. the conditional posterior distribution) via the proposed iterative scheme may be proved (out of the scope of the current work).

6. Numerical Illustrations

6.1 Example 1: Dynamical system identification via a 200-dimensional nonlinear filtering problem

For the state-parameter estimation of a 50 degrees-of-freedom (DOFs) mechanical oscillator, the system model (herein correspondent to a 50-storied shear frame with uncertain damping and stiffness parameters) is considered to be of the form:

$$\ddot{U}(t) + [\mathrm{C}]\dot{U}(t) + [\mathrm{K}]U(t) = R(t) + f\dot{B}_t$$

U, $\dot{U} \in \mathbf{R}^{50}$ respectively denote the displacement and velocity vectors and scalar components define the corresponding quantities for different floors of the frame. The stiffness matrix is given as

$$[\mathrm{K}] = \begin{bmatrix} \mathrm{K}_1+\mathrm{K}_2 & -\mathrm{K}_2 & 0 & ... & 0 \\ -\mathrm{K}_2 & \mathrm{K}_2+\mathrm{K}_3 & -\mathrm{K}_3 & ... & 0 \\ 0 & -\mathrm{K}_3 & \mathrm{K}_3+\mathrm{K}_4 & ... & 0 \\ ... & ... & ... & ... & -\mathrm{K}_{50} \\ 0 & 0 & 0 & -\mathrm{K}_{50} & \mathrm{K}_{50} \end{bmatrix}$$

The viscous damping matrix $[\mathrm{C}]$ is similarly obtained by replacing K_i by C_i in the above matrix, where K_i and C_i are respectively the stiffness and damping parameters corresponding to the i^{th} floor of the frame. $R(t) := \{r_i(t)\}_{i=1}^{n=50}$ is a random forcing vector with the transverse forcing at the i^{th} floor given as $r_i(t) = 500\exp(-t)\,|\,\xi\,|\cos(5t)$ where $\xi \sim N(0,1)$. The aim is to estimate the stiffness and damping coefficients as well as the velocity and displacement states, conditioned only on all the measured velocity components. Note that the present filtering problem is strictly nonlinear as the unknown parameters are taken as augmented states, i.e. the augmented state vector is given by [36; 27]:

$$X := \left\{U^T; \dot{U}^T; \{K_1,...,K_{50}\}^T; \{C_1,...,C_{50}\}^T\right\} \in \mathbf{R}^{200}$$

Indeed the system process model would have been linear if the parameters were known. PFs are likely to diverge or collapse to a single particle for such a large dimensional state-parameter estimation problem with sparse data. Moreover, even for low dimensional problems, PFs may perform poorly with very low-intensity measurement noises, currently employed to reduce random fluctuations in the estimates due to large variance in the measurement noise. To demonstrate the performance of the proposed filter with low measurement noise levels (possible with sophisticated

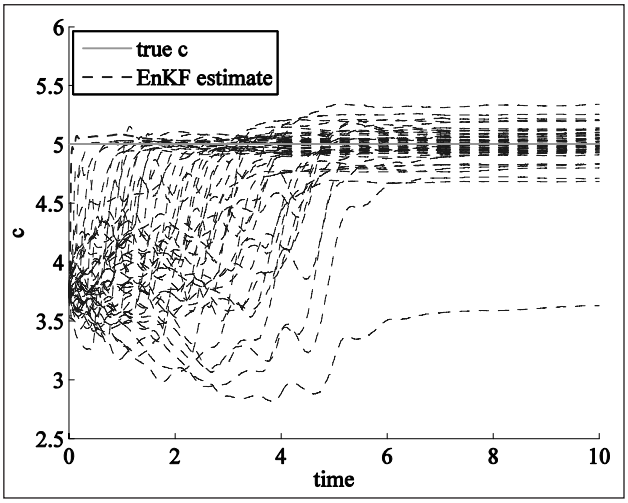

Figure 6.1 (a): Estimates of the damping parameters (C) by EnKF

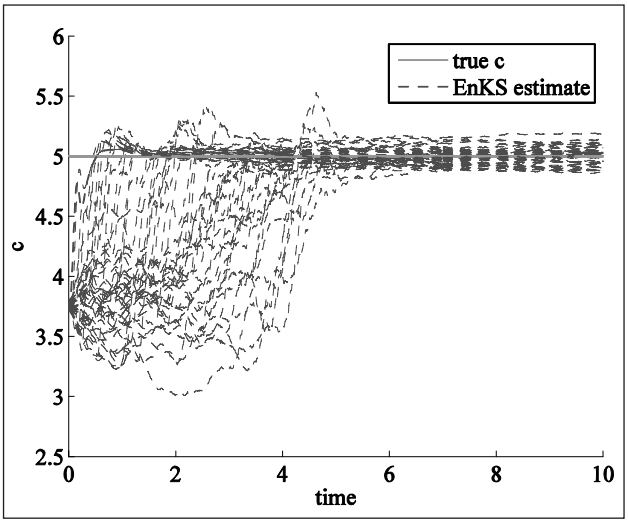

Figure 6.1 (b): Estimates of the damping parameters (C) by EnKS

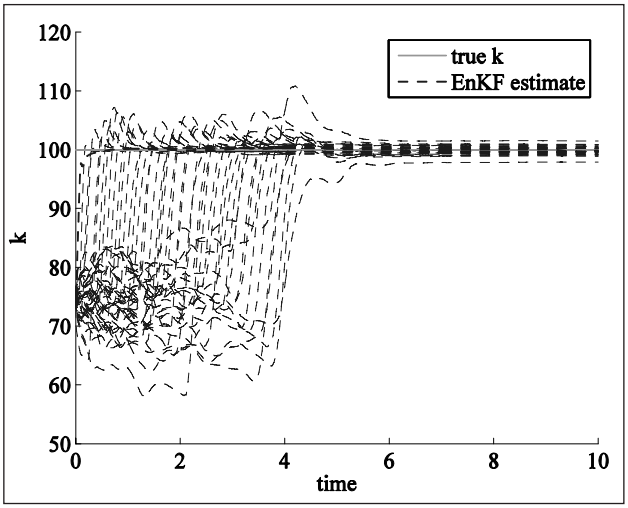

Figure 6.1 (c): Estimates of stiffness parameters (K) by EnKF

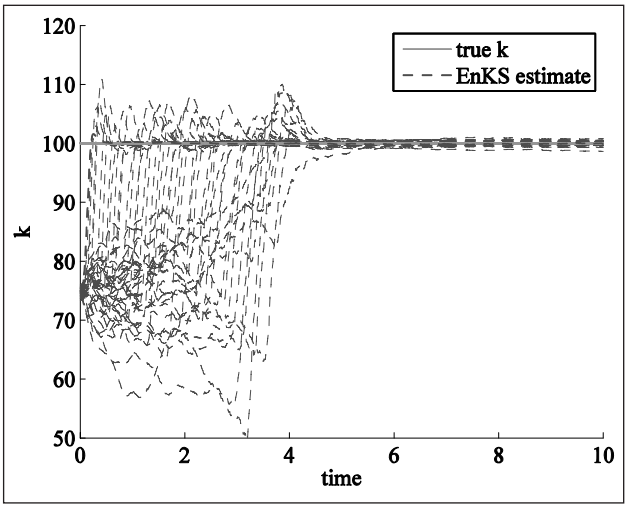

Figure 6.1 (d): Estimates of stiffness parameters (K) by EnKS

measuring devices), very low measurement noise intensity (less than 1%) is considered here for all the 50 components of the measured velocity vector. Since the EnKF (the ensemble Kalman filter as developed and implemented in [20]), is known to work for large dimensional filtering problems, it is used to report the numerical comparisons. An ensemble size $N = 800$ and time step $\Delta t = 0.01$ are taken for both the filters.

The reference stiffness parameters (used to integrate the system process *en route* to the generation of synthetic data by perturbing the computed solutions with appropriate noise) at each degree of freedom is taken as k = 100. Similarly the reference damping parameter at each floor is chosen as c = 5. It may be observed from Figure 6.1 that the EnKF underperforms in comparison to the EnKS and the iterative EnKS (the results via the iterative EnKS are found to be very much similar to those via its non-iterative variant and hence are not reported). Note that the simultaneous adoption of a large system dimension and low measurement noise ensures that the current identification problem is a difficult one.

6.2 Example 2: Damage detection for a 20-DOF mechanical oscillator

Consider once more the oscillator model for a shear frame, albeit of a lower dimension corresponding to 20 DOFs, so that the system model is formally given by:

$$\ddot{X}(t) + [\mathrm{C}]\dot{X}(t) + [\mathrm{K}]X(t) = R(t) + f\dot{B}_t \tag{6.2}$$

Thus the stiffness matrix is given as

$$[\mathrm{K}]=\begin{bmatrix} \mathrm{K}_1+\mathrm{K}_2 & -\mathrm{K}_2 & 0 & \ldots & 0 \\ -\mathrm{K}_2 & \mathrm{K}_2+\mathrm{K}_3 & -\mathrm{K}_3 & \ldots & 0 \\ 0 & -\mathrm{K}_3 & \mathrm{K}_3+\mathrm{K}_4 & \ldots & 0 \\ \ldots & \ldots & \ldots & \ldots & \ldots \\ 0 & 0 & 0 & -\mathrm{K}_{20} & \mathrm{K}_{20} \end{bmatrix}$$

and the viscous damping matrix $[\mathrm{C}]$ is obtained by replacing K_i by C_i in the above matrix. As before, $R(t) := \{r_i(t)\}_{i=1}^{n=20}$ is a random forcing vector whose i-th element, $r_i(t) = 500\exp(-t)|\xi|\cos(5t)$ where $\xi \sim N(0,1)$, denotes the transverse loading at the i-th storey. While the aim remains to estimate the stiffness and damping coefficients along with the velocity/displacement states (conditioned on only the measured velocities of the floors), the reference stiffness parameter K_{10} is kept at a slightly lower

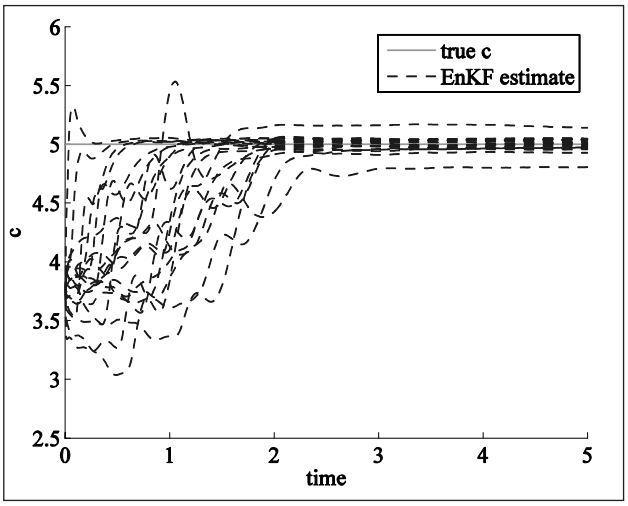

Figure 6.2 (a): Estimates of the damping parameters (C) by EnKF

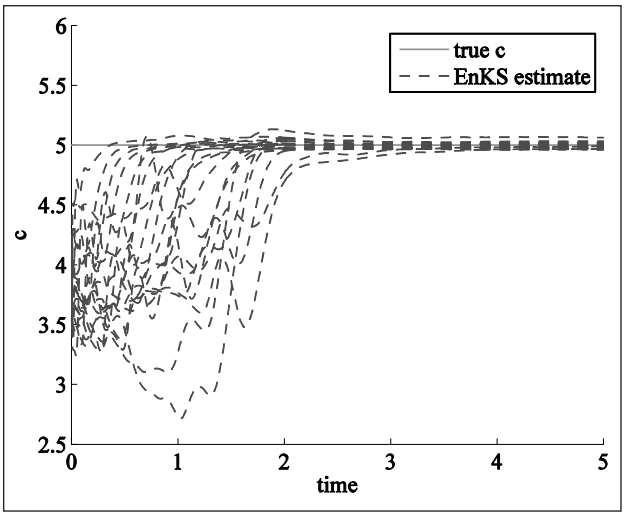

Figure 6.2 (b): Estimates of the damping parameters (C) by EnKS

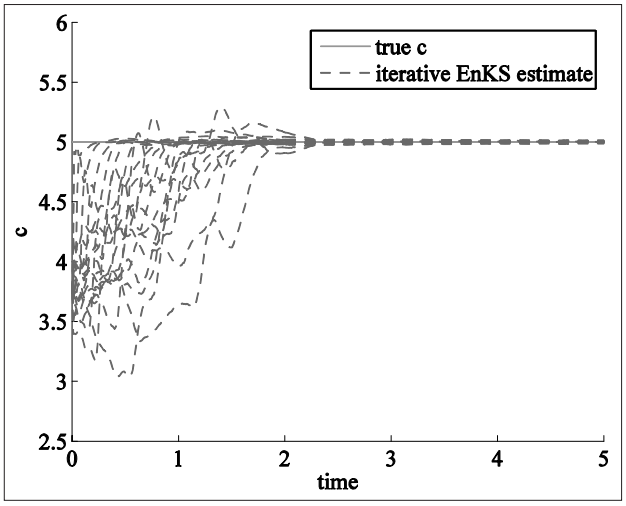

Figure 6.2 (c): Estimates of the damping parameters (C) by iterative EnKS

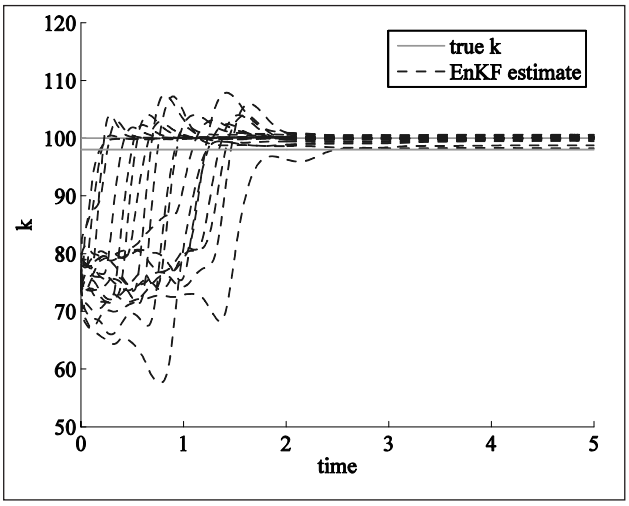

Figure 6.2 (d): Estimates of the stiffness parameters (K) by EnKF

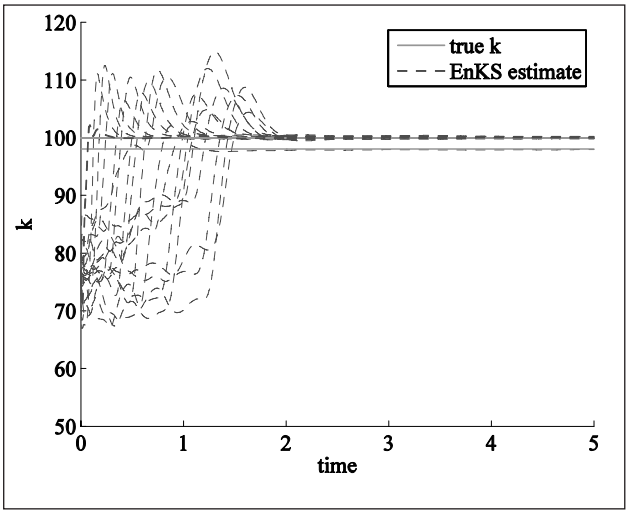

Figure 6.2 (e): Estimates of the stiffness parameters (K) by EnKS

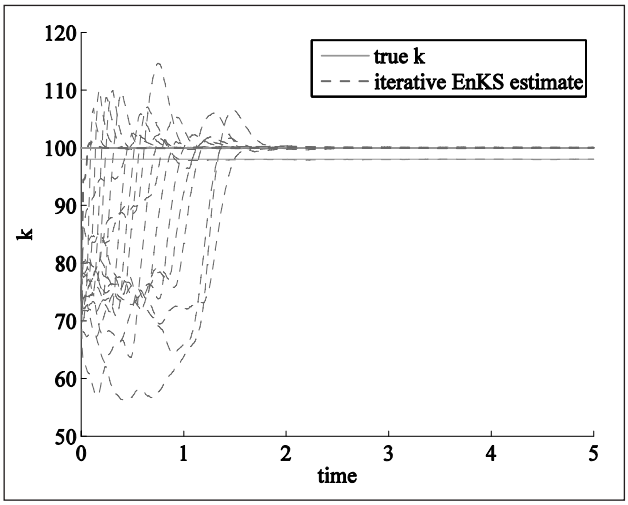

Figure 6.2 (f): Estimates of the stiffness parameters (K) by iterative EnKS

value vis-à-vis the rest $\{K_m \mid m \in [1,20]\} \setminus \{K_{10}\}$. This is a simple representation of a slightly reduced load-carrying capacity at the 10th floor, thereby indicating incipient damage/degradation. Specifically, we take $K_{10} = 98$ even as the rest of the stiffness parameters are maintained at 100. Damping parameter at each floor is chosen as 5. Here the augmented state vector is 80-dimensional and, as in the last example, a low noise intensity (< 1%) is applied in generating the data. An ensemble size of $N = 300$ and time step $\Delta t = 0.01$ are taken for both the EnKF and EnKS filter runs.

A relatively poorer performance of the EnKF in comparison with the EnKS is evident from the estimation results plotted in Figure 6.2. EnKF not only fails to detect the incipient damage (Figures 6.2d, 6.2e), but also yields the estimation of the damping coefficients with poorer resolution (Figures 6.2a – 6.2c). Moreover, as anticipated, the iterative EnKS (broken magenta), performs better than the non-iterative EnKS (broken red) even though the contrast in performance between the two variants is never quite striking. Hence, in the last two examples to follow, only the non-iterative version of the proposed filter is made use of.

6.3 Example 3: Identifying a nonlinear oscillator with nonlinear measurement

Strictly speaking, the EnKF [20] is not quite suited to treating nonlinearity in the measurement model. However, in practice, variants of the EnKF have indeed been applied to filtering problems involving nonlinear measurement models. One thus anticipates a sharper performance contrast between the EnKF and the EnKS in such cases, even if the dimension of the filtering problem were smaller. This point is currently emphasized through a problem of estimating state and parameters of a 1-DOF nonlinear oscillator model, wherein a transducer supplied at the base measures the reaction transferred there (Figure 6.3a).

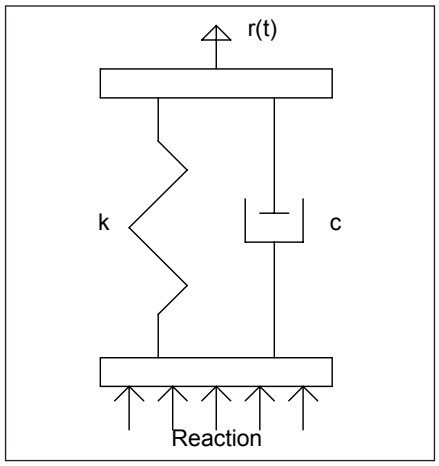

Figure 6.3 (a): A nonlinear oscillator; reaction transferred at the base is measured

The system process and measurement models are respectively given as:

$$\ddot{X}_t + c\dot{X}_t + k\sin(X_t) = r(t) + f\dot{B}_t \tag{18}$$

$$y_t = c\dot{X}_t + k\sin(X_t) + \Delta\eta_t \tag{19}$$

Displacement (X_t), velocity ($\dot{X}_t$), damping (c) and stiffness (k) are estimated using an ensemble size $N = 600$ and time step $\Delta t = 0.01$. A random force $r(t) := 5\exp(-0.01t) \mid \xi \mid \cos(5t)$, $\xi \sim N(0,1)$, is applied at the free end of the oscillator. An assessment of the estimates, reproduced in Figures 6.3b-d, readily reveals a degraded EnKF performance (broken blue), especially in estimating the viscous damping parameter.

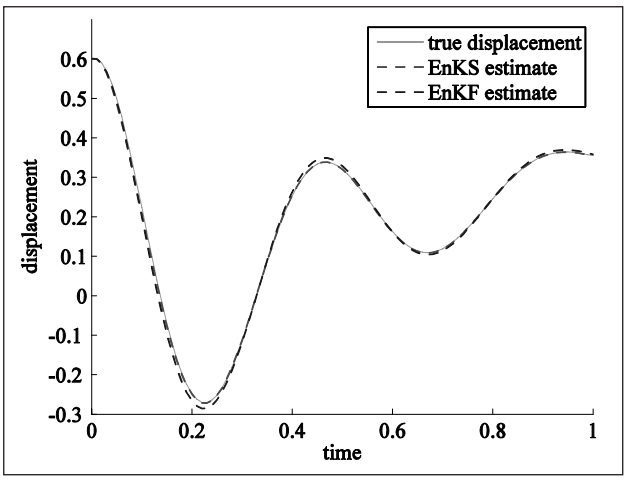

Figure 6.3 (b): Estimate of displacement

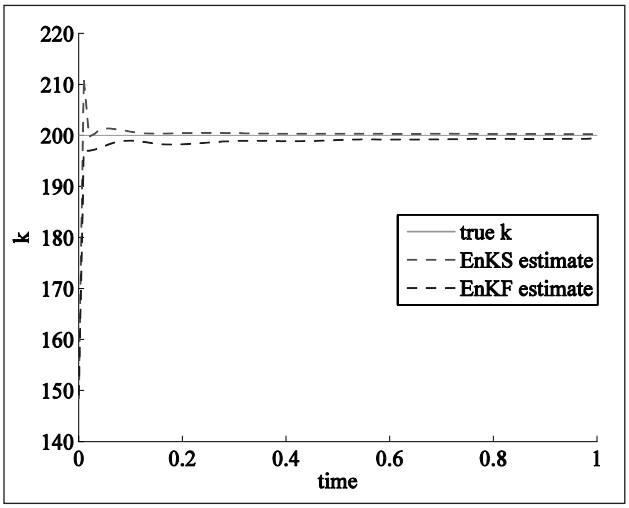

Figure 6.3 (c): Estimate of k

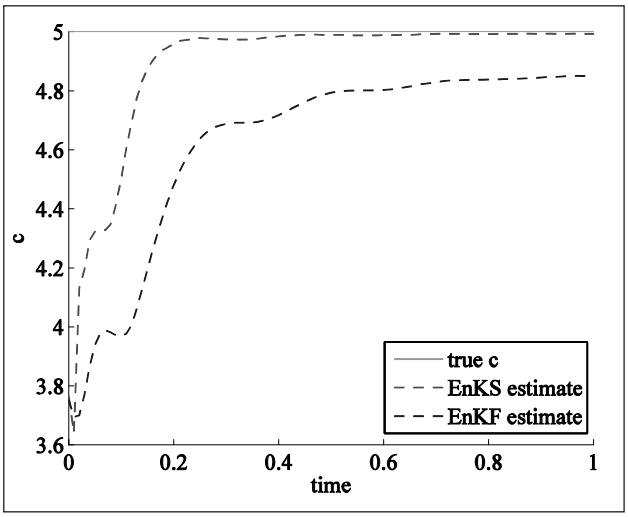

Figure 6.3 (d): Estimate of c

7. Conclusions

The nonlinear and additive particle update in the proposed EnKS, derived through consistent ensemble and time discretizations of the Kushner-Stratonovich SPDE, is essentially aimed at alleviating some of the prominent numerical bottlenecks characteristic of weight-based updates in particle filters. An efficient implementation of the update is made possible through several manipulations on the discretized innovation integral designed to efficiently drive the measurement-prediction misfit to a zero-mean martingale, herein characterized by an Ito integral. Arguably, the most notable development of this work is the non-iterative version of the EnKS that is shown to work quite accurately for nonlinear filtering problems of large dimension and involving sparse data with possibly low measurement noise intensity. This is the regime where a particle filter typically fails to perform. Motivated by the stochastic Picard iteration and implemented using annealing-type inner iterates, an iterative version of the EnKS is also synthesized which, though computationally more intensive, is able to achieve still higher accuracy in the computed estimates. A reflection of the nonlinear nature of the update is in the demonstrably superior performance of both variants of the EnKS over the well known ensemble Kalman filter.

The structure of the EnKS, which shares the familiar gain-based update features of the popular Kalman filter, makes it ideal for nonlinear filtering applications with feedback control. Finally, consistent with the operator-theoretic martingale problem setting as originated by Stroock and Varadhan [37], the EnKS admits a far more general class of non-smooth drift and diffusion fields in the system process and measurement models than is permissible with filters requiring linearizations of these terms.

References

1. Kalman, R. E. and Bucy, R. S. (1961) New results in linear filtering and prediction theory. *Trans. ASME, Ser. D, J. Basic Eng.* 83, 95–107.
2. Kalman, R.E. (1960) A new approach to linear filtering and prediction problems. *Transactions of the ASME- Journal of Basic Engineering*, 82 (1), 35–45.
3. Hoshiya, M and Saito, E. (1984) Structural identification by extended Kalman filter, *Journal of Engineering Mechanics*, 110(12), 1757-1770.
4. Budhiraja, A., Chen, L. and Lee, C. (2007) A survey of numerical methods for nonlinear filtering problems. *Physica D* 230, 27-36.
5. Kallianpur, G. and Striebel, C. (1968) Estimation of stochastic systems: Arbitrary system process with additive white noise observation errors. *The Annals of Mathematical Statistics*, *39*(3), 785-801.
6. Zakai, M. (1969) On the optimal filtering of diffusion processes, *Zeitschrift für Wahrscheinlichkeitstheorie und verwandte Gebiete*, 11(3), 230-243.
7. Kushner, (1964) H. J. On the differential equations satisfied by conditional probability densities of Markov processes, with applications. *SIAM J. Series A: Control* 2.1: 106-119.
8. Ito, K. and Rozovskii, B. (2000) Approximation of the Kushner equation for nonlinear filtering, *SIAM J. Control Optim.* 38(3):893-915.
9. Julier, S. J. and Uhlmann, J. K. (1997) A New Extension of the Kalman Filter to Nonlinear Systems, *In Proc. of AeroSense: The 11th Int. Symp. On Aerospace/Defence Sensing, Simulation and Controls*.
10. Doucet, A., Godsill, S. and Andrieu, C. (2000) On sequential Monte Carlo sampling methods for Bayesian filtering, *Statistics and Computing* 10, 197–208.
11. Fearnhead, P., Papaspiliopoulos, O. and Roberts, G. O. (2008) Particle filters for partially observed diffusions, *Journal of the Royal Statistical Society: Series B (Statistical Methodology)*, 70(4), 755-777.
12. Gordon, N. J., Salmond, D. J. and Smith, A. F. M. (1993) Novel approach to nonlinear/non-Gaussian Bayesian state

estimation, *Radar and Signal Processing, IEE Proceedings F*, 140, 107-113.

13. Pitt, M. and Shephard, N. (1999) Filtering via simulation: Auxiliary particle filters, *J. Amer. Statist. Assoc.* 94, 590–599.
14. Budhiraja, A., Chen, L. and Lee, C. (2007) A survey of numerical methods for nonlinear filtering problems, *Physica D* 230, 27-36.
15. Crisan, D., & Doucet, A. (2000) Convergence of sequential Monte Carlo methods, *Signal Processing Group, Department of Engineering, University of Cambridge, Technical Report CUEDIF-INFENGrrR38, 1.*
16. Chopin, N. (2004) Central limit theorem for sequential Monte Carlo methods and its application to Bayesian inference *The Annals of Statistics* 32(6), 2385-2411.
17. Chorin, A. J. and Tu, X. (2009) Implicit sampling for particle filters, *Proc. Natl. Acad. Sci. USA* 106: 17249-17254.
18. Jeroen, D. H., Thomas, B.S., Gustafsson, F. (2006) On Resampling Algorithms For Particle Filters, *IEEE Nonlinear Statistical Signal Processing Workshop* 79-82, Cambridge, UK.
19. Geweke, J. and Tanizaki, H. (1999) On Markov Chain Monte Carlo methods for nonlinear and non-gaussian state-space models, *Commun. Stat. Simul. C* 28, 867–894.
20. Evensen, G. (2009). *Data assimilation: the ensemble Kalman filter*, Springer.
21. Budhiraja, A. and Kallianpur, G. (1996) Approximations to the solutions of the Zakai equation using multiple Wiener and Stratonovich integral expansions, *Stochastics and Stochastic Reports* 56, 271-315.
22. Gobet, E., Pagès,G., Pham, H. and Printems, J. (2006) Discretization and simulation of the Zakai equation, *SIAM J. Numer. Anal.* 44(6), 2505-2538.
23. Ahmed, N. U. and Radaideh, S. M. (1997) A powerful numerical technique solving Zakai equation for nonlinear filtering, *Dynamics and Control* 7, 293-308.
24. Budhiraja, A. and Kallianpur, G. (1997) The Feynman-Stratonovich Semigroup and Stratonovich Integral Expansions in Nonlinear Filtering, *Appl. Math. Optim.* 35, 91-116.
25. Milstein, G. V. and Tretyakov, M.V. (2009) Solving parabolic stochastic partial differential equations via averaging over characteristics, *Math. Comp.* 78, 2075–2106.
26. Crisan, D. and Lyons, T. (1999) A particle approximation of the solution of the Kushner-Stratonovich equation, *Probab. Theory Related Fields* 115, 549-578.
27. Sarkar, S , Chowdhury, S. R., Venugopal, M., Vasu, R. M., & Roy, D. (2014) A Kushner–Stratonovich Monte Carlo filter applied to nonlinear dynamical system identification, *Physica D: Nonlinear Phenomena* 270, 46-59.
28. Oksendal, B.K. (2003) *Stochastic Differential Equations-An Introduction with Applications*, 6th ed., Springer, New York.
29. Kurtz, T. G. (1998) Martingale problems for conditional distributions of Markov processes, *Electron. J. Probab* 3(9), 1-29.
30. Milstein, G. N., Platen, E., & Schurz, H. (1998) Balanced implicit methods for stiff stochastic systems, *SIAM Journal on Numerical Analysis*, 35(3), 1010-1019.
31. Hartman, P. (1963) On the local linearization of differential equations, *Proceedings of the American Mathematical Society*, 14(4), 568-573.
32. Roy, D. (2004) A family of lower- and higher-order transversal linearization techniques in non-linear stochastic engineering dynamics, *Int. J. Numer. Meth. Eng.* 61:764–790.
33. Roy, D., Saha, N. and Dash, M. K. (2008) Weak Forms of the Locally Transversal Linearization (LTL) Technique for Stochastically Driven Nonlinear Oscillators, *Appl. Math. Model.* 32:1657-1681.
34. Roy, D., & Dash, M. K. (2002) A stochastic Newmark method for engineering dynamical systems, *Journal of sound and vibration*, 249(1), 83-100.
35. Kirkpatrick, S., Gelatt, C. D. and Vecchi, M. P. (1983) Optimization by simulated annealing, *Sci.* 220:671-680.
36. Raveendran, T., Sarkar, S., Roy, D., & Vasu, R. M. (2013) A novel filtering framework through Girsanov correction for the identification of nonlinear dynamical systems. *Inverse Problems*, 29(6), 065002.
37. Stroock, D. W. and Varadhan, S.R. (1972) On the support of diffusion processes with application to the strong maximum principle, *In Proceedings of the Sixth Bercley Symposium on Mathematical Statistics and Probability (Univ. California, Bercley, Calif. 1970/1971)*, 3, 330-359.

Life Cycle Reliability and Safety Engineering
Vol.4 Issue 1 (2015) 14-24

Experimental Studies on Reliability Model Updating of a Building Frame Model under Random Earthquake Loads

V. S. Sundar and C. S. Manohar*
Department of Civil Engineering, Indian Institute of Science, Bangalore, INDIA-560012;
**Email: manohar@civil.iisc.ernet.in*

Abstract

The paper proposes a variance reduction strategy for updating reliability models of dynamical systems driven by random excitations. The basic framework to tackle this problem consist of a system identification step followed by a reliability model updating step. Both these problems are tackled within the framework of Bayesian model updating. Maximum likelihood estimation method is used as a tool for system identification, whereas, the Girsanov transformation based method is made use in obtaining as estimate for the posterior probability of failure with reduced variance. Illustrative example includes shake table studies on an asymmetric, bending-torsion coupled frame.

Keywords: Reliability model updating, existing structures, Girsanov's transformation, system identification, variance reduction.

1 Introduction

During the design phase of a structural system, all the uncertainties associated with the system parameters and external loading are typically characterized by a set of random variables or more generally through random process models. The safety of the structure is quantified through the notion of probability of failure or reliability index [1]. Once the structural system comes into existence, it becomes possible to obtain responses of the structure to ambient and (or) proof loads. Questions on the current state of the structure *i.e.*,damage characterization, system identification, repair and maintenance of the structure becomes relevant.Overviews of issues relevant to this class of problems can be found in the references [1-9]. The monograph by Yao [2] considers the role of structural system identification and its application to structural dynamics, reliability modeling, and damage assessment. Mori and Ellingwood[3] have proposed probabilistic methods to determine the time-dependent reliability of concrete structures. Here the authors also considered the importance of periodic inspection and maintenance of the structural systems.The books by Ditlevsen and Madsen [4] and Melchers [1] contain dedicated chapters on reliability modeling of existing structures. The paper by Melchers [5] outlines the research needs originating from increasing demand for estimation of remaining life of existing structures in the context of widespread desire to extend the life of ageing infrastructure.Frangopol *et al.*, [6], and Ellingwood[7] have reviewed the approaches for modeling deterioration in an existing structure. The models reviewed by these authors are probabilistic in nature, where the deterioration of an existing structure is modeled with the aid of time invariant and (or) time variant reliability methods. The recent monograph by Yuen [8],and the review paper by Yuen and Kouk[9]provide contemporary perspectives on the application of Bayesian methods to problems of structural dynamics in civil engineering applications. The state-of-art report edited by Catbas *et al.*, [10] provides comprehensive account of problem of structural system identification in the context of constructed civil engineering facilities.

Methods of system identification can be broadly classified as being either online or offline. In online methods, the parameters are identified in real time and the measurements are processed sequentially as and when they arrive [11-19]. On the other hand, in offline methods, system identification follows the completion of measurement process, and the measured data are processed in a batch mode[20-24]. The online methods can of course also be used for problems in which there exists no compulsions to identify system parameters in real time.

The work by Beck and Au [25] introduces the application of Markov chain Monte Carlo (MCMC) based methods in the context of structural system identification. Here the authors apply MCMC based

method for model selection and updating the reliability models for existing structures. A comprehensive review of non-linear structural system identification is given in the review paper by Kerschen *et al.,*[26]. Studies on combining MCMC based methods with filtering techniques have been carried out by Khalil *et al.,* [27]. The study by Rosic *et al.,*[28] deals with comparing a few system identification methods (MCMC based, ensemble Kalman filter, polynomial chaos based) in the context of parameter identification of an elasto-plastic system.

In the present study, attention is focused on Bayesian framework to tackle problems associated with existing structures. The template for this framework consists of the following components: (a) mathematical model for the structure, typically based on FE analysis, (b) a set of noisy measurements on structural displacements, strains, applied loads, and (or) reaction transferred to the supports under operating and (or) diagnostic loads, and (c) a mathematical model which relates measured quantities to the system states in the governing mathematical model for structure. Both the models for structural behavior and the measurements are taken to be imperfect, and this is accounted for by including appropriate random noise terms in the models.

Similar studies have been carried out by Soyoz *et al.,*[29]. Here the authors considered parameter identification, and updating the probability of failure of a three span reinforced cement concrete bridge structure subjected to earthquake type excitation on a shake table setup. The authors have identified the stiffness parameters online using the extended Kalman filter. Their study stresses the importance of (a) updating reliability models in the context of post-earthquake damage assessment, and (b) residual reliability estimation.

The aim of the paper is to develop a methodology that efficiently embeds the information contained in the measurement into the mathematical model of the structure and to update the reliability of the structural system. The method broadly consists of a system identification step followed by a reliability model updating step. The maximum likelihood estimation method in conjunction with Genetic algorithms is used to solve the system identification problem, and a variance reduction strategy based on the Girsanov's transformation is employed to tackle the step involving reliability prediction. The contribution of the paper however lies in applying the method developed earlier by the authors [30] to problems with experimental measurement data. Illustrative example consists of shake table studies on an asymmetric bending-torsion coupled frame subjected to non-stationary random excitations and, linear performance function metrics. The predictions from the proposed approximate method are compared with results from appropriate brute force Monte Carlo simulations and a satisfactory mutual agreement is demonstrated.

2. Problem Statement

Consider non-linear dynamical systems governed by the equation of the form

$$\mathbf{M}(\boldsymbol{\Theta})\ddot{\boldsymbol{Y}}(t)+\mathbf{C}(\boldsymbol{\Theta})\dot{\boldsymbol{Y}}(t)+\mathbf{K}(\boldsymbol{\Theta})\boldsymbol{Y}(t)+\boldsymbol{G}\left[(\boldsymbol{\Theta}),\boldsymbol{Y}(t),\dot{\boldsymbol{Y}}(t)\right] = \boldsymbol{F}(t)+\boldsymbol{\xi}(t) \quad \boldsymbol{Y}(0)=\boldsymbol{Y}_0;\dot{\boldsymbol{Y}}(0)=\dot{\boldsymbol{Y}}_0 \tag{1}$$

Here $\boldsymbol{\Theta}$ is a $p\times 1$ vector of uncertain system parameters with joint probability density function $p_{\boldsymbol{\Theta}}(\boldsymbol{\theta})$; $\boldsymbol{Y}(t)$ is a $n\times 1$ displacement vector; **M**, **C**, and **K** are, respectively $n\times n$, structural mass, damping and stiffness matrices; $\boldsymbol{G}\left[\boldsymbol{\Theta},\boldsymbol{Y}(t),\dot{\boldsymbol{Y}}(t)\right]$ is a $n\times 1$ vector of non-linear functions of system states; $\boldsymbol{F}(t)$ is a $n\times 1$ vector of externally applied forces, taken to be a zero mean, stationary/non-stationary Gaussian vector random process.; $\boldsymbol{\xi}(t)$ is a $n\times 1$ is a vector random process representing the errors in arriving at mathematical model for the dynamical system, and is modelled as a zero mean Gaussian white noise vector; $\boldsymbol{Y}_0$ and $\dot{\boldsymbol{Y}}_0$ are, the $n\times 1$ initial displacement and velocity vectors respectively. This model is assumed to a represent the behavior of an existing instrumented structure on which measurements have been made under operating conditions. These measurements typically include displacements, accelerations, strains, reactions transferred to the supports, and (or) applied forces ***F(t)***. The performance of the structure is recorded through a set of s sensors. These quantities are related to the system states through the measurement model given by

$$\boldsymbol{Z}(\boldsymbol{\Theta},t)=\boldsymbol{H}\left[\boldsymbol{\Theta},\boldsymbol{Y}(t),\dot{\boldsymbol{Y}}(t),t\right]+\boldsymbol{\mu}(t),0\le t\le T \tag{2}$$

Here $\boldsymbol{Z}(\Theta,t)$ is a $s\times 1$ vector of sensor records, $\boldsymbol{H}\left[\boldsymbol{\Theta},\boldsymbol{Y}(t),\dot{\boldsymbol{Y}}(t),t\right]$ is a $s\times 1$ vector of functions which relate the measurements with system states, and, $\boldsymbol{\mu}(t)$ is a $s\times 1$ vector of random processes representing the noise in measurements and also the imperfections in relating measured quantities to the system states. $\boldsymbol{\mu}(t)$ is taken to be a zero mean stationary Gaussian vector white noise process with known covariance, and, independent of $\boldsymbol{\xi}(t)$. The

explicit dependence of the measurement on the system parameter vector $\boldsymbol{\Theta}$ mandates for a system identification step prior to updating reliability models. The sample time history of the applied force is taken to arise from the prior model assumed for $\boldsymbol{F}(t)$, if not measured. Prior to the structure coming into existence, the time variant reliability analysis consists of obtaining the probability

$$P_S = \mathrm{P}\left\{h\left[\boldsymbol{\Theta},\boldsymbol{Y}(t),\dot{\boldsymbol{Y}}(t)\right] < h^* \ \forall t \in [0,T]\right\} \tag{3}$$

Here $h\left[\boldsymbol{\Theta},\boldsymbol{Y}(t),\dot{\boldsymbol{Y}}(t)\right]$ is a scalar performance metric and h^* is its permissible limit. Once the structure comes into existence, and, upon the availability of measurement vector $\boldsymbol{Z}(\boldsymbol{\Theta},t),\ 0 \le t \le T$, the posterior reliability can be expressed as

$$P_{S|\boldsymbol{Z}} = \mathrm{P}\left\{ h\left[\boldsymbol{\Theta},\boldsymbol{Y}(t),\dot{\boldsymbol{Y}}(t)\right] \le h^* \ \forall\ t \in [0,T] \ \middle|\ \boldsymbol{Z}(\boldsymbol{\Theta},\tau), 0 \le \tau \le T\right\} \tag{4}$$

To proceed further, $h\left[\boldsymbol{\Theta},\boldsymbol{Y}(t),\dot{\boldsymbol{Y}}(t)\right]$ is replaced by its optimal estimator, given by

$$\hat{h}\left[\boldsymbol{\Theta},\boldsymbol{Y}(t),\dot{\boldsymbol{Y}}(t)\right] = \left\langle h\left[\boldsymbol{\Theta},\boldsymbol{Y}(t),\dot{\boldsymbol{Y}}(t)\right] \ \middle|\ \boldsymbol{Z}(\boldsymbol{\Theta},\tau), 0 \le \tau \le T\right\rangle \tag{5}$$

Here $\langle \bullet \rangle$ denotes the expectation operator taken across the ensemble of process and measurement noises.Thus, Eq. (4) can be rewritten as

$$\begin{aligned} P_{S|\boldsymbol{Z}} &= \mathrm{P}\left\{ \hat{h}\left[\boldsymbol{\Theta},\boldsymbol{Y}(t),\dot{\boldsymbol{Y}}(t)\right] \le h^* \ \forall\ t \in [0,T]\right\} \\ &= \mathrm{P}\left\{ \max_{0\le t\le T} \hat{h}\left[\boldsymbol{\Theta},\boldsymbol{Y}(t),\dot{\boldsymbol{Y}}(t)\right] \le h^*\right\} \end{aligned} \tag{6}$$

The problem on hand now consists of identifying the parameter $\boldsymbol{\Theta}$, and determining the posterior probability of failure, $P_{F|\boldsymbol{Z}} = 1 - P_{S|\boldsymbol{Z}}$. In section 4, an illustrative example involving the application of maximum likelihood estimation method for system identification followed by a reliability model updating step is presented. Considering $\boldsymbol{\Theta}$ to be a deterministic quantity (*i.e,*. after system identification), the method proposed by Sundar and Manohar [30] (*i.e.,* interfacing filtering techniques with the Girsanov transformation based variance reduction method) could be effectively used to determine the posterior failure probability. In the next section the case of linear systems and linear measure models with additive Gaussian noise is considered and the method is reproduced for completeness.

3 Linear Systems - Methodology

Equation (1) can be appropriately modified to obtain a linear system by setting the non-linear term, $\boldsymbol{G}\left[\boldsymbol{\Theta},\boldsymbol{Y}(t),\dot{\boldsymbol{Y}}(t)\right] = 0$. Furthermore, the system is assumed to have been identified through a previous system identification step, and, the uncertainties arise solely due to the external random excitation. Introducing a state vector, $\boldsymbol{X}(t) = \left[\boldsymbol{Y}(t),\dot{\boldsymbol{Y}}(t)\right]^t$, Eq. (1) can be recast into an equivalent state space form with the process equation given by Ito's SDE

$$\begin{aligned} d\boldsymbol{X}(t) &= \mathbf{A}\boldsymbol{X}(t)\,dt + \boldsymbol{f}(t)\,dt + d\bar{\boldsymbol{B}}(t) \\ \boldsymbol{X}(0) &= \boldsymbol{X}_0 \end{aligned} \tag{7}$$

Here $\mathbf{A}$ is a $2n \times 2n$ drift matrix, $\boldsymbol{f}(t) = \left[\boldsymbol{0}, \boldsymbol{F}(t)\right]^t$ and $d\bar{\boldsymbol{B}}(t)$ is taken to be an increment of a zero mean Brownian motion process with $\left\langle d\bar{\boldsymbol{B}}(t)\, d\bar{\boldsymbol{B}}^t(t+\tau)\right\rangle = \mathbf{Q}\delta(\tau)$. Also, the measurement equation is taken to be linear and is given by

$$\boldsymbol{Z}(t) = \mathbf{H}\boldsymbol{X}(t) + \boldsymbol{\mu}(t),\ 0 \le t \le T \tag{8}$$

Here $\mathbf{H}$ is a $2n \times s$ matrix and $\boldsymbol{\mu}(t)$ is the $s \times 1$ measurement noise vector modeled as zero mean Gaussian vector white noise process with $\left\langle \boldsymbol{\mu}(t)\boldsymbol{\mu}^t(t+\tau)\right\rangle = \mathbf{R}\delta(\tau)$. $\boldsymbol{\mu}(t)$ and $d\bar{\boldsymbol{B}}(t)$ are taken to be independent of each other. For the purpose of illustration, it is assumed that the force $\boldsymbol{F}(t)$ is not measured. As mentioned earlier, the system has already been identified, and the system properties are embedded in the matrices $\mathbf{A}$ and $\mathbf{H}$. The problem of dynamic state estimation consists of determining the conditional mean and conditional covariance given by

$$\begin{aligned} \hat{\boldsymbol{X}}(t) &= \left\langle \boldsymbol{X}(t) \middle| \boldsymbol{Z}(\tau), 0 \le \tau \le T\right\rangle \\ \mathbf{P}(t) &= \left\langle \left[\boldsymbol{X}(t) - \hat{\boldsymbol{X}}(t)\right]\left[\boldsymbol{X}(t) - \hat{\boldsymbol{X}}(t)\right]^t \ \middle|\ \boldsymbol{Z}(\tau), 0 \le \tau \le T\right\rangle \end{aligned} \tag{9}$$

It must be noted that expectations mentioned in the above equation are taken across ensemble of process noise $d\bar{\boldsymbol{B}}(t)$ and measurement noise $\boldsymbol{\mu}(t)$, and are evaluated for a given realization of $\boldsymbol{f}(t)$. Given that the process equation (Eq. 7) and the measurement equation (Eq. 8) are linear, and with additive Gaussian noise, an exact solution to the dynamic state estimation problem, based on continuous version of the Kalman filter can be obtained as

$$\frac{d\hat{\boldsymbol{X}}(t)}{dt} = \mathbf{A}\hat{\boldsymbol{X}}(t) + \mathbf{K}_{\mathrm{g}}(t)\left[\boldsymbol{Z}(t) - \mathbf{H}\hat{\boldsymbol{X}}(t)\right] + \boldsymbol{f}(t)$$

$$\hat{\boldsymbol{X}}(0)=\hat{\boldsymbol{X}}_0$$
$$\frac{d\mathbf{P}(t)}{dt}=\mathbf{AP}+\mathbf{PA}^t-\mathbf{PH}^t\mathbf{R}^{-1}\mathbf{HP}+\mathbf{Q}$$
$$\mathbf{P}(0)=\mathbf{P}_0 \tag{10}$$

Here $\mathbf{K}_g=\mathbf{PH}^t\mathbf{R}^{-1}$ is the $n\times s$ Kalman gain matrix. Expressing the covariance matrix as $\mathbf{P}(t)=\boldsymbol{\Omega}(t)\boldsymbol{\Psi}^{-1}(t)$, it can be shown that the functions $\boldsymbol{\Omega}(t)$ and $\boldsymbol{\Psi}(t)$ arise as solutions of the initial value problem [31]

$$\dot{\boldsymbol{\Omega}}=\mathbf{A}\boldsymbol{\Omega}+\mathbf{Q}\boldsymbol{\Psi}$$
$$\dot{\boldsymbol{\Psi}}=\mathbf{H}^t\mathbf{R}\mathbf{H}\boldsymbol{\Omega}-\mathbf{A}^t\boldsymbol{\Psi} \tag{11}$$
$$\boldsymbol{\Omega}(0)=\mathbf{P}_0,\boldsymbol{\Psi}(0)=\mathbf{I}$$

Furthermore, the forcing vector $\boldsymbol{f}(t)$is taken to represent either a vector of white noise processes or as a vector of linearly filtered white noise processes. Thus, Eq. (10) can be rewritten as

$$d\hat{\boldsymbol{X}}(t)=\mathbf{A}\hat{\boldsymbol{X}}(t)dt+\boldsymbol{\Omega}(t)\boldsymbol{\Psi}^{-1}(t)\mathbf{H}^t\mathbf{R}^{-1}\left[\boldsymbol{Z}(t)-\mathbf{H}\hat{\boldsymbol{X}}(t)\right]dt+d\boldsymbol{B}(t) \tag{12}$$

with $\boldsymbol{\Omega}(t)$ and $\boldsymbol{\Psi}(t)$ defined as per Eq. (11). Here $\boldsymbol{f}(t)dt=d\boldsymbol{B}(t)$with$\langle d\boldsymbol{B}(t)\rangle=0$ and $\langle d\boldsymbol{B}(t)d\boldsymbol{B}^t(t+\tau)\rangle=\Sigma\delta(\tau)$. Considering a linear performance function of the form $h[\boldsymbol{X}(t)]=\boldsymbol{\phi}^t\boldsymbol{X}(t)$, where $\boldsymbol{\phi}$ is a $r\times 1$ vector, the required posterior probability is given by

$$\begin{aligned}P_{S|\boldsymbol{Z}}&=\mathrm{P}\left\{\boldsymbol{\phi}^t\boldsymbol{X}(t)\le h^*\ \forall\ t\in[0,T]\ \middle|\ Z(\tau),0\le\tau\le T\right\}\\&=\mathrm{P}\left\{\boldsymbol{\phi}^t\hat{\boldsymbol{X}}(t)\le h^*\ \forall\ t\in[0,T]\right\}\\&=\mathrm{P}\left[\max_{0\le t\le T}\boldsymbol{\phi}^t\hat{\boldsymbol{X}}(t)\le h^*\right]\end{aligned} \tag{13}$$

A Monte Carlo simulation based estimator for the conditional probability of failure,

$P_{F|\boldsymbol{Z}}=1-P_{S|\boldsymbol{Z}}=\left\langle I\left[h^*-\max_{0\le t\le T}\boldsymbol{\phi}^t\hat{\boldsymbol{X}}(t)\le 0\right]\right\rangle$ is obtained as

$$\hat{P}_{F|\boldsymbol{Z}}=\frac{1}{N_s}\sum_{l=1}^{N_s}I\left[\left\{h^*-\max_{0\le t\le T}\boldsymbol{\phi}^t\hat{\boldsymbol{X}}^{(l)}(t)\right\}\le 0\right] \tag{14}$$

Here $\hat{\boldsymbol{X}}^{(l)}(t)$ is the conditional expectation $\hat{\boldsymbol{X}}(t)$ corresponding to the l^{th} realization of $\boldsymbol{f}(t)$. The sampling variance of the unbiased estimator (Eq. 14) is inversely proportional to the sample size N_s [32]. Thus, the computational cost involved becomes increasingly intractable as the probability to be estimated becomes small (of the order of 10^{-4} or smaller). One way to circumvent this problem is by reinforcing the simulation method with suitable techniques to control the sampling variance. The method of Girsanov's transformation, applied in the context of reliability analysis [33,34], is made use in the present study. The drift term in Eq. (12) is modified through addition of a deterministic control force, $\boldsymbol{u}(t)$. Equation (12) now reads as

$$\begin{aligned}d\tilde{\boldsymbol{X}}(t)&=\mathbf{A}\tilde{\boldsymbol{X}}(t)dt+\boldsymbol{\Omega}(t)\boldsymbol{\Psi}^{-1}(t)\mathbf{H}^t\mathbf{R}^{-1}\left[\boldsymbol{Z}(t)-\mathbf{H}\tilde{\boldsymbol{X}}(t)\right]dt+\boldsymbol{\sigma}(t)\boldsymbol{u}(t)dt+\boldsymbol{\sigma}(t)d\boldsymbol{B}(t)\\d\Gamma(t)&=-\Gamma(t)\boldsymbol{u}^t(t)d\boldsymbol{B}(t)\\\tilde{\boldsymbol{X}}(0)&=\boldsymbol{X}_0,\Gamma(0)=\Gamma_0\end{aligned} \tag{15}$$

Here $\boldsymbol{u}(t)$ is a $q\times 1$ vector and $\Gamma(t)$ is a scalar correction process with deterministic initial condition Γ_0. Following the principles of the Girsanov theorem [35, 36], the following equivalence of expectations can be established

$$\left\langle I\left[h^*-\max_{0\le t\le T}\boldsymbol{\phi}^t\hat{\boldsymbol{X}}(t)\le 0\right]\right\rangle=\left\langle\Gamma(T)I\left[h^*-\max_{0\le t\le T}\boldsymbol{\phi}^t\tilde{\boldsymbol{X}}(t)\le 0\right]\right\rangle\Big/\Gamma_0 \tag{16}$$

The expectation on the right side of Eq. (16) can be obtained by setting a Monte Carlo simulation estimator as

$$\tilde{P}_{F|\boldsymbol{Z}}=\frac{1}{N_g}\sum_{l=1}^{N_g}\Gamma(T)I\left[\left\{h^*-\max_{0\le t\le T}\boldsymbol{\phi}^t\tilde{\boldsymbol{X}}^{(l)}(t)\right\}\le 0\right]\Big/\Gamma_0 \tag{17}$$

The control force, $\boldsymbol{u}(t)$is selected so that variance of the estimator given in Eq. (17) is lower than that given in Eq. (14). An optimal control force exists that yields an estimator with zero variance [33]. This being infeasible, we resort to determining a sub-optimal control. The method proposed by Macke and Bucher [33] as applied to system of equations mentioned in Eq. (15) is briefly explained below.

Consider the associated dynamical system

$$\begin{aligned}d\boldsymbol{V}(t)&=\mathbf{A}\boldsymbol{V}(t)dt+\mathbf{K}_g(t)\left[\boldsymbol{Z}(t)-\mathbf{H}\boldsymbol{V}(t)\right]dt+\\&-\boldsymbol{\sigma}(t)\boldsymbol{u}(t)dt;\ 0\le t\le T\\\boldsymbol{V}(0)&=\boldsymbol{X}_0\end{aligned} \tag{18}$$

The control force is selected by solving the following optimization problem

$$\beta\left(\tau^m\right)=\sqrt{\sum_{j=1}^{m}\int_0^{\tau^m}u_j^2\left(t\right)dt}\ \text{subjected to}\ h^*-\phi^t\boldsymbol{V}\left(\tau^m\right)=0,\ 0<\tau^m\le T \tag{19}$$

It is observed that selecting τ^m in the vicinity where the measurement peaks yields better results. This is in contrast to the problem of forward reliability analysis, where, typically one takes $\tau^m=T$. Eq. (15) is discretized using the order 1.5 strong Taylor's scheme [37]. The time step of discretization need not coincide with the sampling interval used in acquiring measurements.

The method outlined here would be inapplicable to problems with non-linear process and measurement models, and non-linear performance metrics. This is because, though it is possible to set up the equations for conditional moments [similar to those in Eq. (11) and (12)], there would be a fundamental problem, since, these equations would constitute an infinite hierarchy of moment equations which at no stage yield sufficient number of equations to solve the problem [20]. This, infact, is similar to moment closure problem encountered in non-linear random vibration problems [38]. Extension of the proposed method to handle such problems, based on the application of bootstrap filter, has been outlined in [30].

4. Five Storey Bending-Torsion Coupled Frame

In this section, a building frame model which is tested on a earthquake shake table is considered, and the combined problem of system identification and reliability model updating is pursued. The building frame studied is the five storey bending-torsion coupled frame (see Fig. 1). Attention here is limited to the case where the system is taken to behave linearly and the base excitation is applied only in one direction. The structure is mounted on a servo-hydraulic controlled, multi-axes, shake table which operates in a displacement controlled mode. The base excitation is modeled as the output of a coupled Kanai-Tajimi-Clough-Penzien filter driven by a non-stationary white noise excitation. The structure is taken to be instrumented with strain gauges, linear variable differential transformers (LVDT-s), and accelerometers which enable the evaluation of performance metric used in reliability calculation, and for the purpose of system identification. Thus the LVDT shown in Fig. 1 measures the inter-storey drift

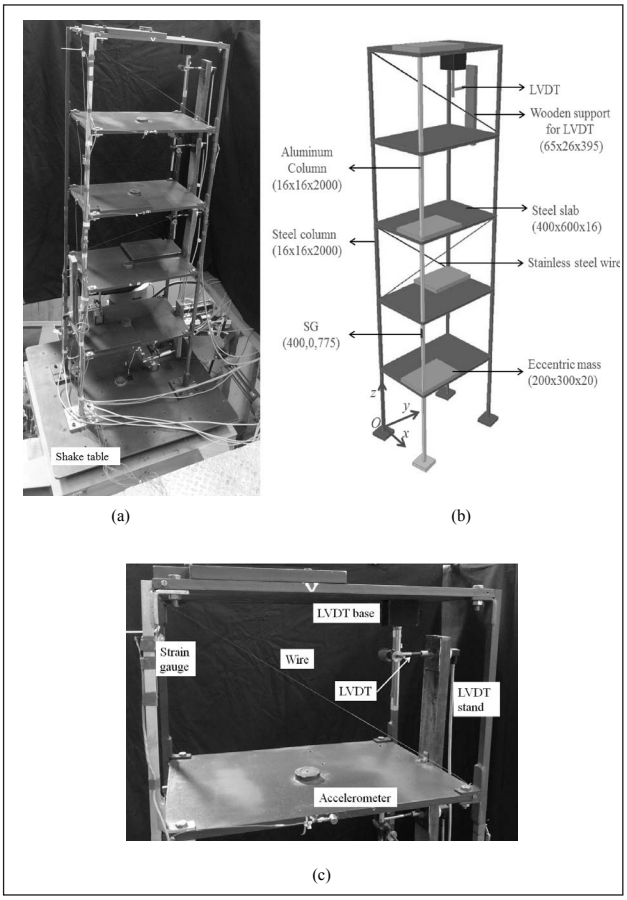

Figure 1. Experimental setup; (a) test structure mounted on a shake table; (b) schematic showing the location of sensors, along with the coordinates of the strain gauge; all dimensions are in mm; (c) details of instrumentation.

between fourth and fifth floors along y -direction and the strain gauge (marked as SG) measures the bending strain in the aluminum column. The frame as shown in Fig. 1 consists of five steel slabs with eccentric mass, and twenty columns (fifteen steel columns and five aluminum columns). The bending and torsional degrees of freedom from the frame are coupled and the study is based on a fifteen dof model as shown in Fig. 2. The mass lumped at each floor level, in the fifteen dof model, are as follows:

$$\begin{aligned}
m_1 &= m_{slab}+\left(3m_s+m_a\right)+m_e+m_{wood}+m_{acc}+m_{magnet}\\
m_2 &= m_{slab}+\left(3m_s+m_a\right)+m_e+2m_{wood}+m_{acc}+2m_{LVDT}\\
m_3 &= m_{slab}+\left(3m_s+m_a\right)+m_e+m_{wood}+m_{acc}+m_{magnet}+m_{LVDT}\\
m_4 &= m_{slab}+\left(3m_s+m_a\right)+m_{wood}+m_{acc}+m_{magnet}+m_{LVDT}\\
m_5 &= m_{slab}+\left(3m_s+m_a\right)/2+m_e+m_{acc}+m_{magnet}+m_{LVDT}
\end{aligned}$$

where m_{slab} = mass of slab, m_e = mass of the additional eccentric slab, m_s = mass of steel column, m_a = mass of aluminum column, m_{wood} = mass of LVDT support wooden stand (0.719 kg), m_{acc} = mass

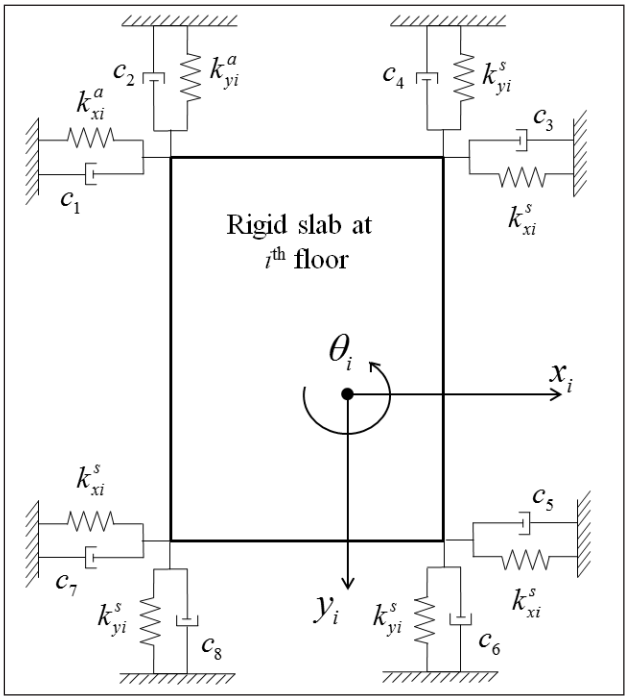

Figure 2. Section 4; schematic showing the dof-s at each floor; the solid circle represents the location of center of gravity at each floor.

of the torsional accelerometer (0.350 kg), m_{magnet} = mass of the magnetic base support for the LVDT (1.315 kg), and m_{LVDT} = mass of the LVDT (0.233 kg). The masses lumped in both the x and y -directions, at each floor, are assumed to be the same. The governing equations are obtained as

$$\begin{aligned} &\ddot{y}_s + 2\eta_s\omega_s\dot{y}_s + \omega_s^2 y_s = e(t)w_1(t) + w_2(t) \\ &\ddot{y}_f + 2\eta_f\omega_f\dot{y}_f + \omega_f^2 y_f = 2\eta_s\omega_s\dot{y}_s + \omega_s^2 y_s \\ &\mathbf{M}\ddot{\boldsymbol{Y}} + \mathbf{C}\dot{\boldsymbol{Y}} + \mathbf{K}\boldsymbol{Y} = -\mathbf{M}\boldsymbol{\Omega}\ddot{y}_f(t) + \boldsymbol{\xi}(t) \end{aligned} \tag{20}$$

Here $\boldsymbol{Y} = (x_1, y_1, \theta_1, x_2, y_2, \theta_2, x_3, y_3, \theta_3, x_4, y_4, \theta_4, x_5, y_5, \theta_5)^t$ is the 15×1 vector of dof-s, **M**, **K**, and **C** are the 15×15 structural mass, stiffness and damping matrices; $\boldsymbol{\Omega}$ is the 15×1 participation factor vector; $y_f(t)$ is the ground displacement in the y -direction; $\boldsymbol{\xi}(t)$ is a zero mean 15×1 process noise vector with ; $w_1(t)$ is the zero mean stationary white noise excitation at the bed rock level with $\langle w_1(t)w_1(t+\tau)\rangle = \sigma_1^2\delta(\tau)$; $w_2(t)$ is the zero mean stationary white noise process with $\langle w_2(t)w_2(t+\tau)\rangle = \sigma_2^2\delta(\tau)$ which represents the process noise in modeling ground motions. The processes $\boldsymbol{\xi}(t)$, $w_1(t)$, and $w_2(t)$ are taken to be independent. The Caughey classical damping model [39], with all the fifteen modes, is used in constructing the **C** matrix from **M**, **K**, and damping ratios. $e(t) = A_0\left(e^{-\alpha_1 t} - e^{-\alpha_2 t}\right)$ is a deterministic envelope function with $A_0 = -2.31$, $\alpha_1 = 0.7$, and $\alpha_2 = 0.2$. The parameters of Kanai-Tajimi-Clough-Penzien model are taken to be $\eta_s = 0.6$, $\omega_s = 5\pi$ rad/s, $\eta_f = 0.8$, $\omega_f = \omega_s/10$ rad/s. Numerical values considered for the standard deviation of the noise terms in the problem are as follows: $\sigma_1 = 0.15$ m/s^2, $\sigma_2 = \sigma_1/10$ m/s^2 and , where **I** is the 15×15 identity matrix.

The task of system identification and reliability model updating are carried out in two separate steps. It is assumed that two sets of measurements are available so that one set could be used for system identification and the other for reliability model updating. In the experimental work, the measurements have been made on the inter-storey drift between fourth and fifth floors and these measurements for two loading cases are shown in Figs. 3 and 4. The base accelerations for these two measurements are shown in Figs. 5 and 6 respectively.

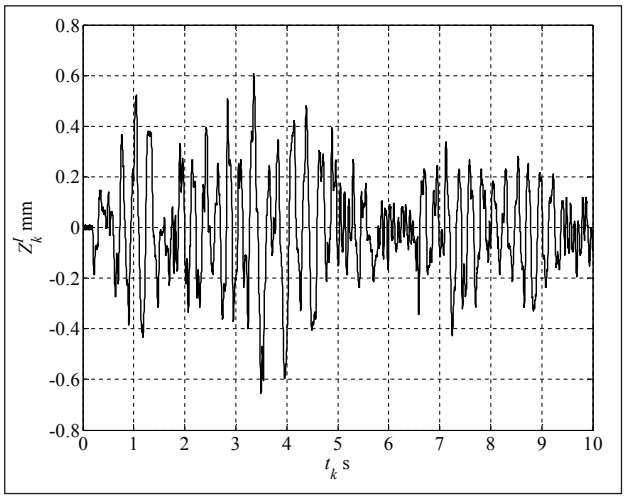

Figure 3. Section 4; measured inter-storey drift used for system identification.

4.1 System Identification

The properties of the frame to be identified are taken to be made up of the following set

1. density of steel in slabs and columns, ρ_s,
2. density of aluminum in the column, ρ_a,
3. stiffness in the x and y-directions for steel columns, $k^s_{xi} = k^s_{yi}$, $i = 1, 2, \cdots, 5$,
4. stiffness in the x and y -directions for aluminum column, $k^a_{xi} = k^a_{yi}$, $i = 1, 2, \cdots, 5$,
5. torsional stiffness at each floor, $k_{\theta i}$, $i = 1, 2, \cdots, 5$, and
6. the fifteen modal damping ratios, $\eta_1, \eta_2, \cdots, \eta_{15}$.

obtained as

1.7090	0	-0.0992	-0.3708	0	0.0068	0	0	0	0	0	0	0	0	0
0	1.7090	-0.1480	0	-0.3708	0.0102	0	0	0	0	0	0	0	0	0
-0.0992	-0.1480	0.2368	0.0217	0.0324	-0.0474	0	0	0	0	0	0	0	0	0
-0.3708	0	0.0217	0.7416	0	-0.0137	-0.3708	0	0.0217	0	0	0	0	0	0
0	-0.3708	0.0324	0	0.7416	-0.0203	0	-0.3708	0.0292	0	0	0	0	0	0
0.0068	0.0102	-0.0474	-0.0137	-0.0203	0.0959	0.0068	0.0102	-0.0473	0	0	0	0	0	0
0	0	0	-0.3708	0	0.0068	0.7416	0	-0.0435	-0.3708	0	0.0137	0	0	0
0	0	0	0	-0.3708	0.0102	0	0.7416	-0.0584	0	-0.3708	0.0163	0	0	0
0	0	0	0.0217	0.0292	-0.0473	-0.0435	-0.0584	0.1023	0.0217	0.0292	-0.0482	0	0	0
0	0	0	0	0	0	-0.3708	0	0.0217	0.7416	0	-0.0275	-0.3708	0	0.0259
0	0	0	0	0	0	0	-0.3708	0.0292	0	0.7416	-0.0326	0	-0.3708	0.0328
0	0	0	0	0	0	0.0137	0.0163	-0.0482	-0.0275	-0.0326	0.0976	0.0137	0.0163	-0.0485
0	0	0	0	0	0	0	0	0	-0.3708	0	0.0137	0.3708	0	-0.0259
0	0	0	0	0	0	0	0	0	0	-0.3708	0.0163	0	0.3708	-0.0328
0	0	0	0	0	0	0	0	0	0.0259	0.0328	-0.0485	-0.0259	-0.0328	0.0537

Let $\boldsymbol{\psi} = \left(k_{x1}^s, k_{x1}^a, k_{\theta 1}, \cdots, k_{x5}^s, k_{x5}^a, k_{\theta 5}, \rho_s, \rho_a, \eta_1, \eta_2, \cdots, \eta_{15}\right)^t$ be the resulting 32×1 vector of unknown parameters. A non-dimensional independent uniform random variable $\boldsymbol{X}$ is introduced such that $\psi_i = \alpha_i X_i$, $i = 1,2,\cdots,32$, where $\boldsymbol{\alpha}$ is a 32×1 vector of reference values of the unknown parameters, details of which are as follows:

1. Stiffness in x and y -directions: $k_x = k_y = 12EI/L^3$ $k_x = k_y = 12EI$, where $E = 210$ GPa for steel and $= 69$ GPa for aluminum.
2. Torsional stiffness: $k_\theta = \left(3G_s + G_a\right)J/L$, where $G = E/\left(1+2\upsilon\right)$ is the rigidity modulus of the material, with $\upsilon = 0.3$. The subscripts *s* and *a* denote steel and aluminum respectively. Here J is the polar area moment of inertia, taken to be the same for all the columns.
3. Density: 8000 kg/m^{3}for steel and 3000 kg/m^{3}for aluminum.
4. Damping ratio: 0.04 for all the fifteen modes.

The random variables X_1 to X_{17} are taken to be uniformly distributed in $[0.42\ 0.98]$, and, X_{18} to X_{32} are assumed to be uniformly distributed in $[0.02\ 0.98]$. The measurement as shown in Fig. 3 is considered for identifying the system. The model for measurements is given by

$$Z_k^I = \boldsymbol{H}_k\left(\boldsymbol{Y}_k\right) + \mu_k,\ k = 1,2,\ldots\bar{N} \tag{21}$$

Here $H_k\left(\boldsymbol{Y}_k\right) = \left(y_{5k} - y_{4k}\right)$, and μ_k is the measurement noise modeled as a sequence of zero mean Gaussian iid random variables with variance, $\Sigma_{\mu_k\mu_k} = 3.6854\times10^{-5}$ mm^2. The system parameters are identified using the maximum likelihood estimation method in conjunction with genetic algorithms. The likelihood function here is given by $p_{\boldsymbol{Z}^I}\left(\boldsymbol{Z}^I \middle| \boldsymbol{x}\right) = \prod_N N\left[Z_k^I, H(\boldsymbol{x}), \Sigma_{\mu_k\mu_k}\right]$. The *ga* toolbox available in the Matlab software is used to solve the problem. Parameters considered for the genetic algorithm are as follows: population size: 50; initial population range: [-1,1]; crossover fraction: 0.85; migration direction: forward; migration fraction: 0.1; migration interval: 5; elite count: 2; generations: 30; time limit: 200000, fitness limit: 10^{-6}, stall generation limit:10; and stall time limit:100000. In order to ascertain that global optimum solution is obtained, a parametric study has been conducted on optimization problems with similar number of variables and the values are fixed based on experience gained.

The genetic algorithm has been run five times giving rise to five solution vectors with the optimal likelihood function values as: 34473, 37175, 38154, 34367, and 38520. Accordingly, the solution obtained on the fifth trial is considered as being acceptable. The identified non-dimensional parameter vector, $\boldsymbol{\alpha}^*$ = [0.8627, 0.6638, 0.5698, 0.9357, 0.9379, 0.7573, 0.7194, 0.5628, 0.9745, 0.6718, 0.6426, 0.9611, 0.4726, 0.5259, 0.9116, 0.9271, 0.8504, 0.9033, 0.0354, 0.0929, 0.6049, 0.0541, 0.4376, 0.4085, 0.0461, 0.5281, 0.4479, 0.6328, 0.1954, 0.0210, 0.8477, 0.1116]^t.

From these non-dimensional factors, the density of steel and aluminum are determined as 7416.80 kg/m^3 and 2551.20 kg/m^3 respectively. Accordingly, the lumped mass, and the mass moment of inertia at each floor are deduced as follows: $m_1 = 45.52$ kg $m_2 = 45.18$ kg , $m_3 = 45.52$ kg , $m_4 = 36.10$ kg , $m_5 = 43.22$ kg , $I_1 = 2.18$ kgm^2 , $I_2 = 2.21$ kgm^2 ,

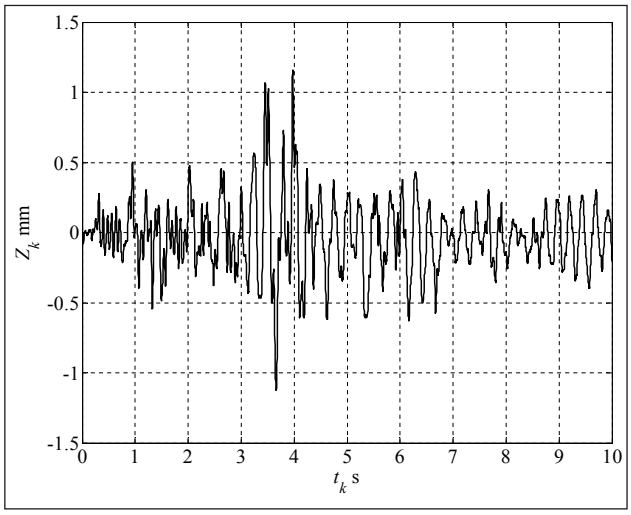

Figure 4. Section 4; measured inter-storey drift used for updating reliability.

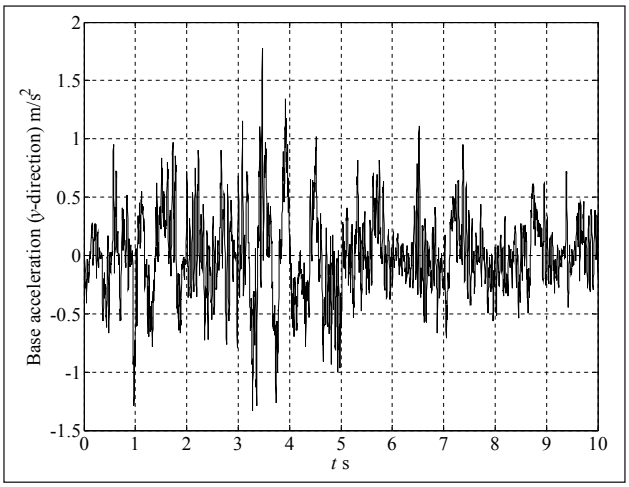

Figure 5. Section 4; measured base accelerationcorresponding to measurement used for system identification.

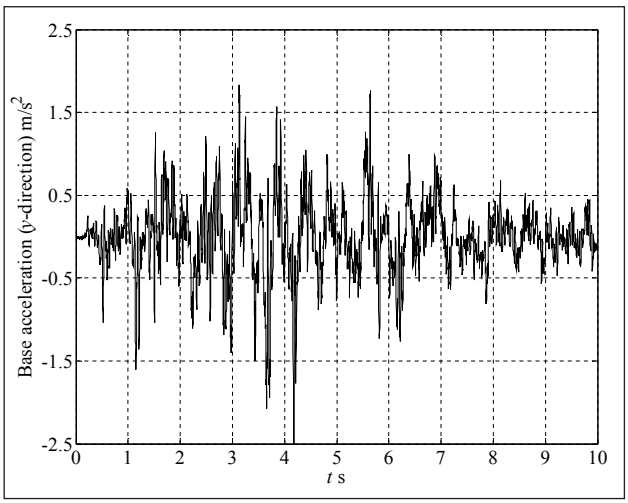

Figure 6. Section 4; measured base accelerationcorresponding to measurement used for updating reliability models.

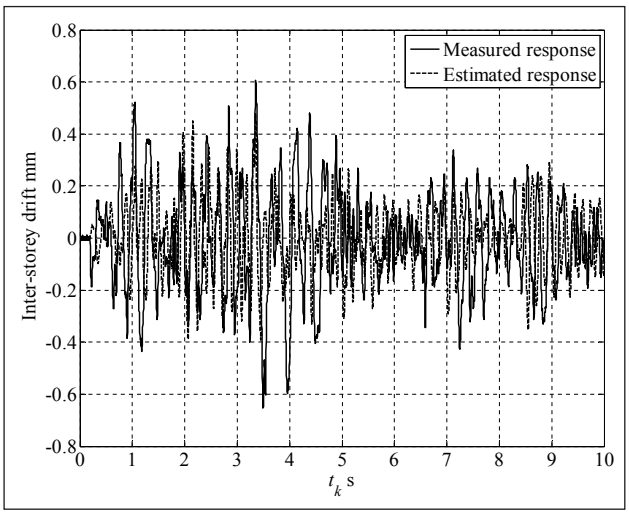

Figure 7. Section 4; comparison of measurement and estimated response

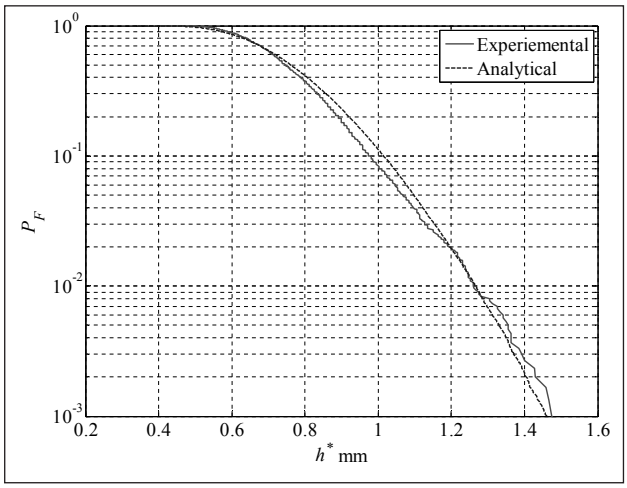

Figure 8. Section 4; comparison of probability of failure determined experimentally and estimated by using the identified model.

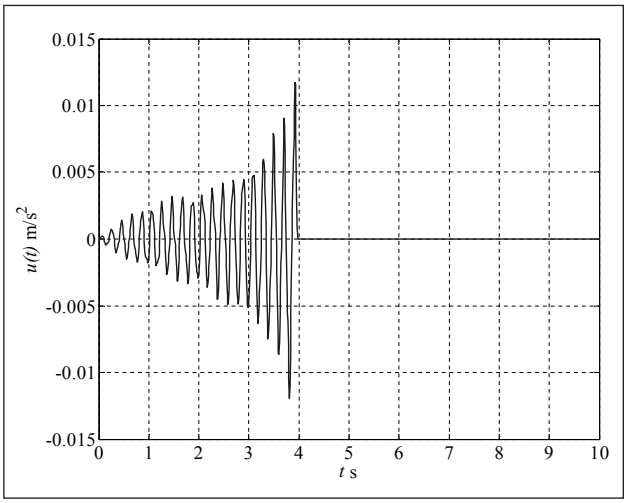

Figure 9. Section 4; control force; $h^* = 1.6$ mm; $\tau^m = 4.0$ s.

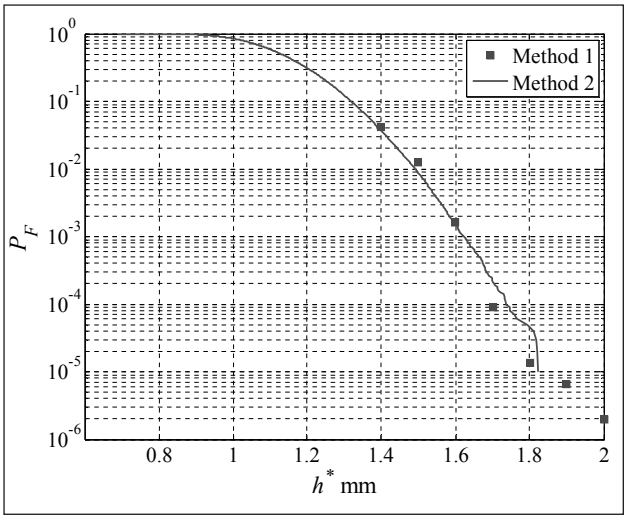

Figure 10. Section 4; estimates of conditional probability of failure.

$I_4 = 1.80\ \text{kgm}^2$, and $I_5 = 1.91\ \text{kgm}^2$. Similarly, the stiffness matrix, **K** is obtained as

The stiffness values in the x and y-directions have the units of MN/m and the torsional stiffness is in MNm/rad. The damping ratios for the fifteen modes are obtained as 0.0361, 0.0014, 0.0037, 0.0242, 0.0022, 0.0175, 0.0163, 0.0184, 0.0211, 0.0179, 0.0253, 0.0078, 0.0048, 0.0339, and 0.0045 respectively. From the above structural matrices, thefifteen natural frequencies are determined as 4.8021, 4.9246, 10.1820, 13.3615, 13.7879, 20.8248, 21.9023, 24.3520, 27.2877, 28.1258, 30.6755, 32.1236, 36.9902, 46.9998, and 55.1148 Hz.Comparison of the measured and estimated response of the inter-storey drift considered for identifying the system is shown in Fig. 7. Fig. 8 shows the comparison of the probability of failure determined experimentally [40] and analytically for different values of the threshold level, h^*. Based on the reasonably good mutual agreement between measured and estimated values evident in this figure, it is concluded that the task of system identification has been accomplished satisfactorily. The next step is to update the reliability model against future random excitations.

4.2 Reliability Model Updating

Measured inter-storey drift between fourth and fifth floors, as shown in Fig. 4 is considered for updating the reliability model. Similar to Eq. (20), the measurement equation is written as

$$Z_k = \boldsymbol{H}_k\left(\boldsymbol{Y}_k\right) + \mu_k,\ k = 1,2,\ldots \bar{N} \tag{22}$$

As before, the measurement noise is taken to be a zero mean Gaussian random process with variance $3.3344\times10^{-3}\ \text{mm}^2$. The performance function is taken to be in terms of the maximum inter-storey drift between fourth and fifth floors. Accordingly, the posterior reliability to be determined is given by

$$P_{S|\boldsymbol{Z}} = \text{P}\left\{\left[y_5(t) - y_4(t)\right] \le h^*\ \forall\ t \in [0,T]\ \middle|\ \boldsymbol{Z}_{1:\bar{N}}\right\} \tag{23}$$

The problem on hand is solved using Methods 1 and 2. The control needed to implement the Girsanov transformation for a threshold, $h^* = 1.6$, and for $\tau^m = 4$ s, is shown in Fig. 9. The conditional probability of failure is estimated using Methods 1 and 2 (10^5 samples) for different threshold values and is plotted in Fig. 10 which demonstrates a good agreement between the two methods. The estimate for Method 1 shown in the plot is the mean of five estimates obtained each with a sample size of 500.

5. Discussions and Conclusions

The numerical work associated with the illustration in section 4 was carried out on a Core ™ i5650 @ 3.20 GHz computer with 8 GB of RAM. The time taken for obtaining the probability of failure using brute force Monte Carlo simulation along with 10^5 number of samples is 43393.24. Whereas, the proposed method takes 2151.37 s (1435.20s for obtaining the control force and 716.17 for 500 number of simulations). It is important to note that these time requirements crucially depend on the sample sizes used and step sizes adopted in various time discretization steps. Within the framework of the choices made, it can be observed that the results from variance reduction (Method 1) show significant reduction in computational time of the order of 70% as compared to brute force Monte Carlo simulation (Method 2).

The work reported in this paper develops a framework for updating reliability models of linear dynamical systems when measured data on the system performance under operating loads become available. The framework combines dynamic state estimation methods with simulation based approaches in estimating the reliability of the system conditioned on measured data and for ensemble of future excitations. The contribution of the paper lies in demonstrating the method earlier developed by the authors to problems with experimental measurement data, and development of a frame work for the problem of combined system identification and reliability model updating.

References

1. Melchers R.E., "Structural Reliability Analysis and Prediction", 2nd edition, John Wiley & Sons, Chichester, 1999.
2. Yao J.T.P., "Safety and Reliability of Existing Structures", Pitman, Boston, 1985
3. Mori Y., and Ellingwood B., "Reliability-based service life assessment of aging concrete structures", ASCE Journal of Structural Engineering, Vol 119, No. 5, pp.1600-1621, 1993.
4. Ditlevsen O., and Madsen H.O., "Structural Reliability Methods", John Wiley & Sons, Chichester, 1996.
5. Melchers R.E., "Assessment of existing structures-approaches and research needs", ASCE Journal of Structural Engineering, Vol 127, No. 4, pp.406-411, 2001.
6. Frangopol D.M., Kallen M.J., and van Noortwijk J.M, "Probabilistic models for life-cycle performance of deteriorating structures: review and future directions," Progress in Structural Engineering and Materials, Vol 6, No. 4, pp.197-212, 2004.
7. Ellingwood B.R., "Risk-informed condition assessment of civil infrastructure: state of practice and research issues," Structure and Infrastructure Engineering, Vol 1, No. 1, pp. 7-18, 2005.
8. Yuen K.V., "Bayesian Methods for Structural Dynamics and Civil Engineering", John Wiley & Sons, Singapore, 2010.
9. Yuen K.V., and Kuok S.C., "Bayesian methods for updating dynamic models", Applied Mechanics Reviews, Vol 64, No. 1, pp. 010802-1-18, 2011.
10. Catbas F.N., Correa T.K., and Aktan A.E, "Structural Identification of Constructed Facilities," A state of art report by ASCE SEI Committee on Structural Identification of Constructed Systems, 2011http://www.cece.ucf.edu/people/catbas/St%20ID%20Report%20(Jan%2011%202011)%20ALL%20Chapters.pdf (as on 4th September 2013).
11. Ljung L.,"Asymptotic behavior of the extended Kalman filter as a parameter estimator for linear systems", IEEE Transactions on Automatic Control, Vol 24, No. 1, pp.36-50, 1979.
12. Wang D., and Haldar A., "An element level SI with unknown input information", ASCE Journal of the Engineering Mechanics Division,Vol 120, No. 1, pp.159-176, 1994.
13. Wang D., and Haldar A., "System identification with limited observations and without input",ASCE Journal of the Engineering Mechanics, Vol 123, No. 5, pp.504-511, 1997.
14. Ching J., Beck J.L., Porter K.A., and Shaikhutdinov, R., "Bayesian state estimation method for nonlinear systems and its application to recorded seismic response", ASCE Journal of Engineering Mechanics, Vol 132, No. 4, pp.396-410, 2006.
15. Ching J., Beck J.L., and Porter K.A., "Bayesian state and parameter estimation of uncertain dynamical systems", Probabilistic Engineering Mechanics, Vol 21, pp.81-96, 2006.
16. Ching J., Muto M., and Beck J.L., "Structural model updating and health monitoring with incomplete modal data using Gibbs sampler", Computer-Aided Civil and Infrastructure Engineering, Vol 21, No. 4, pp.242-257, 2006.
17. Nasrellah H.A., and Manohar C.S., "A particle filtering approach for structural system identification in vehicle-structure interaction problems", Journal of Sound and Vibration, Vol 329,pp.1289-1309, 2010.
18. Nasrellah H.A., and Manohar C.S.,"Particle filters for structural system identification using multiple test and sensor date: A combined computational and experimental study", Structural Control and Health Monitoring, Vol 18, No. 1, pp. 99-120, 2011.
19. Nasrellah H.A., and Manohar C.S., "Finite element based Monte Carlo filters for structural system identification", Probabilistic Engineering Mechanics, Vol 26, pp.294-307, 2011.
20. Maybeck P.S.,"Stochastic Models, Estimation, and Control", Volume 2, Academic Press, New York, 1982.
21. Ghanem R., and Shinozuka M., "Structural-system identification, I: Theory", ASCE Journal of Engineering Mechanics, Vol 121, No. 2, pp.255-264, 1995.
22. Shinozuka M., and Ghanem R.,"Structural-system identification, II: Experimental verification", ASCE Journal of Engineering Mechanics, Vol 121, No. 2, pp.265-273, 1995.
23. Andrieu C., and Doucet A., "Online expectation maximization type algorithms for parameter estimation in general state space models", IEEE International conference on Acoustic, Speech, and Signal processing, April 6-10, Vol 6, pp.69-72, 2003.
24. Ionides E.L., Breto C., and King A.A., "Inference for nonlinear dynamical systems", Proceedings of National Academy of Sciences, Vol 103, No. 49, pp.18438-18443, 2006.
25. Beck J.L., and Au S.K.,"Bayesian updating of structural models and reliability using Markov Chain Monte Carlo simulation", ASCE Journal of Engineering Mechanics, Vol 128, pp.380-391, 2002.
26. Kerschen G., Worden K., Vakakis A.F., and Golinval J.C., "Past, present and future of nonlinear system identification in structural dynamics", Mechanical Systems and Signal Processing, Vol 20, pp.505-592, 2006.
27. Khalil M., Poirel D., and Sarkar A.,"Parameter estimation of a fluttering aeroelastic system in the transitional Reynolds number regime", Journal of Sound and Vibration, Vol 332, pp.3670-3691, 2013.
28. Rosic B.V., Kucerova A., Sykora J., Pajonk O., Litvinenko A., and Matthies H.G., "Parameter identification in a probabilistic setting", Engineering Structures, Vol 50, pp.179-196, 2013.
29. Soyoz S., Feng M.Q., and Shinozuka M., "Structural reliability estimation with vibration-based identified parameters," ASCE Journal of Engineering Mechanics, Vol 136, No. 1, pp.100-106, 2010.
30. Sundar V.S., and Manohar C.S., "Time variant reliability model updating in instrumented dynamical systems based on Girsanov's transformation", International Journal of Non-linear Mechanics, Vol 52, pp.32-40, 2013.
31. Brown R.G., and Hwang P.Y.C., "Introduction to Random Signals and Applied Kalman Filtering", 3rd edition, John Wiley & Sons, New York, 1997.
32. Liu J.S.,"Monte Carlo Strategies in Scientific Computing", Springer, New York, 2001.
33. Macke M., and Bucher C.,"Importance sampling for randomly excited dynamical systems", Journal of Sound and Vibration, Vol 268, pp.269-290, 2003.
34. Olsen A.I., and Naess A., "Estimation of failure probability of linear dynamical systems by importance sampling," Sadhana, Vol 31, No. 4, pp.429-443, 2006.

35. Grigoriu M., "Stochastic Calculus: Applications in Science and Engineering", Birkhauser, Boston, 2002.
36. *Oksendal B., "Stochastic Differential Equations: An Introduction and Applications",6th edition, Springer, New York, 2003.*
37. Kloeden P.E., and Platen E., "Numerical Solution of Stochastic Differential Equations," Springer, Berlin, 1992.
38. Ibrahim R. A., "Recent results in random vibrations of nonlinear mechanical systems," ASME Special 50th Anniversary Design Issue, Vol 117, pp.222-233, 1995.
39. Clough R.W., and Penzien J., "Dynamics of Structures", McGraw Hill, New York, 1993.
40. Sundar V. S., and Manohar C.S., "Random vibration testing with controlled samples", Structural Control and Health Monitoring,Vol 21, No. 10, pp.1269-1283, 2014.

Life Cycle Reliability and Safety Engineering
Vol.4 Issue 1 (2015) 25-34

Health Assessment of Nonlinear Structural Systems

Abdullah Al-Hussein and Achintya Haldar*
Department of Civil Engineering and Engineering Mechanics, University of Arizona, P.O. Box 210072, Tucson, AZ 85721, USA;
**Email: haldar@u.arizona.edu*

Abstract

A novel structural health assessment procedure for nonlinear structural systems is presented. It is developed by integrating the unscented Kalman filter concept with the weighted global iteration procedure with an objective function. It is denoted as unscented Kalman filter with weighted global iteration (UKF-WGI). It is a finite elements-based time-domain system-identification technique. It can be used to assess structural health at the element level using only a limited number of noise-contaminated responses. The efficiency and accuracy of the procedure are demonstrated by identifying a realistic frame. Defect(s) with different level of severity is simulated in single and multiple member(s) and then the capabilities of the procedure are examined. The examples confirmed that the method is capable of identifying defect-free and defective states of structures. The proposed method is compared with the extended Kalman filter with weighted global iteration (EKF-WGI) procedure. The proposed UKF-WGI is superior to EKF-WGI in all aspects, particularly when the level of nonlinearity is severe. Since the level of nonlinearity is expected to be unknown at the initiation of the inspection, to be on the safe side, the proposed UKF-based procedure should be used to assess structural health in the future.

Keywords: ***Unscented Kalman filter, nonlinear structural system, structural heath assessment, damage detection, parameter identification***

1. Introduction

Structures deteriorate with time during their normal use. They also suffer damages when exposed to natural events like large earthquakes or high winds. Man-made events like impacts or explosions can also cause different levels of damages to them. To maintain the intended use of the structures and economic activities of the region, it is important to detect the location and severity of defects as early as possible to that required remedial actions can be promptly initiated. All defects are not equally important in maintaining the use of the structure. It is also important to decide whether the structure is beyond repair; it needs to be replaced. The topic has recently attracted serious multi-disciplinary research interests. This is generally known as structural health assessment (SHA) in the literature. Due to lack of available resources, developing objective SHA techniques is now one of the very active research areas in the profession. It has many different components including the study of structural behavior, development of sensors, presence of uncertainty in every phase of the investigations, and integrating all available information to objectively assess the current health of a structure. The authors and their team members are active in developing inspection-based SHA techniques. Some of their recent work is presented in this paper.

The most common technique used for SHA is the visual inspection or assessment. By tapping a structure and listening to the generated sound to assess its health was used over centuries. Obviously, its success will depend on the experience of the inspector. A structure consisting of numerous structural elements, SHA can be very challenging using visual inspections. If defects are hidden behind walls, fire proofing material, facades, etc., they cannot be visually inspected. Sometimes, some parts of the structure can be inaccessible. If visual inspection indicates the location and type of defects, and if they are accessible, we have technological sophistication to inspect them more thoroughly using many techniques including radiographs, magnetic, ultrasonic, etc. However, their success will depend on the knowledge of locations and types of defects a *priori*. For real civil engineering structures, this type of information will be unavailable in most cases. These are generally known as non-model approaches. Alternatives to visual or

specialized instrument-based techniques need to be developed.

To address numerous deficiencies of non-model based approaches, several model-based approaches were developed. The research team at the University of Arizona proposed several model-based approaches by representing structures by finite elements (FEs). The basic intent is that by tracking changes in the properties of these elements, the location and severity of defects can be detected. The FE-based formulation can be developed for the static or dynamic application of loading. Due to its numerous advantages, the formulation based on dynamic application of loading is very popular with researchers. Dynamic behavior can be studied in two ways: (a) frequency domain using modal properties and (b) time domain. Since modal properties represent global behavior, i.e., whether the structure is defect-free or defective without giving information on the structure at the local level, only time domain approaches were exclusively considered by the research team. It is not possible to present the state-of-the-art in the related areas here but it can be found in the literature [1-5].

2. Challenges in Structural Health Assessment

Before presenting a new concept, it is necessary to briefly discuss the challenges in structural health assessment and the contributions already made by the team. The overall basic idea in all activities of the team is related to the finite element-based time domain system identification (SI) concept and how to implement it in the most effective way. A typical SI-based concept has three essential elements: (a) characteristics of the dynamic loading to excite the structure, (b) the system to be identified, generally represented by finite elements, and (c) dynamic responses measured at different locations in the structure. By knowing the excitation and response information, the system can be identified using an inverse transformation technique. The signature hidden in the response time histories will give the information on the heath of the structure. The dynamic properties of a system are generally expressed in terms of mass, stiffness, and damping. The mass of elements is generally assumed to be known. At present, damping properties may not be confidently correlated with the damage state of a structure. Thus, by tracking the changes in the stiffness properties of elements, or using information on them from the previous inspections, if available, or deviation from other similar structural elements, the location and severity of defects can be assessed.

The concept appears to be straightforward. However, to increase its implementation potential, few challenges will have to be resolved. Outside the laboratory environment, it is extremely difficult to record excitation time history. Just after an earthquake, it may not even be available at the location of interest. It will be extremely desirable, if the system can be identified using only response information, completely ignoring the excitation information. It will be mathematically challenging since two of the three elements of SI will be unknown. It is also not possible to instrument the whole structure to collect response information. Thus, the structure needs to be identified using only limited responses measured at a small part of the structure. The dynamic responses, in our case, acceleration time histories must be measured by sensors (accelerometers). However, no sensor is noise-free. Thus, a structure needs to be identified using only a small number of noise-contaminated responses. Considering the complexity and nature of challenges, Maybeck [6] suggested that the SI-based concept might not be appropriate to assess structural health. The team successfully demonstrated that the above statement is not correct. If different sources of uncertainties are treated appropriately with advanced data processing algorithms and other innovative approaches, a system can be identified using the SI-based concept and thus the health of a structure can be assessed.

3. SHA approaches developed by the research team: a brief review

The team addressed all the challenges identified in the previous section. To address the excitation information-related problem, the team sequentially proposed several SI techniques with unknown input (UI). Using the least-squares based concept, the team members developed several techniques including iterative least-squares with unknown input (ILS-UI) [7], modified ILS-UI [8], generalized ILS-UI [9], and three dimensional generalized ILS-UI [10]. The measured response information can be noise-contaminated. The major weakness of these procedures is that they require dynamic response information to be available at all dynamic degrees of freedom (DDOFs). This led to the development of several procedures that can identify the structural system using only limited number of noise-contaminated responses. These procedures used the extended Kalman filter (EKF) concept. They are known as iterative least-squares extended Kalman filter with unknown input (ILS-EKF-UI) [11], modified ILS-EKF-UI [12], generalized

ILS-EKF-UI [13], and three dimensional generalized ILS-EKF-UI [14].

4. Necessity for a New SHA Procedure

All the discussions made in the previous sections are essentially for linear structural systems. Most civil structural systems behave nonlinearly; therefore, a new SI-based SHA procedure is necessary for highly nonlinear systems and it is presented in this paper.

The nonlinear system identification using measured dynamic responses has attracted attention of researchers in the last decades. Nonlinearity is generic in nature and linear behavior is an exception [15]. However, the estimation of nonlinear systems is not easy. There are many sources of uncertainties in the state of the system; model uncertainties, measurement uncertainties, and uncertainties due to different sources of noise acting on the system. To get the optimal solution to the nonlinear filtering problem, a complete description of the conditional probability density is necessary. Unfortunately, unbounded number of parameters is required to get the exact description [16]. Many techniques of suboptimal approximation have been developed for nonlinear structural system identification. Kerschen et al. [15] presented a review of the past and recent developments in system identification of nonlinear dynamical structures.

Of the various reported methods, the Kalman filter is one of the best known and widely used algorithms for SI. It is robust and requires only the first and second moment of probabilistic description because the filter is well established on the basis of the linear Gaussian assumption. For nonlinear SI, EKF was developed to account for the nonlinearities. The EKF accounts for nonlinearities by linearizing the system about its last-known best estimate with the assumption that the error incurred by neglecting the higher-order terms is small in comparison to the first-order terms. The basic Kalman filter is then applied to the linear system, resulting in a suboptimal solution. In the field of structural identification, EKF has been one of the most widely used tools. As mentioned earlier, it was used by the research team in the past and by other researchers [17-20]. Although EKF has been used successfully in many applications, in the presence of severe nonlinearities it can become unstable and accuracy of the estimates can be unacceptable.

Julier et al. [21-23] proposed the unscented Kalman filter (UKF) concept considering the fact that it is easier to approximate a probability distribution than to approximate an arbitrary nonlinear function. They used unscented transformation (UT) to make probabilistic inference. The unscented transformation uses a set of sample or sigma points that are determined from a *priori* mean and covariance of the state. The sigma points undergo the nonlinear transformation. Then the *posterior* mean and covariance of the state are determined from the transformed sigma points. This approach gives UKF better convergence characteristics and greater accuracy than EKF for nonlinear systems.

UKF has been shown to be a superior alternative to EKF in a variety of applications in the areas of nonlinear state estimation and parameter identification including nonlinear dynamical system identification, navigation and tracking, visual tracking, neural network training and position determination. Despite the fact that UKF apparently surpasses EKF, UKF has not been used widely in the field of civil engineering. Only few papers are available in the literature [24-27]. In all these studies, the UKF procedure was applied to simple structural systems, shear-type building, with a few dynamic degrees of freedom (DDOFs). This simplification may not represent the real structural systems. Damage detection was not considered in these applications. In addition, at least one of dynamic responses (displacement, velocity or acceleration) was assumed to be measured at all DDOFs. It makes the procedure difficult to implement for large structural systems. The authors [28, 29] addressed these deficiencies and introduced a weighted global iteration (WGI) procedure with an objective function into the UKF algorithm to obtain stable and convergent solutions. The integrated procedure is denoted as unscented Kalman filter with weighted global iteration (UKF-WGI). The WGI procedure with an objective function was first introduced by Hoshiya and Saito [18] in the EKF algorithm and denoted as extended Kalman filter with weighted global iteration (EKF-WGI).

In the following sections, the mathematical concept of UKF enhanced by WGI is briefly presented followed by several illustrative examples to verify and compare with EKF-based approaches and to demonstrate the implementation potential of the concept.

5. Mathematical Formulation

The UKF-WGI procedure is generally used when the response information is limited and noise contaminated. The use of UKF-WGI also helps to

incorporate error in the basic mathematical model representing the structure as well as the presence of noise in the response information. To implement any UKF-based approach, the excitation information and the state vector must be available. Obviously, the excitation information is unknown in the proposed approach. Also, at the initiation of the inspection, the vector will be unknown; it needs to be identified for SHA. The authors generated the necessary information using a substructure approach and the ILS-UI approach by considering responses are measured at a small part of a structure. The identification of the substructure produces the information on the excitation. It also helps to estimate the initial state vector. The procedure is discussed in detail by the authors elsewhere [28, 29]. Using the information on excitation and state vector, the whole structure can be identified by the UKF-WGI procedure. The mathematics behind UKF-WGI is emphasized in the following discussions. As mentioned earlier, the locations and severity of defects are assessed by comparing the identified stiffness parameters with expected or previous values if inspected previously, or deviation from other similar structural elements.

5.1 Concept of UKF Procedure

For the implementation of UKF procedure, it is necessary to describe the dynamic system by a set of nonlinear differential equations expressing in the state-space form as:

$$\dot{\mathbf{X}}_t = f(\mathbf{X}_t, t) \tag{1}$$

where $\mathbf{X}_t$ is the state vector at time t; $\dot{\mathbf{X}}_t$ is the time derivative of the state vector; f is a nonlinear function of the state; and $\mathbf{X}_t$ can be mathematically expressed as:

$$\mathbf{X}_t = \begin{bmatrix} \mathbf{X}(t) \\ \dot{\mathbf{X}}(t) \\ \widetilde{\mathbf{K}} \end{bmatrix} \tag{2}$$

where $\mathbf{X}(t)$ and $\dot{\mathbf{X}}(t)$ are the vectors containing displacement and velocity responses of the system, respectively, at time t; and $\widetilde{\mathbf{K}}$ vector contains the unknown system parameters.

Equation (1) can be rewritten as:

$$\dot{\mathbf{X}}_t = \begin{bmatrix} \dot{\mathbf{X}}(t) \\ \ddot{\mathbf{X}}(t) \\ 0 \end{bmatrix} = \begin{bmatrix} \dot{\mathbf{X}}(t) \\ -\mathbf{M}^{-1}\left[\mathbf{K}\mathbf{X}(t) + (\alpha\mathbf{M} + \beta\mathbf{K})\dot{\mathbf{X}}(t) - \mathbf{f}(t)\right] \\ 0 \end{bmatrix} \tag{3}$$

where $\mathbf{M}$ and $\mathbf{K}$ are the global mass and stiffness matrix, respectively; $\mathbf{f}(t)$ is the input excitation vector at time t; and α and β are the mass and stiffness proportional Rayleigh damping coefficients, respectively.

The nonlinear discrete time measurements with additive noise at $t = k\Delta t$ can be expressed as:

$$\mathbf{Y}_k = h(\mathbf{X}_k, \mathrm{t}) + \mathbf{V}_k \tag{4}$$

where h is the function that relates the state to the measurement; $\mathbf{X}_k$ is the state vector at $t = k\Delta t$; Δt is the constant time increment; and $\mathbf{V}_k$ is a vector of zero mean white noise Gaussian processes with covariance matrix $\mathbf{R}_k$. The noise covariance matrix is generally assumed to be diagonal. In the present study, the value of diagonal entries of $\mathbf{R}_k$ is considered to be 10^{-4}.

To initiate the filtering algorithm, it is necessary to have an initial estimate of the uncertain state vector. The initial value of displacement and velocity not measured at DDOFs can be assumed to be zero. The initial value of stiffness parameters for the whole structure was considered to be their theoretical value of defect-free case.

The initial error covariance matrix contains information on the errors in the observed displacement and velocity responses and in the initial values assigned to the unknown stiffness parameters of the whole structure. It is generally assumed to be a diagonal matrix with positive numbers. Jazwinski [30] and Al-Hussein and Haldar [29] pointed out that the diagonal entries for the covariance values for the system parameters should be large positive numbers to accelerate the convergence of the iteration process. A value of 1000 is used in this study.

The UKF procedure comprises three steps as following [31, 32]:

a. Sigma vector calculation step

At current state vector $\widehat{\mathbf{X}}_{k|k}$, sets of $2n+1$ symmetric sigma vectors are generated so that they have the same mean and covariance of $\widehat{\mathbf{X}}_{k|k}$ as following:

$$\begin{aligned} \boldsymbol{\chi}_{0,k|k} &= \widehat{\mathbf{X}}_{k|k} \\ \boldsymbol{\chi}_{i,k|k} &= \widehat{\mathbf{X}}_{k|k} + \sqrt{(\lambda + n)}\,\mathbf{C}_{col.i} \qquad i = 1, \ldots, n \\ \boldsymbol{\chi}_{i+n,k|k} &= \widehat{\mathbf{X}}_{k|k} - \sqrt{(\lambda + n)}\,\mathbf{C}_{col.i} \qquad i = 1, \ldots, n \end{aligned} \tag{5}$$

where $\lambda = \varphi^2(n+\gamma) - n$; n is the dimension of the state vector; φ is a scaling parameter which determines the spread of the sigma points; γ is a secondary scaling parameter; $\mathbf{C}$ is a square root of the covariance matrix such that $\mathbf{P}_k = \mathbf{C}\mathbf{C}^{\mathbf{T}}$; and $\mathbf{C}_{col.i}$ is the i^{th} column of $\mathbf{C}$'s matrix. Note that $\mathbf{P}_k$ must be symmetric and positive definite which allows us to find the square root using Cholesky decomposition.

b. Prediction step

In the prediction step, it is necessary to transform the sigma vectors through the nonlinear dynamic equation as:

$$\boldsymbol{\chi}_{i,k+1|k} = \boldsymbol{\chi}_{i,k|k} + \int_{k\Delta t}^{(k+1)\Delta t} f(\mathbf{X}_t, t)dt \qquad i = 0, \dots, 2n \tag{6}$$

The predicted state vector can be shown to be:

$$\widehat{\mathbf{X}}_{k+1|k} = \sum_{i=0}^{2n} W_i \, \boldsymbol{\chi}_{i,k+1|k} \tag{7}$$

and its predicted error covariance matrix is:

$$\mathbf{P}_{k+1|k} = \sum_{i=0}^{2n} W_i \left(\boldsymbol{\chi}_{i,k+1|k} - \widehat{\mathbf{X}}_{k+1|k}\right)\left(\boldsymbol{\chi}_{i,k+1|k} - \widehat{\mathbf{X}}_{k+1|k}\right)^T + (1 - \varphi^2 + \delta)\left(\boldsymbol{\chi}_{0,k+1|k} - \widehat{\mathbf{X}}_{k+1|k}\right)\left(\boldsymbol{\chi}_{0,k+1|k} - \widehat{\mathbf{X}}_{k+1|k}\right)^T \tag{8}$$

where δ is a parameter added to the weight on the zeroth sigma point of the calculation of the covariance. The weight factor W_i can be shown to be:

$$W_0 = \frac{\lambda}{\lambda + n} \qquad i = 0 \tag{9}$$

$$W_i = \frac{1}{2(\lambda + n)} \qquad i = 1, \dots, 2n$$

For the measurement model, acceleration time-histories will be measured during an inspection. Then the acceleration time-histories will be successively integrated to obtain velocity and displacement time-histories [33-35]. Therefore, the discrete time measurement model can be expressed in a linear form as:

$$\mathbf{Y}_k = \mathbf{H} \cdot \mathbf{X}_k + \mathbf{V}_k \tag{10}$$

where $\mathbf{Y}_k$ is the measured displacement and velocity at $t = k\Delta t$; and $\mathbf{H}$ is the measurement matrix.

Since the measurement model is linear, Kalman filter (KF) will be used to compute the predicted measurement vector, its error covariance and cross correlation matrix as suggested by Hao et al. [36] instead of using the sigma points used in the UKF algorithm.

The predicted measurement vector $\widehat{\mathbf{Y}}_{k+1|k}$ can be expressed as:

$$\widehat{\mathbf{Y}}_{k+1|k} = \mathbf{H}\widehat{\mathbf{X}}_{k+1|k} \tag{11}$$

and its error covariance matrix $\mathbf{P}_{k+1}^{\mathrm{YY}}$ as:

$$\mathbf{P}_{k+1}^{YY} = \mathbf{H}\mathbf{P}_{k+1|k}\mathbf{H}^T + \mathbf{R}_{k+1} \tag{12}$$

and the cross correlation matrix $\mathbf{P}_{k+1}^{\mathrm{XY}}$ can be estimated as:

$$\mathbf{P}_{k+1}^{XY} = \mathbf{P}_{k+1|k}\mathbf{H}^T \tag{13}$$

c. Updating step:

The state vector and the error covariance matrix are updated as follows:

$$\mathbf{K}_{k+1} = \mathbf{P}_{k+1}^{XY}(\mathbf{P}_{k+1}^{YY})^{-1} \tag{14}$$

where $\mathbf{K}_{k+1}$ is the Kalman gain matrix.

$$\widehat{\mathbf{X}}_{k+1|k+1} = \widehat{\mathbf{X}}_{k+1|k} + \mathbf{K}_{k+1}\left(\mathbf{Y}_{k+1} - \widehat{\mathbf{Y}}_{k+1|k}\right) \tag{15}$$

$$\mathbf{P}_{k+1|k+1} = \mathbf{P}_{k+1|k} - \mathbf{K}_{k+1}\mathbf{P}_{k+1}^{YY}\mathbf{K}_{k+1}^{I} \tag{16}$$

where $\widehat{\mathbf{X}}_{k+1|k+1}$ is the updated state vector and $\mathbf{P}_{k+1|k+1}$ is the updated error covariance matrix.

5.2 Integration of Weighted Global Iteration Procedure with UKF

The iteration processes between successive time points in the UKF procedure, i.e. generating sigma vectors, prediction, and updating steps, are termed as local iterations and the iteration processes for all q time points in the time history are termed as a global iteration. After the initial values are assigned to the state vector and its error covariance matrix, the local iterations are successively carried out for each q time point used in the identification to complete the first global iteration. To implement the next global iterations, the authors [29] incorporated the weighted global iteration with an objective function in the UKF algorithm to obtain a stable and convergent solution. In the second global iteration, the initial values of the stiffness parameters are the same as that of obtained

at the completion of first global iteration. A weight factor w is introduced in the stiffness covariance matrix obtained at the completion of the first global iteration to amplify it and then used it as the initial stiffness covariance in the second global iteration. The same processes of local iterations are carried out for all the time points and a new set of state vector and error covariance matrix are obtained at the completion of second global iteration. The global iteration processes are continued until the estimated error in the identified stiffness parameters at the end of two consecutive global iterations becomes smaller than a predetermined convergence criterion (ε). If they diverge, the best estimated values based on minimum objective function $\bar{\theta}$ are considered, as discussed elsewhere by Hoshiya and Saito [18].

6. Verification of the Proposed UKF-based Approach and Comparison with Previous EKF-based Approach

Before the proposed UKF-based approach can be accepted, it needs verifications by identifying relatively large realistic structures exhibiting nonlinear behavior. To establish its superiority, it is also necessary to compare the identified results with the EKF-based procedure. For appropriate verification, both defect-free and defective states of the structure are considered. For the defective state, the presence of one or multiple defects of different levels of severity is considered. The optimum number of dynamic responses required to identify structural parameters is used in all cases.

6.1 Description of the Frame

A one-bay three-story steel frame, as shown in Figure 1, is considered. The same frame was tested in the laboratory by the research team at the University of Arizona [37]. To fit the testing facilities, the frame was scaled to one-third of its actual dimensions. The scaled frame has a bay width of 3.05 m and story height of 1.22 m. The frame consists of 9 members; 6 columns and 3 beams. Steel section of size S4x7.7 was used for all the beams and columns in order to minimize the effects of fabrication defects and differences in material properties. The frame is represented by the finite element (FE) with 9 elements and 8 nodes. Each node has three DDOFs; two translational and one rotational. The support condition at the bases is considered to be fixed. Therefore, the total number of DDOFs for the frame is 18. The actual stiffness parameters k_i, defined in terms of $(E_i I_i/L_i)$, for the beam and column are estimated to be 96500 N-m and 241250 N-m, respectively. The first two natural frequencies of the defect-free frame are estimated to be f_1 = 9.90 Hz and f_2 = 34.77 Hz. Then, the two Rayleigh damping coefficients α and β are estimated using the procedure suggested by Clough and Penzien [38]. The value of α and β is found to be 1.1628328 and 0.00008559, respectively for an equivalent modal damping of 1.201%. The frame is excited by a sinusoidal load $f(t)$ = 1400 sin (58.23t) N applied at node 1 as shown in Figure 1. For the theoretical verification of the methods, the responses of the frame in the presence of geometric nonlinearity are numerically generated using a commercial software ANSYS (ver. 15.0) [39]. The responses in terms of displacement, velocity and acceleration time histories are collected at 9 DDOFs (responses at nodes 1, 2 and 3). The responses used in the health assessment process are from 0.02 to 0.32s with time increment of 0.00025s providing a total of 1201 time points.

6.2 Health Assessment of Frame

The capabilities of the proposed UKF and EKF-based procedures are examined in this paper by considering the following cases:

1. Defect-free and a small defect in a single member
2. Moderate to severe defect in a single member
3. Defects in multiple members

6.2.1 Defect-free and a small defect in a single member

The optimum number of responses required to identify the frame is found to be 9. Using only responses at 9 DDOFs (nodes 1, 2 and 3), the stiffness parameters of all members in the frame are identified for the defect-free state and the results are summarized in Table 1, Column 3. The maximum error in the identification (percentage changes in identified stiffness parameters with respect to the actual values) is about 0.1%. The acceptable error in the identification process was reported to be about 10% [40, 41]. Obviously, the proposed UKF-WGI is very accurate. Since the identified stiffness parameter did not vary significantly from one member to another and from the expected values, the proposed method correctly identified the defect-free state of the frame.

The same frame is then identified using the EKF-WGI procedure and the results are summarized in Column 4 of Table 1. The maximum error in the identification is about 0.8%. It is still within the acceptable level but not as good as the proposed

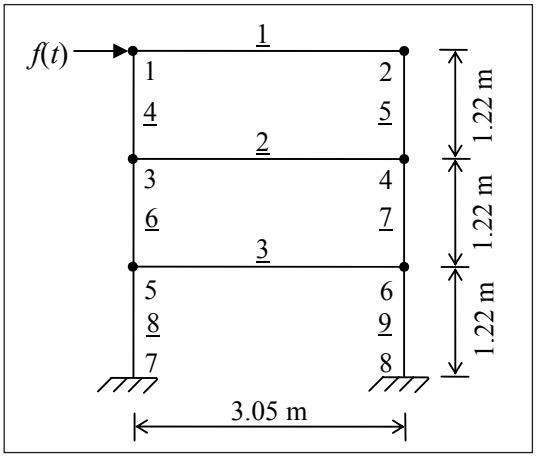

Figure 1. Finite element representation of three-story frame

Table 1. Change (%) in identified stiffness parameter (*EI/L*) for defect-free and small defect cases

Member	Theoretical (N-m)	Defect-Free		Defect 1		Defect 2	
		UKF	EKF	UKF	EKF	UKF	EKF
(1)	(2)	(3)	(4)	(5)	(6)	(7)	(8)
k_1	96500	0.0	-0.1	-0.1	0.0	0.1	0.2
k_2	96500	0.0	0.2	0.1	0.1	-0.1	-0.5
k_3	96500	0.0	-0.2	-4.3	-4.3	-9.6	-9.1
k_4	241250	0.0	-0.1	0.1	-0.1	0.2	-0.1
k_5	241250	0.1	*-0.8*	-0.1	*-0.8*	0.2	-0.5
k_6	241250	0.1	0.1	-0.2	-0.1	0.1	-0.2
k_7	241250	0.0	-0.2	0.0	-0.2	0.0	-0.3
k_8	241250	0.0	0.2	-0.3	-0.1	-0.5	-0.5
k_9	241250	0.0	0.1	-0.3	-0.2	-0.4	*-0.6*

Table 2. Change (%) in identified stiffness parameter (*EI/L*) for moderate to severe defect cases

Member	Theoretical (N-m)	Defect 3		Defect 4		Defect 5	
		UKF	EKF	UKF	EKF	UKF	EKF
(1)	(2)	(3)	(4)	(5)	(6)	(7)	(8)
k_1	96500	0.2	-1.6	-0.5	-7.2	**-79.9**	**-80.4**
k_2	96500	-0.4	2.9	**-29.3**	**-19.9**	-0.5	6.7
k_3	96500	**-19.1**	**-23.1**	-1.1	-17.8	0.7	-16.9
k_4	241250	0.4	-2.3	-0.5	-5.9	0.0	-0.2
k_5	241250	0.5	*-5.1*	-1.0	-15.0	0.8	-15.7
k_6	241250	-0.2	4.8	1.9	17.5	-0.5	15.1
k_7	241250	0.1	-2.8	-1.3	-27.0	1.8	-13.0
k_8	241250	-0.9	2.4	-0.6	*46.7*	-1.1	*47.7*
k_9	241250	-0.9	2.0	1.9	-10.0	-0.1	-17.2

Table 3. Change (%) in identified stiffness parameter (*EI/L*) for multiple defects

Member	Theoretical (N-m)	Defect 6		Defect 7		Defect 8	
		UKF	EKF	UKF	EKF	UKF	EKF
(1)	(2)	(3)	(4)	(5)	(6)	(7)	(8)
k_1	96500	**-60.1**	**-62.0**	-0.2	-7.5	**-30.0**	**-34.7**
k_2	96500	**-29.7**	**-23.2**	**-24.8**	**-14.2**	**-20.0**	**-9.8**
k_3	96500	-0.8	-16.4	**-15.0**	**-32.2**	**-9.9**	**-27.6**
k_4	241250	-0.2	-3.9	-0.1	-6.7	0.1	-5.8
k_5	241250	-0.6	-14.8	-0.2	-15.8	0.2	-15.9
k_6	241250	1.0	18.9	0.7	19.3	0.3	19.8
k_7	241250	-0.4	-21.8	-0.4	-21.2	0.0	-20.5
k_8	241250	0.3	*44.3*	-0.4	*37.8*	-0.3	*36.9*
k_9	241250	0.8	-12.3	0.0	-3.1	-0.1	-3.0

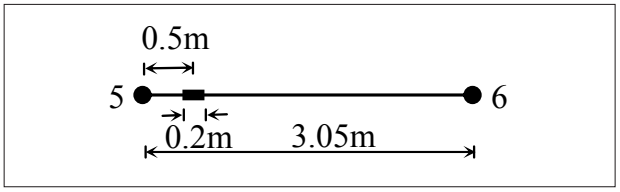

Figure 2. Defect 1 representation

method. For this case also, the defect-free state can be predicted but with less confidence.

After the successful verification of the defect-free state, the following two defect scenarios are considered:

a. Defect 1 - loss of cross-sectional area over a finite length in member 3

b. Defect 2 – reduction in stiffness of member 3 by 10%

For Defect 1, the cross-sectional area of member 3 is considered to be corroded over a length of 20 cm, located at a distance of 0.5 m from node 5, as shown in Figure 2. The web and flange thicknesses are considered to be reduced by 40% of their original values. The loss of thicknesses will result in the reduction of the cross-sectional area by 38.70% and the moment of inertia by 35.46% from the nominal values. For Defect 2, the moment of inertia of member 3 over the entire length is considered to be reduced by 10% of the defect-free value.

Using only responses at 9 DDOFs (nodes 1, 2 and 3), the stiffness parameters of all members in the frame are identified for the above-mentioned two cases using both UKF and EKF-based procedures and the results

are summarized in Table 1. The results indicate that both the UKF and EKF-based procedures identified the location and severity of defects correctly. However, UKF-WGI appears to be superior to EKF-WGI in identifying Defect 2.

It can be concluded that both methods are capable of identifying defect-free and defective states of the frame but the proposed method appears to be better than EKF in the overall sense.

6.2.2 Moderate to severe defect in a single member

In this case, the following three defective scenarios are considered:

a. Defect 3 - reduction in stiffness of member 3 by 20%
b. Defect 4 - reduction in stiffness of member 2 by 30%
c. Defect 5 - reduction in stiffness of member 1 by 80%

In these defects, the moment of inertia of the member over the entire length is considered to be reduced by the specified percentage from the defect-free value. The results of all three defects using UKF-WGI and EKF-WGI are summarized in Table 2. For Defect 3 with 20% reduction, both procedures appear to locate the defective member correctly. However, in detecting the severity of the defect, EKF-WGI is less accurate. Also, by considering the changes in the stiffness parameter of all the members, EKF-WGI is less conclusive. Differences of the two approaches become very significant for Defects 4 and 5. In fact, one can conclude that EKF-WGI failed to identify the defective states. Changes in the stiffness parameter for defect-free members for Defect 4 are higher than the defective member. For Defect 5, one can erroneously conclude that more than one member are defective. An inspector should not have any such assessment difficulties if UKF-WGI is used. The proposed method is accurate and superior to EKF-WGI in every aspect.

6.2.3 Defects in multiple members

In this case, the following three defective scenarios are considered:

a. Defect 6 - reductions in stiffness of members 1 and 2 by 60 and 30%, respectively
b. Defect 7 - reductions in stiffness of members 2 and 3 by 25 and 15%, respectively
c. Defect 8 - reductions in stiffness of members 1, 2, and 3 by 30, 20, and 10%, respectively

In these defects, the moment of inertia of more than one member over the entire length is considered to be reduced by the specified percentage from the defect-free value. The identified stiffness parameters of all the members for all the defect scenarios using UKF-WGI and EKF-WGI are summarized in Table 3. All the observations made for Defects 3- 5 in the previous section are also applicable for these defective states. The proposed UKF-WGI not only identified the defective members correctly, it also estimated the severity of the defects accurately. On the other hand, EKF-WGI failed to identify the frame and cannot be used for the SHA of the frame under consideration.

From the examples given in the paper and considering other examples given by the team using EKF-WGI elsewhere, it can be concluded that the applicability of the two procedures will depend on the level of nonlinearity. Both methods will be appropriate for linear or mildly nonlinear cases. However, since the level of nonlinearity is expected to be unknown at the initiation of the inspection, to be on the safe side, the UKF-based proposed procedure should be used to assess structural health in the future.

7. Conclusions

A novel structural health assessment procedure for nonlinear structural systems is presented. It is developed by integrating the unscented Kalman filter concept with the weighted global iteration procedure with an objective function. It is denoted as unscented Kalman filter with weighted global iteration (UKF-WGI). It is a finite elements-based time-domain system-identification technique. It can be used to assess structural health at the element level using only a limited number of noise-contaminated responses. The efficiency of the procedure is demonstrated by identifying a realistic frame. Defect(s) with different level of severity is simulated in single and multiple member(s) and then the capability of the procedure is examined. The examples confirmed that the method is capable of identifying defect-free and defective states of structures. The proposed method is compared with the EKF-WGI procedure. The proposed UKF-WGI is superior to EKF-WGI in all aspects, particularly when the level of nonlinearity is severe. Since the level of nonlinearity is expected to be unknown at the initiation of the inspection, to be on the safe side, the proposed UKF- based procedure should be used to assess structural health in the future.

Acknowledgments

This study is based on work partly supported by the Iraq's Ministry of Higher Education and Scientific Research. Any opinions, findings, conclusions, or recommendations expressed in this paper are those of the writers and do not necessarily reflect the views of the sponsor.

References

1. Doebling S. W., Farrar C. E., and Prime M. B., "A Summary Review of Vibration-Based Damage Identification Methods," The Shock and Vibration Digest, Vol. 30, No. 2, pp. 91-105, 1998.
2. Sohn H., Farrar C. R., Hemez F. M., Shunk D. D., Stinemates D. W., Nadler B. R., and Czarnecki J. J., "A Review of Structural Health Monitoring Literature: 1996-2001," Los Alamos National Laboratory, LA-13976-MS, 2004.
3. Fan W. and Qiao P., "Vibration-Based Damage Identification Methods: A Review and Comparative Study," Structural Health Monitoring, Vol. 10, No. 1, pp. 83-111, 2011.
4. Haldar A. and Das A. K., "Past, Present, and Future of Structural Health Assessment," Proceedings of International Symposium on Engineering under Uncertainty: Safety Assessment and Management (ISEUSAM), Shibpur, India, 2012a.
5. Haldar A. and Das A. K., "Past, Present, and Future of Structural Health Assessment," International Journal of Life Cycle Reliability and Safety Engineering, Vol. 1, No. 4, pp. 33-43, 2012b.
6. Maybeck P. S., "Stochastic Models, Estimation, and Control Theory," Academic Press, Inc., UK, 1979.
7. Wang D. and Haldar A., "Element-Level System Identification with Unknown Input," Journal of Engineering Mechanics, ASCE, Vol. 120, No. 1, pp. 159-176, 1994.
8. Ling X. and Haldar A., "Element Level System Identification with Unknown Input with Rayleigh Damping," Journal of Engineering Mechanics, ASCE, Vol. 130, No. 8, pp. 877-885, 2004.
9. Katkhuda H., Martinez-Flores R., and Haldar A., "Health Assessment at Local Level with Unknown Input Excitation," Journal of Structural Engineering, ASCE, Vol. 131, No. 6, pp. 956-965, 2005.
10. Das A. K. and Haldar A., "Structural Integrity Assessment under Uncertainty for Three Dimensional Offshore Structures," International Journal of Terraspace Science and Engineering (IJTSE), Vol. 2, No. 2, pp. 101-111, 2010.
11. Wang D. and Haldar A., "System Identification with Limited Observations and without Input," Journal of Engineering Mechanics, ASCE, Vol. 123, No. 5, pp. 504-511, 1997.
12. Ling X., "Linear and Nonlinear Time Domain System Identification at Element Level for Structural Systems with Unknown Excitations," PhD Dissertation, Department of Civil Engineering and Engineering Mechanics, University of Arizona, Tucson, Arizona, 2000.
13. Katkhuda H. and Haldar A., "A Novel Health Assessment Technique with Minimum Information," Structural Control and Health Monitoring, Vol. 15, No. 6, pp. 821-838, 2008.
14. Das A. K. and Haldar A., "Health Assessment of Three Dimensional Large Structural Systems - A Novel Approach," Life Cycle Reliability and Safety Engineering, Vol. 1, No. 1, pp. 1-14, 2012.
15. Kerschen G., Worden K., Vakakis A. F., and Golinval J. C., "Past, Present and Future of Nonlinear System Identification in Structural Dynamics," Mechanical Systems and Signal Processing, Vol. 20, No. 3, pp. 505-592, 2006.
16. Julier S. J. and Uhlmann J. K., "A New Extension of the Kalman Filter to Nonlinear Systems," Proceedings of Aerospace/Sense: The 11th Int. Symp. On Aerospace/ Defence Sensing, Simulation and Controls, 1997.
17. Yun C. B. and Shinozuka M., "Identification of Nonlinear Structural Dynamic Systems," Journal of Structural Mechanics, Vol. 8, No. 2, pp. 187-203, 1980.
18. Hoshiya M. and Saito E., "Structural Identification by Extended Kalman Filter," Journal of Engineering Mechanics, ASCE, Vol. 110, No. 12, pp. 1757-1770, 1984.
19. Loh C. H. and Tsaur Y. H., "Time Domain Estimation of Structural Parameters," Engineering Structures, Vol. 10, No. 2, pp. 95–105, 1988.
20. Koh C. G. and See L. M. "Identification and Uncertainty Estimation of Structural Parameters," Journal of Engineering Mechanics, ASCE, Vol. 120, No. 6, pp. 1219-1236, 1994.
21. Julier S. J., Uhlmann J. K., and Durrant-Whyte H., "A New Approach for Filtering Nonlinear Systems," In Proceedings of the American Control Conference, pp. 1628-1632, 1995.
22. Julier S. J. and Uhlmann J. K., "New Extension of the Kalman Filter to Nonlinear Systems," Proc. SPIE 3068, Signal Processing, Sensor Fusion, and Target Recognition VI, Vol. 182, pp. 182-193, 1997.
23. Julier S., Uhlmann J., and Durrant-Whyte H. F., "A New Method for the Nonlinear Transformation of Means and Covariances in Filters and Estimators," IEEE Transactions on Automatic Control, Vol. 45, No. 3, pp. 477-482, 2000.
24. Mariani S. and Ghisi A., "Unscented Kalman filtering for nonlinear structural dynamics," Nonlinear Dynamics, Vol. 49, No. 1, pp. 131-150, 2007.
25. Wu M. and Smyth A.W., "Application of the Unscented Kalman Filter for Real-Time Nonlinear Structural System Identification," "Structural Control and Health", Vol. 14, No. 7, pp. 971–990, 2007.
26. Chatzi E. N. and Smyth A. W., "The Unscented Kalman Filter and Particle Filter Methods for Nonlinear Structural System Identification with Non-Collocated Heterogeneous Sensing," Structural Control and Health Monitoring, Vol. 16, No. 1, pp. 99-123, 2009.
27. Chatzi E. N., Smyth A. W., and Masri S. F., "Experimental Application of On-Line Parametric Identification for Nonlinear Hysteretic Systems with Model Uncertainty," Journal of Structural Safety, Vol. 32, No. 5, pp. 326–337, 2010.
28. Al-Hussein A. and Haldar A., "A Novel Unscented Kalman Filter for Health Assessment of Structural Systems with Unknown Input," Journal of Engineering Mechanics, ASCE, 2015a, (accepted for publication).
29. Al-Hussein A. and Haldar A., "Unscented Kalman Filter with Unknown Input and Weighted Global Iteration for Health Assessment of Large Structural Systems," Structural Control and Health Monitoring, 2015b, (under review).
30. Jazwinski A. H., "Stochastic Process and Filtering Theory," Academic Press, Inc., UK, 1970.
31. Al-Hussein A., Das A. K., and Haldar A., "A New Approach for Structural Health Assessment Using Unscented Kalman Filter," 11th International Conference on Structural Safety

and Reliability (ICOSSAR'13), Columbia University, New York, N.Y., 2013.

32. Al-Hussein A. and Haldar A., "A New Extension of Unscented Kalman Filter for Structural Health Assessment with Unknown Input," in Sensors and Smart Structures Technologies for Civil, Mechanical, and Aerospace Systems, Proceedings of SPIE Vol. 9061, 2014c.
33. Vo P. H. and Haldar A., "Post Processing of Linear Accelerometer Data in System Identification," Journal of Structural Engineering, Vol. 30, No. 2, pp. 123-130, 2003.
34. Das A. K., "Health Assessment of Three Dimensional Large Structural Systems Using Limited Uncertain Dynamic Response Information", PhD Dissertation, University of Arizona, Tucson, AZ, 2012.
35. Haldar A., Das A. K., and Al-Hussein A., "Data Analysis Challenges in Structural Health Assessment Using Measured Dynamic Responses," Advances in Adaptive Data Analysis, Vol. 5, No. 4, pp. 1-22, 2013.
36. Hao Y., Xiong Z., Sun F., and Wang X., "Comparison of Unscented Kalman Filters," Proc. IEEE Int. Conf. Mechatron. Autom., Harbin, China, pp. 895-899, 2007.
37. Martinez-Flores R. and Haldar A., "Experimental Verification of a Structural Health Assessment Method without Excitation Information," Journal of Structural Engineering, Vol. 34, No. 1, pp. 33-39, 2007.
38. Clough R. W. and Penzien J., "Dynamics of Structures," Third Edition, Computers and Structures, CA, USA, 2003.
39. ANSYS version 15.0, The Engineering Solutions Company, 2013.
40. Toki K., Sato T., and Kiyono J., "Identification of Structural Parameters and Input Ground Motion from Response Time Histories," Structural Engineering / Earthquake Engineering, Vol. 6, No. 2, pp. 413-421, 1989.
41. Koh C. G., See L. M., and Balendra T., "Estimation of Structural Parameters in Time Domain: A Substructure Approach," Earthquake Engineering and Structural Dynamics, Vol. 20, No. 8, pp. 787-801, 1991.

Life Cycle Reliability and Safety Engineering
Vol.4 Issue 1 (2015) 35-43

Performance of Alternative Wavelet Basis for Feature Based Damage Detection in Structures

Suprateek Roy[1], Sudib K. Mishra[1]*, Subrata Chakraborty[2]
[1]Department of Civil Engineering, Indian Institute of Technology, Kanpur, UP, India,
[2]Department of Civil Engineering, Indian Institute of Engineering Science and Technology, Shibpur, Howrah, West Bengal, India,
[*]Email: smishra@iitk.ac.in

Abstract

The Wavelet Transforms have been used to enhance damage sensitive features for structural health monitoring. Although, the Continuous Wavelet Transforms have also been employed, the Discrete Wavelet Transform (DWT) becomes a natural choice in view of its capability to optimally localize the space/time and frequency/scale resolution. Whereas, a number of alternative DWT families exist; the choice of a particular basis for enhancement of damage features is somehow arbitrary. In the present study, the feature enhancement capability of several most commonly employed wavelet families are compared in order to assess their relative efficacy. The superior performance of Cohen-Daubechies-Feauveau family is observed and appears to be the sole choice where the damage onset is at immediate vicinity of the boundary. The relative efficiencies of enhancements are demonstrated considering the possible variations of the damage locations, extents, as well as alternate features.

Keywords: Damage Detection, Wavelets, Mode Shape Curvature, Damage Feature, Sensitivity analysis

1. Introduction

Assessment of structural health and prognosis becomes an increasing concern to the structural engineering research community. This includes detection, classification, identification of location and determination of severity of damage, estimation of the remaining service life and if necessary proposing suitable retrofitting options. Though, the traditional nondestructive techniques are quite popular for the detection of damage in structures, they required manual intervention and can only identifies local damage. The aim of modern Structural Health Monitoring (SHM) is the real time, automatic and continuous assessment of structures in service with minimum manual intervention. They also aim to be global i.e. can detect damage in any location of the structure. Further, the SHM methodologies must be robust i.e. tolerant to environmental noise. Therefore, the research in modern SHM strives at exploring and deriving features from the structural response, which can faithfully indicate the onset of structural damage.

A number of investigations in search of damage sensitive features have been taken up in the past. A brief review of these can be seen in Doebling et al. [1]. Most of these features are based on measured vibration signal of the structure and the typical features are based on changes in their natural frequencies, mode shapes [2], changes in modal curvature [3], changes in Frequency Response Function (FRF) [4] and so on. All such features are based on the assumption that the changes in the properties of the structure are essentially reflected in changes of these parameters. Although these techniques perform well in some cases, they often suffer from the fact that it is not easy to extract local information caused by small damage from modal parameters, which is rather a global characteristic [5]. The development of time domain based methodologies in the recent past which do not require data reduction and feature extractions is notable. The time domain approach was employed for damage detection in beam using vibration data with a moving oscillator as an excitation source [6]. The time domain methodology has been extended to damage detection in smart structures [7] as well. Time domain identification of structure by Extended Kalman Filter was introduced by Hoshiya and Saito [8]. This has been extended and generalized by Ling and Haldar [9], which was also validated experimentally by Vo and Haldar [10]. More details on time domain based

methodology can be obtained from Sohn and Farrar [11].

The wavelet transform has been appeared to be one of the most prominent techniques[12,13]to enhance the sensitivity of damage features with respect to the incipient damage in structures. Wang and Deng [5] proposed a damage detection technique using Wavelet and demonstrated it on a damaged beam with a crack. The technique avoids complete analysis of structure and does not require prior knowledge on the reference structure. Hou et al. [12] demonstrated the Wavelet based approach for structural damage detection with reference to a model, consisting of multiple breakable springs, to show the effectiveness of the technique in detecting fatigue induced damage. It is shown that the technique is robust against noise intensity and damage severity. The relatively lower frequency resolution capability of Wavelet transforms have been overcome by usage of Wavelet Packet Transform, as reported by Sun and Chang [13] for SHM applications. In their study, the Wavelet packet based damage features were corroborated to the damage severity through regression analysis by means of Neural Network. The Wavelet based damage detection methodology has been implemented in frame structure by Ovanesova and Suarez [14]. The two dimensional Haar wavelet has been used by Kim et al. [15] for nondestructive damage evaluation of plates using multi-resolution analysis. Rucka and Wilde [16] studied the application of Continuous Wavelet Transform in vibration based damage detection of beams and plates, considering the mode shapes containing the damage features. The Wavelet Transform of the mode shape difference has been identified as a potential damage feature by Poudel et al. [17]. Although, the mode shape curvature has been well established as an effective damage feature, Wang and Qiao [18] has shown the potential of the irregularity in mode shapes as a good damage indicator in beam, achieved through Wavelet based processing of irregular profile.

The choices of Wavelet basis are somewhat arbitrary in most of the aforementioned studies. In certain instances, the Continuous Wavelet family has been adopted, whereas, in others, the Discrete Wavelet Transform is a choice. In both the discrete and continuous Wavelet Transform, specific basis has also been used for extraction of damage sensitive features. The usage of Wavelet is attractive due to the fact that the Wavelet transforms are quite efficient to amplify the hidden singularities in the response signal of the structure [19]. Further, the Wavelets also pose excellent capability of localizing an event in time and/or space, which make effective for analysis of non-stationary signals [20]. However, with these facts, the choice of the class of Wavelet or particular basis function for this purpose is still somewhat ad hoc in nature. A particular choice does not essentially ensure that for a given scenario, the selection of basis is optimal. In this context, it is of worth mentioning here that a number of studies have been reported in the past on the optimal selection of wavelet basis for various other applications for example in signal de-noising [21], texture classifications [22] and multi-scale data representation [23]. Motivated with these applications, the feature enhancement capabilities of most commonly employed wavelet families are compared in this study to assess their relative efficacy. For demonstration purpose, the well acclaimed modal curvature difference (with respect to reference structure) and its hierarchical scale-wise wavelet decompositions are adopted as the damage sensitive features. The superior performance of Cohen-Daubechies-Feauveau (CDF) family is observed and appears to be the sole choice where the damage onset is at immediate vicinity of the boundary. The relative efficiencies of enhancements are demonstrated with regard to the possible variations of damage locations, extents as well as alternate feature.

2. Background and Formulations

2.1 Mode Shape Curvature as a damage sensitive feature

The mode shapes of a structure are obtained by solving the respective generalized eigenvalue problem as:

$$[K]\{\phi\} = \omega^2 [M]\{\phi\} \tag{1}$$

The relevant formulations are available in standard textbooks [24] of structural dynamics. For damage assessment purpose, the mode shape values at particular modes are obtained from experimental measurements by modal testing. The details of Modal testing and relevant analysis procedure of the measured data can be found elsewhere [25]. Once the mode shape for any i^{th} mode (denoted as $\phi^{(i)}$) is obtained, its curvature can be numerically evaluated in finite difference form as:

$$\phi''^{(i)}_{,jj} = \left(\phi^{(i)}_{j+1} - 2\phi^{(i)}_{j} + \phi^{(i)}_{j-1}\right) \Big/ \left(\Delta x\right)^2 \tag{2}$$

in which double subscripts of j refers to the second order derivative with respect to the spatial coordinate j and Δx is the spatial resolution of the mode shape. The mode shape curvature is related to the flexural stiffness of beam section as:

$$\phi'' = (M/EI) \tag{3}$$

Where, M is the bending moment at a section, E is the modulus of elasticity, and I is the second moment of inertia of the cross sectional area. The reason of sensitivity of mode shape curvature to the damage is due to the reduction in flexural rigidity (EI), which leads to locally increased curvature around the location of damage. Therefore, the mode shape curvature feature becomes useful for detecting and localizing damage. Furthermore, the change in the mode shape curvature can be correlated to the changes in the flexural rigidity (EI), from which an estimate of the extent of damage can be derived.

It may be noted here that the present study does not emphasize or advocate for the usage of only modal curvature feature, but adopt this as a feature to demonstrate the wavelet enhancement of the feature sensitivity with respect to damage. In fact, as far as the wavelet enhancement is concerned, any damage feature can be adopted for the purpose and the present formulation is not restricted to any particular damage feature.

2.2 Feature Enhancement by the Wavelet Transform

The Wavelet Transform is an important mathematical tool for multi-resolution analysis to represent hierarchical data. The transform uses certain wavelet basis which are derived from basic templates by scaling and shifting the respective mother wavelets. A variety of different wavelet exists and particular families of wavelet are suitable over the others for case specific applications. The major advantage of wavelet analysis of a function is that it enables one to extract and examine its features on different scales and locations. In one dimension, a continuous wavelet $\psi(x)$ transforms a function $f(x)$ as [19,20]:

$$W_f(a,b) = \int_{-\infty}^{\infty} f(x)\psi_{a,b}(x)\,dx \tag{4}$$

The two-parameter family of functions, $\psi_{a,b}(x)$ is derived from a single mother wavelet function ($\psi_{a,b}(x)$) as:

$$\psi_{a,b}(x) = \left(1/\sqrt{a}\right)\psi\left[(x-b)/a\right] \tag{5}$$

In the above, the symbol a refers to a scaling factor used for dilation and b is a translational factor. The factor $\left(1/\sqrt{a}\right)$ outside is included for normalization. The parameter a can take any positive real value and the fluctuations of $f(x)$ at position b are measured at scale a. All the wavelet transform algorithms essentially perform the convolution operations expressed in equation (4) by some form or others. Once the transform coefficients $(W_f(a,b))$ are available along all the scales a (with positions b), it is possible to reconstruct f at a range of scales for x between s_1 and s_2 $(s_1 \le s_2)$ through the inverse wavelet transform as:

$$f_{s_1,s_2}(x) = (1/c_\psi)\int_{s_1}^{s_2}\int_{-\infty}^{\infty} W_f(a,b)/\psi_{a,b}(x)\,db\,da/a^2 \tag{6}$$

Where c_ψ is a constant evaluated from the properties of the wavelet basis.

The wavelets can be broadly categorized as continuous or discrete wavelets. In continuous wavelet, the wavelet basis function is expressed as a continuous function whereas, the discrete wavelets are expressed as a discrete filters defined by the coefficients' values and positions. An arbitrary level of frequency resolution is possible to attain through the Continuous Wavelet Transform (CWT), whereas, the Discrete Wavelet Transform (DWT) will only provide the transform in terms of a number of discrete scales, the resolution of which is dictated by the sampling resolution of the function/ signal and the resolution of that scale. Unlike the spectrum of scales (frequencies) provided by the CWT, the DWT optimally adjust its localization in space/time and in frequencies/scales. In doing so, a balance must be established between the two, since arbitrary resolution cannot be achieved. An improved resolution in one is always at the expense of compromise in the other, which is analogous to the uncertainty principle (resolution in position and momentum) in quantum mechanics [26].

The DWT algorithm is implemented as a fast algorithm. A digitized function of length n is alternatively convolved with the low and high pass filters to result into fine and coarse information respectively, which are subsequently grouped into two halves of length $(n/2)$ by down sampling the signal. The process is repeated by choosing the next coarser part of the signal of length $(n/2)$. At the end, a number of scales containing increasingly finer and coarser information are obtained. The aforementioned DWT operation for obtaining hierarchical scale-wise

decompositions of a signal is schematically shown in Figure 1.

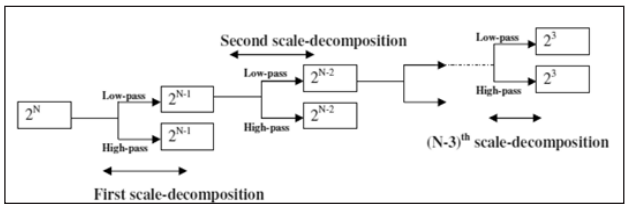

Figure 1: Hierarchical scale-wise decomposition of a function through DWT

Although the application of CWT in SHM is reported in literature [16], the DWT is naturally a better choice for feature enhancement, keeping in view the ability of DWT to localize the scale/frequency and time/location of a signal/field variations in an optimal manner [26, 27]. However, there exist a number of discrete wavelet families to carry out the DWT, which are broadly classified as orthogonal and bi-orthogonal wavelets. In the Orthogonal wavelet the basis wavelets (i.e. the analysis filter for the forward transform and the synthesis filter for the inverse wavelet transform) are orthogonal. Whereas in Bi-orthogonal two different sets of filters are employed, in which, the analysis and synthesis filters are mutually orthogonal among themselves. Thus requires two set of orthogonality conditions to be satisfied. Due to this, the bi-orthogonal wavelets allow more degrees of freedom than the orthogonal wavelets while designing the filter and hence allow the possibility of designing symmetric filter [23, 28].

The wavelets transform defined until now assume that the function is either periodic and/or fixed at its ends. Most of these wavelet transform cannot take care of the finite interval on which the signal/field is defined. Recently, some special class of wavelets are developed which are defined on the exact interval of the real line, termed as Wavelets in the interval, which can adaptively adjust their number of coefficients in the filter as it perform the convolution operations increasingly closer to the boundaries [29]. The Bi-orthogonal family offers such flexibility for treatment of the finite boundary, while designing/modifying the filters for wavelet transform near the boundary.

This class of wavelets is designed based on lifting scheme, which also offer much convenience for developing such wavelets. One of the earliest wavelet that was defined on the interval was that of CDF wavelet, which is adopted in the present study for processing the damage feature for enhancement. Such class of wavelet, due to their capability of exactly representing the data on and around the immediate vicinity of the boundary is expected to perform better when the damage is particularly localized around the boundaries of the domain. The underlying analysis filters (CDF filter) are shown in Figure 2(a) and 2(b). The symmetric nature of these wavelets is particularly notable as offered by the bi-orthogonal family only. However, near the boundary of the signal the filters modify its length and value of the coefficients as well. The details of such wavelet can be found elsewhere [27, 29].

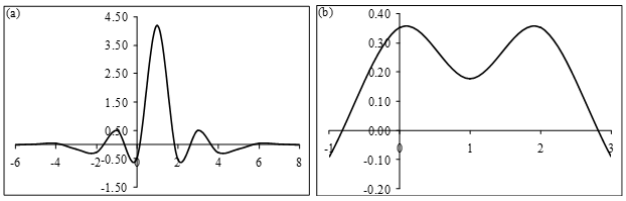

Figure 2: The analysis wavelet filters for the CDF wavelets

With the above discussion in view, the wavelet transform from various families have been applied on the mode shape curvature based damage feature to enhance the sensitivity of the same. The feature enhancements are qualitatively presented in the subsequent discussion. A comparison among the relative enhancements is also presented in order to identify the best suitable family of wavelet basis for such purposes.

3. Wavelet Based Enhancement of Mode Shape Curvature Based Damage Feature

The difference in the i^{th} mode shape curvature can be evaluated as:

$$\left\{\Delta\phi''\right\}^i = \left\{\phi_d''\right\}^i - \left\{\phi_u''\right\}^i \tag{7}$$

Where, $\left\{\phi_d^{ii}\right\}^i$ and $\left\{\phi_u^{ii}\right\}^i$ are the i^{th} mode shape curvatures of the damaged and undamaged structure, respectively. These can be readily obtained from equation (2) using $\left\{\phi_d\right\}^i$ and $\left\{\phi_u\right\}^i$, the i^{th} mode shape from the damaged and undamaged structure. This provides a legitimate damage feature as indicated by many investigators [3]. This is chosen as the feature for demonstration of further enhancement that can be achieved through wavelet transform technique.

In this context, it is worth mentioning that the difference in modal curvature itself is an excellent feature to detect and localize damage in structure and further enhancement of the feature might not be necessary except in some pathological cases. One such case is considered herein which the damage lays at

the boundary of the structural domain. Although the efficacy of the wavelet enhancement is demonstrated here with respect to the mode shape curvature feature, the procedure is general enough to be applied to any type of damage feature and can be useful in enhancing features to facilitate damage detection and localization which is otherwise not possible or obscure in many circumstances. Once established, the wavelet based enhancement and the optimal choice of the underlying wavelet basis for the same can be extended for more cases where the identification of damage through conventional damage feature poses problem.

The wavelet transform is applied on the difference in the mode shape curvature, and the respective vector quantity is decomposed into number of scales (denoted by $s_l, l \in 1,n$) following the fast DWT algorithm as

$$W_{\left\{\Delta\phi''\right\}^i}(s,x) = W_{\left\{\Delta\phi''\right\}^i}(s_1,x) \otimes W_{\left\{\Delta\phi''\right\}^i}(s_2,x) \otimes \ldots\ldots\ldots \otimes W_{\left\{\Delta\phi''\right\}^i}(s_n,x) \tag{8}$$

Where $W_{\left\{\Delta\phi''\right\}^i}(s,x)$ is the wavelet transform of the difference in mode shape curvature along n number of scales $(s \in s_1 \otimes s_2 \ldots . s_n)$ and spatial coordinates with varying degree of resolutions, given as $2^n\Delta x, 2^{n-1}\Delta x, \ldots\ldots, 2\Delta x$ in the transformed domain. Thus, each of these transformed scales represents the transformed data in varying resolution $\left(2^{l-1}\Delta x\right)$ and varying scale (s_l).

It is well known that the wavelets are good in exploring hidden singularity in the signal at the transformed domain. This particular property is relied on in employing the wavelet transform for feature enhancement. The degree of enhancement can be expressed as:

$$E^i_{w,j}(s_l,x_j) = \left(W_{\left\{\Delta\phi''\right\}^i_j}(s_l,x_j) \Big/ \left\{\Delta\phi''\right\}^i_j \right) \tag{9}$$

It depends on the mode shape considered for modal curvature, the wavelet scale (s_l) and the spatial coordinate (x_j). It is obvious that for curvature corresponding to a particular mode shape (i) and wavelet scale (s_l), the feature enhancement is provided by a vector of length equal to that of the spatial coordinates (x_j) and a damage in any location of the structure (such as beam, plate and shells), will be reflected by the sudden jump in the feature. Such singularity/jump will be significantly amplified in its enhanced form than its corresponding value in its respective base feature.

Before presenting the wavelet based feature enhancement, the capability of exploring/enhancing singularity in a signal, through wavelet transform is demonstrated by taking a simple and most commonly adopted example, the Dirac delta function or singularity function, which takes a value of unity at its support ($x = x_0$) and elsewhere it is zero, i.e.

$$\delta(x - x_0) = \begin{cases} 1 & x = x_0 \\ 0 & x \neq x_0 \end{cases}$$

The Wavelet transform (with Daubechies basis 6.8) of the same is presented in Figure 3 along hierarchy of scales with varying spatial resolutions along the scales. It is observed that, as one moves from coarser (low frequency resolution) to finer (higher frequency resolution) scales, the spatial resolutions get compromised. The implications of this in feature enhancement (the singular function is the feature itself) is that with increasingly finer scales, the enhancement increases (as shown by the numerical values) but that is simultaneously accompanied by an increasingly reduced level of localization capability. The enhancement is evaluated and its efficiency is demonstrated in enhancing the feature in the following section for case specific damage scenarios.

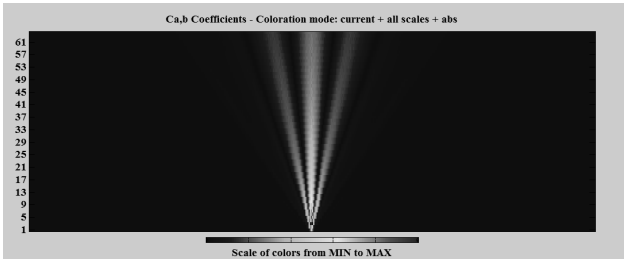

Figure 3: Schematic of the wavelet enhancement, presented in terms of wavelet transform of singular function

4. Numerical Illustration and Discussions

A cantilever beam is selected for numerical illustration on the present Wavelet based damage feature enhancement strategy. The idealized beam is inflicted with artificial damage by locally reducing its stiffness, i.e. its flexural rigidity (EI). The respective mode shapes are obtained by modal analysis. The curvature of the mode shapes are then obtained by finite difference approximation. First, the damage is inflicted at the middle of the beam and the respective modal curvature values at different nodes along the length of the beam are processed through the DWT. The beam is discretized into 512 numbers of nodes for finite element based analysis used for demonstration

Table1: Scale-wise enhancement of damage feature for alternative wavelet families

Scale	Spatial resolution (Δx)	Orthogonal		Bi-orthogonal		CDF	
		$\max\left(W_{\{\Delta\phi^{''}\}_j^i}\right)$	$\max\left(E_{w,j}^i\right)$	$\max\left(W_{\{\Delta\phi^{''}\}_j^i}\right)$	$\max\left(E_{w,j}^i\right)$	$\max\left(W_{\{\Delta\phi^{''}\}_j^i}\right)$	$\max\left(E_{w,j}^i\right)$
0	$32\,\Delta x$	-0.0159	110.5974	0.04055	544.6793	0.0706	799.7615
1	$32\ \Delta x$	0.02186	91.8418	0.05546	184.6975	0.0835	278.1366
2	$16\ \Delta x$	0.02778	138.9493	0.07204	218.4493	0.0911	276.3821
3	$8\ \Delta x$	0.03306	123.1602	0.08158	297.4308	0.0865	315.3744
4	$4\ \Delta x$	0.03478	126.2369	0.06148	232.1592	0.0588	222.0589
5	$2\ \Delta x$	0.02713	124.3579	0.01487	48.9159	0.0149	48.9160

purpose. In this regard, it is worth mentioning that it is often practically not feasible to instrument a realistic structure with many numbers of sensors to get its responses at all nodes. The wavelet analysis of the data, on the other hand, requires sufficient data length for its processing through fast algorithms. In such situation, some expansion technique must be employed in order to extend the measured data to sufficient length to make it amenable to wavelet processing [30,31].

The mode shapes of damaged and undamaged structures are processed for their curvatures and the differences are obtained. The enhancement of this feature, as attained through alternative families of wavelet transforms are shown in Figure 4(b), whereas the feature itself (difference in mode shape curvature) is shown in Figure4(a).The particular wavelet basis that has been employed in generating these plots are Daubechies 4, bi-orthogonal spline10.4 and CDF 4.6 [19,20].

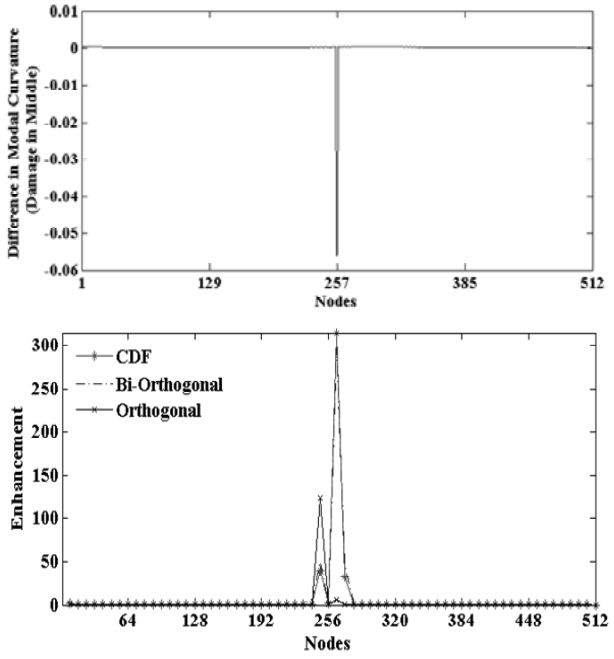

Figure 4: (a) Difference in the first mode shape curvature with damaged location at the middle and (b) Enhanced feature through hierarchical scale-wise decomposition through alternative wavelet transforms

Although the difference in the mode shape curvature itself has been proved to be an excellent candidate for feature based detection of damage, the present results show that the sensitivity of the same has been improved by an order of magnitude (around 300) with the application of the Wavelet Transform. Further, all the wavelets are not equally effective in enhancing the feature. Figure4(b) clearly indicates to the relative superiority of the CDF Wavelet over the Orthogonal or Bi-orthogonal ones. Also notable is the much improved efficiency of enhancement attained through the Bi-orthogonal family while compared with its orthogonal counterparts.

It must be mentioned here that the wavelet enhanced feature as depicted in Figure4(b) belongs to a specific scale for each family of wavelets. However, it is observed that the specific scale at which the maximal enhancement occurs varies from one wavelet family to the others. The scale-wise variations of such enhancement are further illustrated in Table 1 for each wavelet family. It is observed that the maximum enhancement in each wavelet family corresponds to different scale, which may be termed as the dominant scale for enhancement of damage features. Results in Table 1 also clearly show that the enhancement capability of the Bi-orthogonal family is much more than the orthogonal ones and the maximum enhancement is obtained by using the CDF family, which is a special class of bi-orthogonal wavelet defined on the exact interval of the real line.

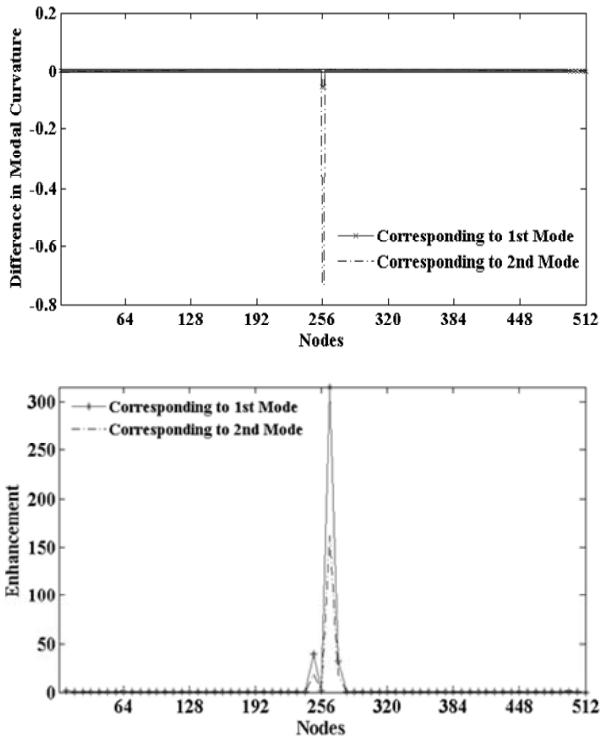

Figure 5: (a) Difference in higher mode shape curvature (second and third mode) with damaged location at the middle and (b) Enhanced feature through hierarchical scale-wise decomposition through alternative wavelet transforms

The wavelet based feature enhancement capability is further studied with respect to the same modal curvature but corresponds to higher modes (the second and third modes) which can be treated as alternate features. The difference in mode shape curvature from these two higher modes are shown and compared in Figure 5(a), whereas the respective mode specific wavelet enhancements are shown in Figure 5(b). As it is already established from the previous results (Figure 4(b)) that the CDF is the preferred choice among the other alternative wavelet family, the results from the CDF is only presented and compared in these plots. It is observed that the mode shape curvature in higher modes (second/third modes) shows much higher sensitivity in their respective feature value. However, comparing their wavelet enhanced counterparts, it can be inferred that the first mode enrichment rather shows better feature than the higher (second) mode enrichment. In this regard, it is important to note that, though the sensitivity of the mode shape curvature feature increases substantially in increasingly higher modes, exciting the structure in higher modes poses difficulty [25]. Thus, the wavelet feature enhancement to provide much better feature in the first mode itself (over the higher ones) provide an important alternative to bypass the requirement and difficulties associated with exciting the higher modes in search for more sensitive damage feature.

Until now, the discussion is limited to the damage that are occurring in the mid span (or close to the mid span) or far from the boundaries of the structure. In next, the damage at the immediate vicinity of the boundary of the domain is considered. The cantilever with a localized damage very close to the free end is considered. Respective difference in mode shape curvature value is then obtained and shown in Figure 6(a). It is observed that the damage near the boundary cannot be represented by the mode shape curvature feature, as there is no marked discrepancies (singularity) observed in the plot, which is unlike to the observations made earlier (Figure 4(a)), in case of damage in the middle of the domain or at

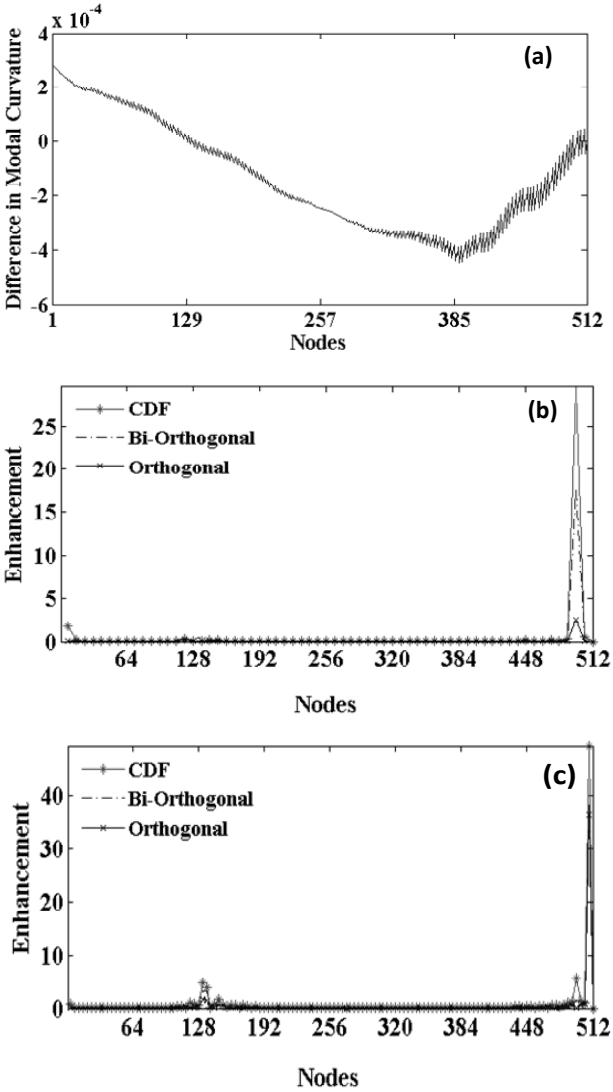

Figure 6: (a) Difference in Mode Shape curvature for a beam damaged at the boundary and respective wavelet enhanced feature (b) at scale resolution 64Δx) and (c) at scale (128Δx)

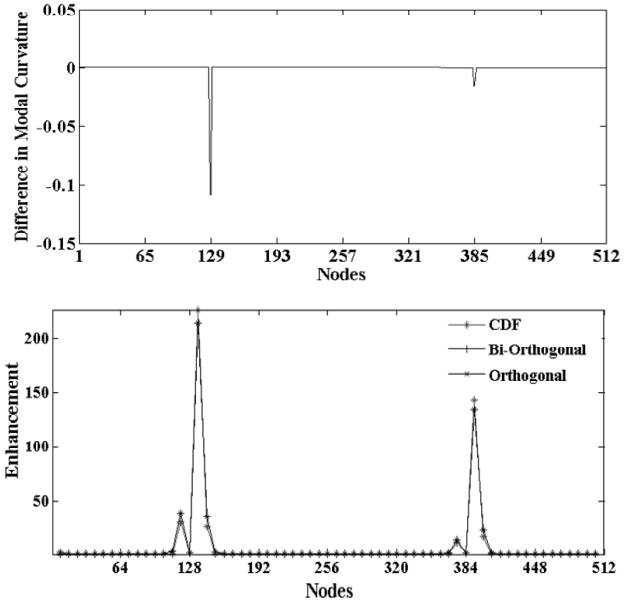

Figure 7: Multiple damage scenarios and their reflections in the (a) Difference in mode shape curvature (b) Wavelet enhancement of the same feature using alternative family of wavelets

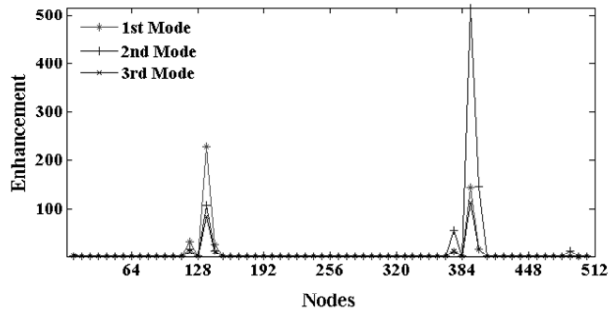

Figure 8: Comparison of wavelet based feature enhancement in different modes

least not arbitrarily close to the domain boundary. Thus, the mode shape curvature cannot serve as a legitimate candidate as a sensitive feature that can indicate damage near the boundary. The three classes of wavelet families are then tried to see their consequences. Respective wavelet enhanced features at two different scales are shown and compared in Figures6(b) and 6(c). It is observed that though the mode shape curvature difference fails, its wavelet enhancement is able to provide a feature which can clearly indicate the presence of damage around the boundary. The superior performance of CDF is also notable to represent this kind of damage. Although the bi-orthogonal family provides the feature at certain scales, it has been observed (but not shown herein) that the behavior of the enhanced features along the hierarchy of scales is not consistent. Thus the CDF appears to be the only option for such damage scenario. The reason for the superiority of CDF over the other is due to the fact that this particular wavelet family is exactly defined over the finite interval [28,29] and the respective transform can exactly represent the minute details at the boundary, which is not possible to achieve by using the other class of wavelet basis.

The performance of the wavelet enhancement scheme is further tested in case of multiple damage scenarios. The damage is initiated in two segments of the beam, at 1/3 and 2/3 of the span. The magnitudes of damage, as defined by the respective reductions in stiffness properties of the section are adopted to be identical. Respective difference in the mode shape curvatures are shown in Figure 7(a), in which the occurrence of the damage are clearly reflected by the two jumps. The enhancements of these features are further achieved following the procedure of wavelet transform, and the enhanced features are shown in Figure 7(b).It can be observed that the enhancements are achieved for both the damage scenarios as reflected in the peaks shown in Figure 7(b). However, comparisons among the various wavelet families show that the CDF and the bi-orthogonal basis provide much better enhancement of the feature than the orthogonal one. Further, the CDF basis performs better than the bi-orthogonal. These results clearly indicate the feature enhancement efficiency offered by the CDF over the orthogonal family in case of multiple damage scenarios.

The efficiency of enhancement attained through CDF wavelet families in different modes are now compared in Figure 8. In general, it is noted that the higher modes provide better localization and indication of damage. However, after enhancement, it is observed that the enhanced features do not significantly vary from one mode to another and the lower modes (preferably the fundamental mode) can also be as efficient as the higher ones provided the modal feature extracted from this is used in conjunction with the wavelet enhancement.

5. Conclusions

An attempt has been made to compare the feature enhancement capability of several most commonly employed wavelet families in order to assess their relative efficacy. The results from the study provide some insights about the relative efficacy of alternative wavelet basis in enhancing/extracting damage sensitive features useful to detect, localize and quantify damage. It is demonstrated than in general transform based on the bi-orthogonal wavelet family provides better results than the orthogonal basis for enhancing

damage features. In particular, the CDF family is found to be superior for this purpose. Further, the CDF family, which is defined on the exact interval of the real line, takes care of the finite length of the structural domain and becomes the only choice to detect damage features in case the damage is localized in the boundary regions. The robustness of the feature enhancement technique as presented is also verified by numerical studies involving variations in the extent, location and number (single/multiple) of damage. Although the conclusion in the present study is solely based on the mode shape curvature based feature, the findings from this study can be useful for selection of specific wavelet family in order to enhance/extract damage features, which are otherwise difficult to assess.

References:

1. Doebling S. W., Farrar C. R., Primee M. B., Shevitz D. W., "Damage Identification and Health Monitoring of Structural and Mechanical Systems from Changes in Their Vibration Characteristics: A Literature Review", Report LA-13070-MS, UC-900, Los Alamos National Laboratory, New Mexico, 1996.
2. Salawu O. S., "Detection of Structural Damage Through Changes in Frequency: A Review", Engineering Structure, 19,9,718-723,1997.
3. Pandey A. K., Biswas M., Samman M. M. "Damage Detection from Changes in Curvature Mode Shapes", Journal of Sound and Vibration, 145(2), 321-332, 1991.
4. Wang Z., Lin R. M., Lim M. K., "Structural Damage Detection Using Measured FRF Data", Computer Methods in Applied Mechanics and Engineering, 147, 1-2, 187-197, 1997.
5. Wang Q., Deng X., "Damage detection with spatial wavelets", International Journal of Solids and Structure, 36: 3443–68, 1999.
6. Majumder L., Manohar C. S., "A Time-Domain Approach For Damage Detection in Beam Structures Using Vibration Data With a Moving Oscillator as An Excitation Source", Journal of Sound and Vibration, 268, 699-716, 2003.
7. Cattarius J., Inman D. J., "Time Domain Analysis for Damage Detection in Smart Structures", Mechanical System and Signal Processing, 11,3,409-423, 1997.
8. Hoshiya M., Saito E., "Structural Identification by Extended Kalman Filter", Journal of Engineering Mechanics, ASCE, 110, 12, 1757-1770, 1984.
9. Ling X., Haldar A., "Element Level System Identification with Unknown Input with Rayleigh Damping", Journal of Engineering Mechanics, ASCE, 130,8,877-885, 2004.
10. Vo P.H., and Haldar A., "Post Processing of Linear Accelerometer Data in System Identification", Journal of Structural Engineering,30, 2, 123-130, 2003.
11. Sohn, H., Farrar, C. R., "Damage Diagnosis Using Time Series Analysis of Vibration Signals",Smart Materials AndStructures, 10, 446-451, 2001.
12. Hou Z., Noori M., Amand R. St., "Wavelet-Based Approach for Structural Damage Detection", Journal of Engineering Mechanics,126,7,2000.
13. Sun Z., Chang C. C., "Structural Damage Assessment Based on Wavelet Packet Transform", Journal of Structural Engineering, ASCE, 128,10, 2002.
14. Ovanesova A. V., Suarez L. E. "Applications of Wavelet Transforms to Damage Detection in Frame Structures", Engineering Structures, 39-49, 2004.
15. Kim B. H., Kim H., Park T., "Nondestructive Damage Evaluation of Plates Using Multi-Resolution Analysis of Two Dimensional Haar Wavelet", Journal of Sound and Vibration, 292, 82-104, 2006.
16. Rucka M., Wilde K., "Application of Continuous Wavelet Transform in Vibration Based Damage Detection Method for Beams and Plates", Journal of Sound and Vibration, 297, 536-550, 2006.
17. Poudel U. P., Fu G., Ye J., "Wavelet Transformation Of Mode Shape Difference Function For Structural Damage Location Identification", Earthquake Engineering and Structural Dynamics, 36, 1089-1107, 2007.
18. Wang J., Qiao P., "On Irregularity Based Damage Detection Method for Cracked Beams", Journal of Solids and Structures, 45, 688-704, 2008.
19. Daubechies, I., Mallat, S., and Willsky, A. S., "Special Issue on Wavelet Transforms and Multiresolution Signal Analysis—Introduction". IEEE Trans. Info. Theory.,38:529–531, 1992.
20. Cohen, A., Daubechies, I., Jawerth, B., and Vial, P., "Multiresolution Analysis, Wavelets and Fast Algorithms on an Interval". Compt. Rend Acad. Sci. Math.316: 417–421, 1993.
21. Luisiera F., Blua T., Forsterb B., and Unser M., "Which Wavelet Bases are the Best for Image Denoising?", Proceedings of the SPIE Optics and Photonics, Conference on Mathematical Methods: Wavelet XI, pp. 1-12, 2005 (San Diego CA, USA, 2005).
22. Arivazhagan S. and Ganesan L., "Texture Classification Using Wavelet Transform", Pattern Recognition Letters, 24,1513-1521, 2003.
23. Cohen, A., Daubechies, I., Jawerth, B., and Vial, P., "Multiresolution Analysis, Wavelets and Fast Algorithms on an Interval", Compt. Rend Acad. Sci. Math.316:417–421,1993.
24. Clough R. W., Penzien J., "DynamicsofStructures",McGrawHill,NewYork,1975.
25. Ewins D. J.,"Modal Testing: Theory and Practice", Research Studies Press, Letchworth, 1984.
26. Daubechies I., "The Wavelet Transform, Time-Frequency Localization and Signal Analysis", IEEE Transactions on Information Theory, 36, 5, 1990.
27. Jense A., Cour-HarboA., "Ripples in Mathematics: The Discrete Wavelet Transform", First Edition, Springer, Berlin, ISBN: 3540416625, 2001.
28. Cohen A., Daubechies I., Feauveau J. C., "Biorthogonal Bases of Compactly Supported Wavelets", Communications in Pure and Applied Mathematics, 45, 5, 485-560, 1992.
29. Cohen A., Daubechies I., Vial P., "Wavelets on The Interval and Fast Wavelet Transform", Applied and Computational Harmonic Analysis, 1,1, 54-81, 1993.
30. O'Callahan J., Avitabile P., and RiemerR.,"System Equivalent Reduction Expansion Process(SEREP)", 7th / MAC, Las Vegus, January,1989,29-37.
31. Sastry C.V.S., Roy Mahapatra D., Gopalakrishnan S., Ramamurthy T.S., "An Iterative System Equivalent Reduction Expansion Process for Extraction of High Frequency Response from Reduced Order Finite Element Model", Computer Methods in Applied Mechanics and Engineering, 192, 1821-1840, 2003.

Life Cycle Reliability and Safety Engineering
Vol.4 Issue 1 (2015) 44-48

Condition and Health Assessment of Wind-Turbine Tower Structures

Mehdi Modares
Department of Civil, Architectural, and Environmental Engineering; Illinois Institute of Technology;
Alumni Memorial Hall Room 213;3201 South Dearborn St., Chicago, USA
Email: mmodares@iit.edu

Abstract

A major cost and management issue related to wind turbine structures is condition assessment, which, when conducted according to state-of-the-art protocols, produces very subjective and highly variable results. This paper reports on the development of a new onsite structural condition assessment for a wind turbine tower structural system based on a wireless sensor system that is remote, compact, and quick to install. This condition assessment tool offers a cost-effective monitoring system that can be effective in increasing the safety of wind turbine tower structures and hence, enhancing their reliability of performance.

Keywords: *Wind Turbines, Structural Condition Assessment, Sensors, Health Monitoring, Structural Reliability*

1. **Introduction**

By the year 2030, the United States targets 20% wind-based electricity generation, over 300 GW, [1]. In order to obtain more stable wind speeds for increased energy generation, taller wind turbine towers are being built. The size of wind turbines has increased over the years, now ranging from 35 to more than 100 meters in height [2]. A wind turbine, including its supporting pillar and foundation, forms a complex structural system that is subject to a unique set of forces. In addition to a dynamic non-uniform wind pressure on blades, the entire structure is also subject to the dynamic action of the rotating blades, additional wind forces on the pillar and, in offshore cases, forces from sea waves. In addition to fluctuating stresses that would affect the integrity of blades, a combination of these forces will result in the system instability that, if not properly controlled, may dramatically affect the operation of the turbine and compromise its safety.

The complexities and increase in the size of wind turbines have made it difficult to perform inspection and maintenance work. In addition, locations of wind turbines, in remote mountainous or rough sea regions, have made it difficult to maintain and repair such structures. Due to these remote locations and turbine downtime, wind turbines have a high cost of operation and maintenance. Thus, condition monitoring and fault diagnosis of wind turbines are crucial in their sustainable operation. Reactive maintenance dominated the early practices as turbines were operated until failure occurred. More recently, preventative or condition-based maintenance have been adopted for periodic inspections based on predictions on when subsystems in wind turbines would fail.

Therefore, there must be routine monitoring of the turbines in order to improve safety considerations, minimize the down time, and lower the frequency of sudden breakdowns. Benefits of a fault detection system, in this case a Structural Health Monitoring (SHM) system, are: 1) avoidance of premature breakdown, 2) reduced maintenance cost, 3) supervision at remote sides and remote diagnosis, 4) improvement of energy capacity output, and 5) support for further development of wind turbine technology as efficient fault detection would allow more resourceful spending in advances. Although current state-of-the-art structural health monitoring systems have been implemented on wind turbines for several years, a feature enabling SHM procedure to specifically target structural anomalies (including structural stability and active control in addition to traditional damage assessment analysis) have not been addressed in currently available systems. Moreover, most state-of-the-art SHM systems for wind turbines are focused on the blades and rotating systems and not on the wind turbine towers. As many reported failures of wind turbine structures are based on the failure of their towers, mostly due to extreme environmental conditions such as extreme wind, there is a crucial need for protocols to specifically address the SHM procedures for wind turbine towers. And as such, the

developed protocols will ultimately be utilized for the condition assessment of the entire wind turbine systems [3-8].

In order to address the aforementioned shortcomings with SHM systems for wind turbine structures, this paper discusses the development of, and a conceptual design for, an onsite structural condition assessment and control tool for the entire structure of a wind turbine system, with a focus on the tower structure, based on a wireless sensor fusion platform that is remote, compact, and quick to install. This innovative tool, in addition to the implementation of a wireless sensor system for structural health monitoring of wind turbines, is also able to continuously communicate with the sensor platform and conduct on-time analyses in order to advise on:

(a) System performance
(b) System's critical conditions in terms of stress concentrations, large movements or unusual structural behavior
(c) Critical loading patterns (especially in offshore turbines) that may compromise stability
(d) Blade usage and potential damage growth and structural worthiness as operation continues
(e) Critical time for scheduled maintenance and repair

This onsite structural condition assessment and control tool will work as an "active control" system that can monitor and alter the system dynamic characteristics in order to control and reduce potential damage to the structure. It is anticipated that the onsite structural condition assessment and control tool proposed in this research will equip a turbine with a powerful system that not only addresses the traditional damage potentials of the blades, but also further addresses other issues related to the safe performance of the entire turbine structure (Figure 1).

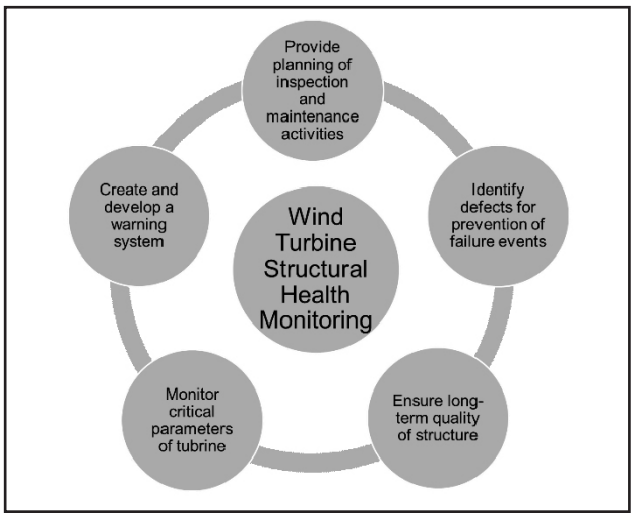

Figure 1. Schematic depiction of the developed method

This development and design concepts reported in this paper are part of an ongoing research by the author at Illinois Institute of Technology. The developed framework represents the results and finding that constitutes a "phase-one" type of study. Currently, the prototype design and field investigations are planned for the continuation of the study.

The system, once fully operational, has a direct impact on the overall safety of wind turbine systems and increasing their reliability of performance. This will further impact the operation of turbines in reducing their down time and increasing their productivity and efficiency of service. Upon success of this project, and with the enhanced safety anticipated with the turbine operations, the power industry is expected to benefit in terms of higher efficiency and lower maintenance.

1.1 Condition Assessment Procedures

The structural health and condition of in-service structures is usually assessed through visual inspections and nondestructive testing and evaluation (NDT/NDE) methods conducted on a pre-set schedule. In general, attempts to quantify the performance of older structures using visual inspection have resulted in subjective and relatively unorganized protocols [9]. Objective evaluation of system level behavior of structures based on sensor network systems is desirable for structural condition assessment purposes.

1.2 Sensor-based Structural Measurements

The goal of sensor-based structural measurements is to employ sensing instruments to provide information pertaining to the condition of the structure [10]. Today's practice of structural measurements involves a host of structural parameters. For those parameters, the sensor-based data is compiled either continuously or intermittently. There are several existing techniques to measure those parameters in structures. There are contact methods that place various sensors, such as strain gauges, accelerometers and Fiber Bragg Grating (FBG) sensors along a structure. Conversely, there exist non-contact methods such as Laser Doppler Vibrometer (LDV), Global Positioning System

(GPS), and Terrestrial Laser Scanning (TSL) [11]. The availability of compact data acquisition systems along with the wireless technology has made the process of data compilation more affordable and convenient. It is envisioned that in the near future, more wind-turbine authorities will take the advantage of the wireless instrumentation and data acquisition process in developing systems that can continuously be used to monitor the state of this structures

1.3 Failure Locations (Hot Spots) - Wind turbine Tower Possible Anomalies

The most common type of damage incurred is rotor or blade damage along with tower damage. Blades account for 15-20% of the total turbine cost and their damage is the most expensive type of damage to repair [12]. The most critical load is the flap wise bending load that arises when the turbine has been brought to a standstill due to high wind, and the blade is hit by the fifty year extreme wind gust [12]. Researchers have examined blade failures; and the work on improving blade performance (with the aid of condition monitoring) is progressing. However, the tower failures are those that are overlooked and are amongst the most dangerous failure types often resulting in damage to other structures as well as causing the total destruction of the system itself. The hot spot for such a failure occurs at the welded or bolted joints of the tripod of the structure. This is prevalent for offshore wind turbines for which the central joint of the tripod constitutes as the most critical location for fatigue and fracture design consideration. In the case of a marine atmosphere, the splash zone of the tower due to exposure is also vulnerable to such failures. More specifically within towers, cracks are generally detected in many of the circumferential welded joints between lower rings and the flanges that connect the towers to the foundations [12].

Most cracks are associated to fatigue phenomena caused by: 1) inadequate weld geometrical design, 2) inadequate weld process parameters, 3) material-process incompatibilities, 4) inadequate weld process execution, and 5) unanticipated service requirements. Analyses at the location of the most stressed section of the tower (close to the foundation) show that failure is due to maximum bending moments on the lower section of the tower. Ultrasonic testing on previous towers has found that the cracks that appear are greater on the inner side of the section than the outer side [5]. This signals that the cracking process probably begins from the inside (internal crack) and propagates as a through crack. Hardness measurements generally yield no significant variations; while it is conceivable that the fatigue process from wind, along with its variation in forces and moments, cause the cracking in the towers. A useful tool is Fatigue Damage Assessment where nominal stresses are used to estimate elastic stress values in the location of interest. From such an analysis, a nominal stress permissible for the component's life is derived, which is compared to applied stress. The method uses hot spot stress or notch stress for this purpose. However, this is appropriate for components with stress concentrators in which hot spot stresses are calculated along with known stress-number of cycles to failure (SN) information for failure analysis. In situations when complex geometries exist (such as for example in connections and joints), this process may result in overestimation of fatigue life, unless SN relations specific to the type of geometry is known. Furthermore, most current methods of fatigue damage use non-random load patterns. However, towers have loading sequences that could be categorized as random; and as it has been reported, a majority of the random nominal stresses are within the range of 10 MPa to 200 MPa [13], which is quite large in terms of variation.

1.4 Failure Case Study

A failure case study is presented regarding a collapsed wind turbine located in Taichung Harbor on September 28, 2008 [2]. The wind turbine tower was broken in three sections; the lower two parts buckled and snapped during a typhoon. The collapse was investigated to see if it followed one of the causes of engineering disasters: human factors, design flaws, material failures, extreme conditions or environments, or a combination of these. It is noted that observations from other wind turbine collapses had found that the primary cause of collapse was strong winds and storms in 52.2% of the cases [2].When testing intact and fractured bolts, it was found that all the bolts that fractured failed to meet the yield and ultimate strength requirements per design specifications. Thus, bolt strength was inadequate as a result of either poor bolt quality control or that the bolts may have had a locked-in stress when screwed into the flange; leading to continuous deformation. A re-analysis was conducted in order to predict the tower response under different wind loads specified in original design. Failure modes of tower collapse, incorporated in the analysis, included excessive deformation, fatigue, fracture, yielding, and plastic collapse. The re-analysis suggested that the bolts of the tower merely met

strength specifications for a lesser wind speed than they were originally designed. Recent specifications were not checked specifically in regards to the bolts. The fact that the tower studied was damaged more than other turbines in the same type of wind load environment suggests that a crosswind, such as vortex shedding or wake galloping, could have been the primary cause of damage to the structure. Main causes of the collapse were found to be due to strong winds, insufficient bolt strength, and poor bolt quality during construction. By analyzing the construction procedure, design specifications and a managerial system, the severity of a similar failure or its damage in the future can be minimized effectively.

2. Methodology Framework

The developed framework for condition assessment for a specific existing wind turbine tower constituted four major steps described below:

Step 1: Preliminary Investigations

As part of the development of the monitoring system, preliminary investigations were conducted to specifically address the basic requirements for the system. Specific studies concentrated on:

a) Surveys of potential sources of dynamic loads (including wind load) to obtain (i) the severity of vibrations induced; (ii) their significance on various structural and non-structural components; and (iii) the critical components that will need to be monitored on a short-term or long-term basis.

b) Review of current local standards and design guidelines of various code bodies that address issues related to, and assess the acceptable levels of, vibrations and deflections for wind turbine systems.

c) Studies of current and available monitoring systems for wind turbine systems.

d) Investigation of traditional and modern sensor technologies used to monitor the structural parameters of wind turbine systems. A variety of sensors measuring structural parameters such as transducers for displacements, accelerometers for vibrations, strain gauges and fiber optics for strains can be assessed for their potential applications in monitoring. The accuracy, measurement ranges, operating temperatures, advantages and disadvantages of the sensors needs to be investigated.

Step 2: Development of a Framework for Monitoring

In this step, appropriate sensors (e.g. acoustic emission, strain gauges, and accelerometers) were studied to develop a design for a sensor fusion framework for the health monitoring for wind turbine system. As part of the findings in our study, the basic features of the system was identified and determined to be a framework that can: 1) monitor critical parameters, 2) identify potential problems, 3) plan inspection and maintenance schedules, and 4) create an alarming system as a means to offer warnings in cases where critical conditions prevail that need immediate actions to remedy and/or correct problems in an effort to prevent potential failures and to enhance safety. Furthermore, the monitoring framework includes measurement sensors, software and hardware for data acquisition, processing and transmission units, as well as data management system.

Step 3: Field Measurements and Data Quality Assurance

This step is currently under way and constitutes sensor installation at critical locations to measure parameters and monitor the structural behavior. The data anticipated to include: a) structure information and identifying number, b) type of sensors and their performance, c) date and time of recording, c) results of damage identification, and d) string of data specific to each sensor. Table 1 summarizes the sensor platform used in this work.

Table 1. Sensor Platform

Sensors	Parameter	Location
Accelerometers	Vibration	Base of tower outside perimeter
Strain Gauges	Strain	Connecting bolts
Joint Meters	Displacement	Baseplate/ foundation

As large amount of raw data is gathered from the sensors, collection, interpretation and analysis of, and the quality assurance procedures for, the collected data must be provided by a data management system.

The data quality assurance (QA) is a critical step to ensure the accuracy and robustness of the data compiled. The QA procedure includes statistical analysis of trends in the data; and specific correlations that exist between measured parameters and certain key structural features and/or the input loads. Similar

QA procedures have been successfully used by others in a variety of health monitoring applications [14].

Step 4: Development of a Warning System

As data enters the central station and is processed, it is expected to be used to pinpoint areas where additional investigations are needed or corrective actions must be taken preemptively to abate the damaging effects of existing anomalies. This warning system can: a) pinpoint to areas where there are potentials for short-term or long-term damage, b) provide advices and/or solutions that can be implemented to prevent damage and d) suggest the types of corrective actions that will need to be taken. Using this framework, if any anomaly is sensed, the structure must be inspected, and proper repair recommended by engineers will be executed.

3. Summary and Conclusions

The failure of infrastructural systems particularly those related to sustainable energy generation has significant societal and human consequences. The work develops an objective condition assessment platform for wind turbines that integrates reconfigurable sensors, finite element models, and structural measurements. This framework enhances the ability to assess the structural condition of in-service wind turbine structures, particularly in cases with unknown design validation. The condition assessment tool can be used for asset management of structures using visual inspection reports, collected non-destructive-test measurements and mathematical modeling with a greater level of confidence due to the inclusion of uncertainty into the protocol. The resulting information can be implemented into structural asset management programs for wind turbine systems to provide more accurate information to the owners for decision making on the structure's condition. This improves the planning and a more cost-effective process for repair, and rehabilitation of wind turbine structures.

This tool increases the overall safety of wind turbines and in their reliability of performance, their operation in terms of reducing their down time and increasing their productivity and efficiency of service. The result of this work, in future, can lead to establishment of a protocol for sustainable management for operation of wind turbine systems.

4. Acknowledgement

The author acknowledges the support of the Wanger Institute for Sustainable Energy Research for the preliminary studies of this work. The author also acknowledges the guidance and assistance of Professor Jamshid Mohammadi, Professor Jafar Saniie, Professor Erdal Oruklu and Mr. Afshin Zahraee on this paper.

References

1. Quilligan, A., O'Connor, A., & Pakrashi, V. (2011). Fragility Analysis of Steel and Concrete Wind Turbine Towers. Engineering Structures, 270-282.
2. Chou, J. s., & Tu, W. T. (2011). Failure Analysis and Risk Management of a Collapsed Large Wind Turbine Tower. Engineering Failure Analysis, 295-313.
3. Wiser R. and Bolinger M., (2008) "Annual report on U.S. wind power installation, cost, performance trend: 2007," U.S Department of Energy, Washington, DC, Tech. Rep.
4. Byon E., Ntaimo L., Singh C. and Ding Y. (2013), "Wind Energy Facility Reliability and Maintenance" in Handbook of Wind Power Systems, Springer.
5. Mcmillan D., and Ault G.W., (2007) "Towards quantification of condition monitoring benefit for wind turbine generators", European Wind Energy Conference & Exhibition, Milan.
6. Swartz R. A., Lynch J. P., Zerbst S., Sweetman B. and. Rolfes R, (2010) "Structural Monitoring of Wind Turbines using Wireless Sensor Networks", Smart Structures and Systems, pp. 183-196.
7. Nagayama, T., & Spencer, Jr., B. F. (2007). Structural Health Monitoring Using Smart Sensors. Urbana: Newmark Structural Engineering Laboratory University of Illinois at Urbana-Champaign.
8. Ciang, C. C., Lee, J.-R., & Bang, H.-J. (2008). Structural Health Monitoring for a Wind Turbine System: A Review of Damage Detection Methods. Measurement Science and Technology, 1-20.
9. Roberts, J.E. and Shepard, R. (2000). Bridge Management for the 21st Century. Proc. Of the Fifth International Bridge Engineering Conference, TRB, (1696) A197-A203.
10. Chang, F. K. (2003). Structural Health Monitoring 2003 From Diagnostics and Prognostics to Structural Health Management, DEStech Publications.
11. Park, H. S., and H. M. Lee (2007) "New Approach for Health Monitoring Structures: Terrestrial Laser Scanning." Computer-Aided Civil and Infrastructure Engineering 22, 19-30.
12. Lavassas, I., Nikolaidis, G., Zervas, P., Efthimiou, E., Doudoumis, I. N., & Baniotopoulos, C. C. (2003). Analysis and Design of the Prototype of a Steel 1-MW Wind Turbine Tower. Engineering Structures, 1097-1106.
13. Guo, P., & Infield, D. (2012). Wind Turbine Tower Vibration Modeling and Monitoring by the Nonlinear State Estimation Technique (NSET). Energies, 5279-5293.
14. Braun, J. F., and Mohammadi., J. (2004) "Structural Monitoring as a Non-Destructive Test Method in Fatigue Reliability Assessment of Aging Aircraft." In NDT Methods Applied to Fatigue Reliability Assessment of Structures. Published by the American Society of Civil Engineers, ASCE.

SRESA JOURNAL SUBSCRIPTION FORM

Subscriber Information (Individual)

Title	First Name	Middle Name	Last Name
_____	_____	_____	_____

Street Address Line 1	Street Address line 2
_____	_____

City	State/Province	Postal Code	Country
_____	_____	_____	_____

Work Phone	Home Phone	E-mail address
_____	_____	_____

Subscriber Information (Institution)

Name of Institution/ Library _____

Name and Designation of Authority for Correspondence _____

Address of the Institution/Library _____

Subscription Rates

	Subscription Quantity	Rate	Total
Annual Subscription (in India)	_____	Rs. 15, 000	_____
(Abroad)	_____	$ 500	_____
	_____		_____
	_____		_____

Payment mode (please mark)

Cheque ☐ Credit Card ☐ Master Card ☐ Visa ☐ Online Banking ☐ Cash ☐ De mand Draft ☐

Credit card Number _____

Credit Card Holders Name _____

Credit Card Holde _____

Guidelines for Preparing the Manuscript

A softcopy of the complete manuscript should be sent to the Chief-Editors by email at the address: editor@sresa.org.in. The manuscript should be prepared using 'Times New Roman' 12 font size in double spacing, on an A-4 size paper. The illustrations and tables should not be embedded in the text. Only the location of the illustrations and tables should be indicated in the text by giving the illustration / table number and caption.

The broad structure of the paper should be as follows: a) Title of the paper – preferably crisp and such that it can be accommodated in one or maximum two lines with font size of 14 b) Name and affiliation of the author(s), an abstract of the paper in ~ 100 words giving brief overview of the paper and d) Five key words which indicates broad subject category of the paper. The second page of the paper should start with the title followed by the Introduction

A complete postal address should be given for all the authors along with their email addresses. By default the first author will be assumed to be the corresponding author. However, if the first author is not the corresponding author it will be indicated specifically by putting a star superscript at the end of surname of the author.

The authors should note that the final manuscript will be having double column formatting, hence, the size of the illustration, mathematical equations and figures should be prepared accordingly.

All the figures and tables should be supplied in separate files along with the manuscript giving the figure / table captions. The figure and table should be legible and should have minimum formatting. The text used in the figures and tables should be such that after 30% reduction also it should be legible and should not reduced to less than font 9.

Last section of the paper should be on list of references. The reference should be quoted in the text using square bracket like '[1]' in a chronological order. The reference style should be as follow:

1. Pecht M., Das D, and Varde P.V., "Physics-of-Failure Method for Reliability Prediction of Electronic Components", Reliability Engineering and System Safety, Vol 35, No. 2, pp. 232- 234, 2011.

After submitting the manuscript, it is expected that reviews will take about three months; hence, no communication is necessary to check the status of the manuscript during this period. Once, the review work is completed, comments, will be communicated to the author.

After receipt of the revised manuscript the author will be communicated of the final decision regarding final acceptance. For the accepted manuscript the author will be required to fill the copy right form. The copy right form and other support documents can be down loaded from the SRESA website: http://www.sresa.org.in

Authors interested in submitting the manuscript for publication in the journal may send their manuscripts to the following address:

Society for Reliability and Safety
RN 68, Dhruva Complex
Bhabha Atomic Research Centre,
Mumbai – 400 085 (India)
e-mail : editor@sresa.org.in

The Journal is published on quarterly basis, i.e. Four Issues per annum. Annual Institutional Subscription Rate for SAARC countries is Indian Rupees Ten Thousand (Rs. 10,000/-) inclusive of all taxes. Price includes postage and insurance and subject to change without notice. For All other countries the annual subscription rate is US dollar 500 ($500). This includes all taxes, insurance and postage.

Subscription Request can be sent to SRESA Secretariat (please visit the SRESA website for details)

SRESA's International Journal of

Life Cycle Reliability and Safety Engineering

Contents

Vol.4 **Issue No.1** **Jan-March 2015** **ISSN – 2250 0820**